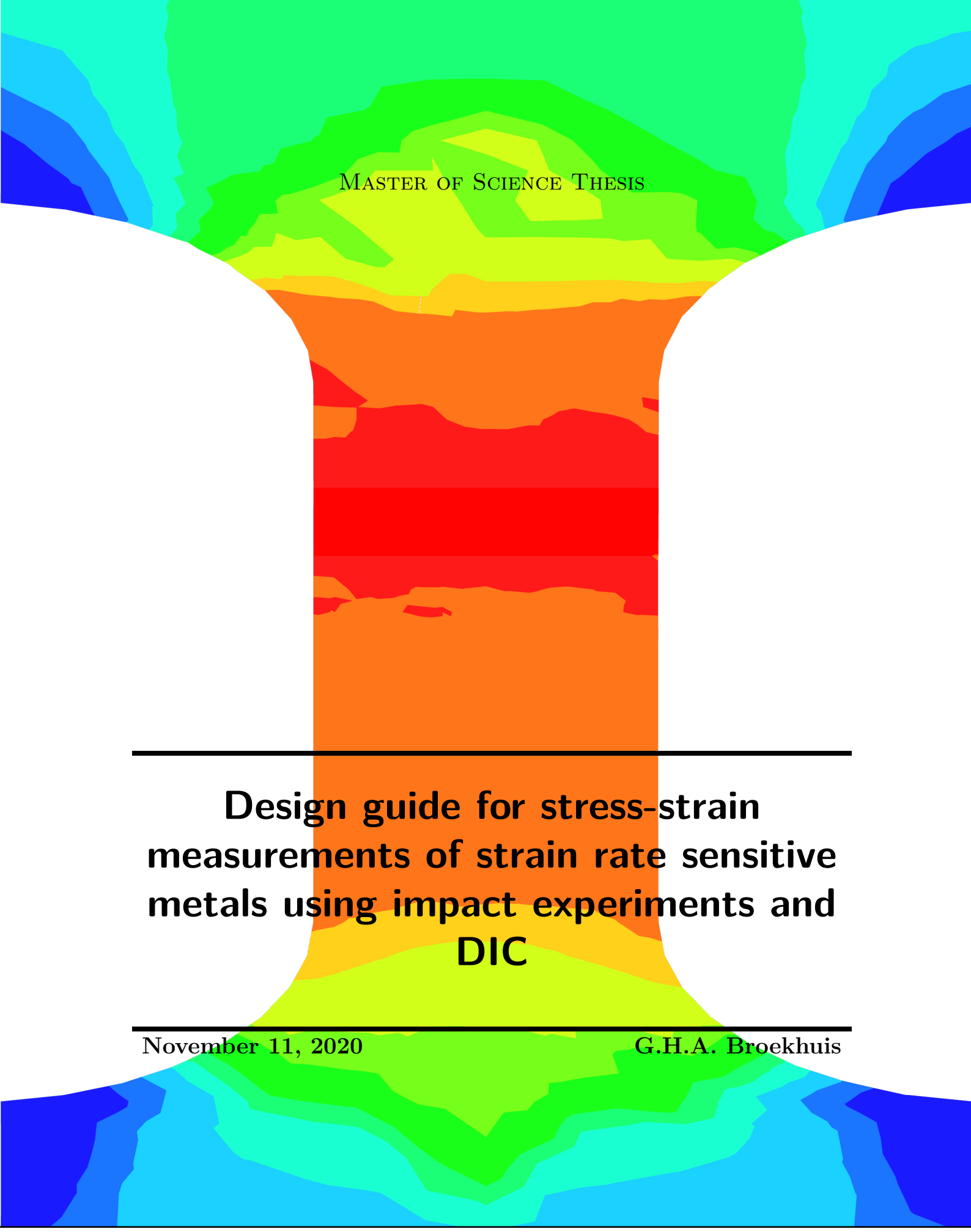

Master of Science Thesis

Design guide for stress-strain measurements of strain rate sensitive metals using impact experiments and DIC

November 11, 2020

G.H.A. Broekhuis

TU Delft Delft University of Technology

Design guide for stress-strain measurements of strain rate sensitive metals using impact experiments and DIC

Master of Science Thesis

For the degree of Master of Science in Marine Technology at Delft University of Technology

G.H.A. Broekhuis

November 11, 2020

Faculty of Mechanical, Maritime and Materials Engineering (3mE) · Delft University of Technology

Delft University of Technology
Department of
Marine Technology

The undersigned hereby certify that they have read and recommend to the Faculty of Mechanical, Maritime and Materials Engineering (3mE) for acceptance a thesis entitled

Design guide for stress-strain measurements of strain rate sensitive metals using impact experiments and DIC

by

G.H.A. Broekhuis

in partial fulfillment of the requirements for the degree of

Master of Science Marine Technology

Dated: November 11, 2020

Supervisor:

Dr. C.L. Walters

Committee members:

Prof. dr. C. Kassapoglou MSc

Dr. L. Pahlavan MSc

Ir. O.J. Coppejans

Preface

Dear reader,

Thank you for taking the time to read the preface, it is the beginning of a document which I have come to love over the last year. It has grown with me as I progressed trough the process of graduation. I hope you will find it useful or, if you are my parents, the best thesis in the entire world.

This thesis is the destination of my journey as a student. In 2012, I started this journey when I came to Delft to study Maritieme techniek. A halfway point came in 2017, when I received my Bachelor's degree, after which I went on to earn a Master's degree. That is where I am now, but I would never have gotten here without the help of my friends, family and teachers.

First, my supervisor dr. Carey Walters. During our weekly meetings, we sometimes wandered off the path of my research, only to come back after a huge but interesting detour. Thank you Carey, for encouraging me, your endless patience and fishing a comma splice out of every other sentence.

I would also like to thank Prof. dr Christos Kassapoglou, Dr. Pooria Pahlavan and Ir. Okko Coppejans for completing my committee and providing me with helpful commentary.

My gratitude also extends to the teachers and staff who taught me valuable (life) lessons, especially (in alphabetical order): Laura Chant, Henk de Koning Gans and Gillian Saunders-Smits.

I would also like to thank my friends, who made my time as a student the time of my life: de Mutszen, mijn lieve middelbare school vriendinnen, de meiden van Stoffig, board game night friends, the friends from DFC, study friends, oud-Huischgenoten, friends who fit none of these categories and everyone I forgot to mention.

Wat zou ik moeten zonder mijn leukste nicht dicht in de buurt? Ze haalde me 's nachts van het station, knuffelde mijn heimwee weg en ik mag altijd even babbelen, dankjewel Yvonne.

Voor alle liefde en warmte waarmee jullie me opnamen in de familie, wil ik graag mijn lieve schoonfamilie bedanken: Paul en Arline, Thieu en Esther, Rob en Tosca en natuurlijk oma.

Mijn eigen warme nest waar ik altijd weer terug kan komen: Lieve papa en mama, Silke, Joris en Mauw, bedankt voor al jullie steun, de belletjes als ik er even doorheen zat, de trots als ik vertelde over mijn studie maar vooral jullie onvoorwaarlijke liefde.

Achter elke grote vrouw, staat een sterke man. Nu weet ik niet zeker of ik groot ben, maar achter mij staat zeker een sterke man: Noud. Als ik het niet meer zag zitten, liet jij me weer een zonnige kant zien. Je gaf me eindeloos veel knuffeltjes, troostte me bij elke huilbui en bleef altijd koppig in me geloven. Ik weet niet hoe ik dit allemaal zou hebben gedaan zonder jouw liefde, je eindeloze geduld en al die flauwe geintjes.

I hope you enjoy reading my thesis as much as I enjoyed finishing it.

Hilde Broekhuis
October 28, 2020
Delft

Summary

Strain rate, how fast a material is strained, is known to have an effect on the behaviour of metals. Being able to measure the effect of strain rate in a material provides more reliable material data as input for material models. Strain rates up to 10 s^{-1} can be tested using a (fast) hydraulic testing machine. Strain rates upwards from 500 s^{-1} can be tested using a Split-Hopkinson bar, but for the strain rates in between no such standard method is available.

The goal of this thesis is to provide a design guide for a reliable experiment that measures the effect of strain rate, in the range 10-100 s^{-1}, on the tensile stress-strain curve of a metal. The test method proposed in this thesis consists of two parts. The first part is a test using a universal testing machine to determine material behaviour at low strain rates of 0.001-10 s^{-1}. A regular dogbone specimen with a longer grip section is used for the UTM tests, which provides the material data to design specimens for the second part. The second part is an impact test where a drophead impacts a specimen, causing it to strain. The specimens are U-shaped strips with a dogbone at either side to test material behaviour at higher strain rates of 10-100 s^{-1}. For both tests, strains are recorded in the grip and gauge sections by means of a DIC system.

The main advantages of the proposed test method are (i) that no sensors are required in the drophead as the load is extracted from strain measurements in the linear elastic grip section, while the gauge section is allowed to deform plastically and (ii) by using DIC, unobtrusive measurements are taken of the strain field in the recorded area.

Two analytical models have been developed, one for the universal testing machine tests and one for the impact tests. The analytical models for the UTM tests and the impact tests have been compared to a finite element model of the same specimen. When plastic strain in the gauge section becomes the most dominant component of the strain, both analytical and FE strain curves show good agreement.

Numerical simulations of the impact test have been done by means of an explicit, dynamic, non-linear impact simulation using finite element analysis. A parametric study has been done using the FE model to determine the effect of drophead mass, impact velocity and specimen dimensions on the strain rate in the gauge section and the measurement accuracy. Based on

the results of this study, a guideline is presented for performing the experiment.

In conclusion, a novel test method and corresponding guideline to determine the stress-strain curve of metals at intermediate strain rates in the range of 10-100 s^{-1} has been presented and demonstrated by means of numerical simulations. As a future step, a set of experiments should be performed to prove the validity of the proposed test method.

Table of Contents

Nomenclature

Roman Symbols

A	Area	mm^2
b	Width	mm
D	Coefficient Cowper-Symonds relation	1/s
dy	Horizontal distance	mm
dz	Vertical distance	mm
E	Young's modulus	GPa
E_{pl}	Plastic Young's modulus	MPa
F	Force	N
h	Thickness	mm
K	Strength coefficient for power law	MPa
L	Length	mm
m	Mass	kg
N	Number of data points	-
n	Strain hardening exponent for power law	-
N	Recording resolution	px
P	Reference point	-
f_c	Friction coefficient	-
q	Coefficient Cowper-Symonds relation	-
C	Constant	-
r	Radius	mm
R	Radius	mm
t	Time	s
u	Displacement	mm
v	Velocity	m/s
x	x-coordinate	mm

y	y-coordinate	mm
z	z-coordinate	mm

Greek Symbols

α	Angle dogbone part of specimen	$^\circ$
β_0	Object displacement accuracy	mm
β_1	Image displacement accuracy	px
δt	Time step	s
$\Delta\bar{\varepsilon}_{pl}$	Incremental change in equivalent plastic strain	–
Δt	Time increment	s
ε	Strain	-
$\dot{\varepsilon}$	Strain rate	s^{-1}
ν	Poisson's ratio	-
ρ	Density	kg/m^3
σ	Stress	N/m^2
ω	Factor in determination of strain rate factor	rad/s

Sub/Superscripts

0	flow
0	Initial
abq	As given by Abaqus
c	Parallel in the gauge section
clamp	In the clamp section
down	In the downward direction
d	Drophead
d	Dynamic
e	Engineering
$\sigma\varepsilon$	As given by the stress-strain input curve
ε	Strain
FoV	Field of view
gauge	In the gauge section
grip	In the grip section
m	Measurement
moving	Is moving
p	In point p
q	In point q
σ	Stress
s	Specimen
s	Quasi-static

tm	In the section toward the middle
t	True
u	Ultimate
up	In the upward direction
x	In x-direction
y	Yield
Z	In Z-direction

Abbreviations

DIC	Digital image correlation
FE	Finite element
FEA	Finite element analysis
FEM	Finite element method
PEEQ	Plastic equivalent strain
SHB	Split-Hopkinson bar
SRF	Strain rate factor
UTM	Universal testing machine

Chapter 1

Introduction

Strain rate, how fast a material is strained, is known to have an effect on the behaviour of metals. This effect comes, for example, into play when ships collide or a car crashes. The damage done in such unfortunate events can be predicted by models. Being able to measure the effect of strain rate in a material provides more reliable material data as input for material models and therefore improves our understanding of a ship's or car's structural integrity during a collision. This information can then, for example, be used to improve safety features to keep everyone and everything involved as safe as possible.

Therefore, in order to obtain more reliable material data at various strain rates, this thesis presents a design guide for an experiment to measure the effect of strain rate on a sample of steel in the strain rate range typical for colliding ships. Before going into the experiment in the following chapters, this chapter presents background information on strain rate testing. It is split in five parts. First the current state-of-the-art of strain rate testing is presented to determine the research gap, which is then addressed by the research question in the second part. The final three sections provide some general definitions, a general discussion on the effect of strain rate on the stress-strain curve for metals, and some general background on measurements by camera, respectively.

Following the introduction, the thesis is split in 7 additional chapters starting with the proposed test method for the experiment in chapter 2. Next, chapters 3 and 4 discuss the analytical approach and numerical simulation of the experiment. In order to determine the correct experimental setup, chapter 5 presents a parametric study of various parameters that influence the experiment to assess their impact. Finally, this results in a guideline for the experiment, as presented in chapter 6 and the conclusions and recommendations in chapters 7 and 8.

1.1 Literature on tensile strain rate testing

The enormous amount of research done on the effects of strain rate on material behaviour is enough to fill several books on the subject. Test methods can be roughly divided by range of strain rates covered by each method. The lowest strain rates, up to about 10 s^{-1}, can be

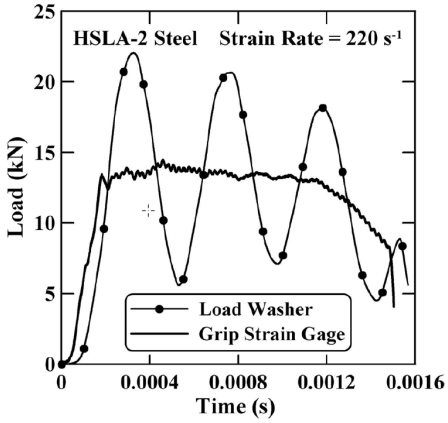

Figure 1.1: Piezoelectric load washer data and strain gauge measurement data for the same experiment (Source: Bruce et al. (2004))

tested using a universal testing machine. Standards such as ISO 6892-1 (2016) and ASTM E8 (2016) are clear guidelines for this test method.

In order to measure the material behaviour at intermediate strain rates, up to 500 s^{-1}, two categories can be distinguished by their test method: (i) measurements using a high-speed servo hydraulic machine and (ii) dropped-weight methods. Material behaviour at higher strain rate, higher than 500 s^{-1}, is commonly measured using a Split-Hopkinson bar. In the following paragraphs, an overview of the different studies using these methods will be given, after which I will summarise their advantages and disadvantages and illustrate the potential for a new test methodology.

One example of the use of high-speed servo hydraulic test machines is the work by Bruce et al. (2004), who used strain gauges and a piezoelectric load washer to the determine the effect of strain rate in several types of automotive sheet steel. Figure 1.1 shows a comparison between the measurements by a piezoelectric sensor and strain gauges. As can be seen, oscillations are observed in the measured load by the piezoelectric sensor, while the strain gauge shows a much smoother curve. These oscillations are caused by stress waves due to the high-speed load introduction by the servo which is required to reach the desired strain rate. Their impact on the material behaviour, however, is limited and they are not of interest for the measurement. Therefore, the piezoelectric sensor proved to be impractical as it picks up all dynamic waves at higher strain rates. A similar situation is described by Pape (2002), who uses an adapted high-speed servo hydraulic machine to determine strain rate effects on flow stress. Therefore, he applies filters on the piezoelectric sensor data to smooth out the oscillations in post-processing of the measurement. An important parameter in these filters is the cut-off frequency. This cut-off frequency has been investigated in more detail by Rusinek et al. (2008). Figure 1.2 shows the effect of filtering using three different frequency domains on the same data. Based on this Rusinek et al. (2008) concluded that, for example, “the yield stress cannot be determined precisely.” and that the results of the measurements are highly dependent on the chosen cut-off frequency in filtering the measurement data and care should be taken in choosing this frequency.

Another important aspect in the measurements of the material behaviour is the potential presence of bending waves resulting in large differences in strain throughout the thickness.

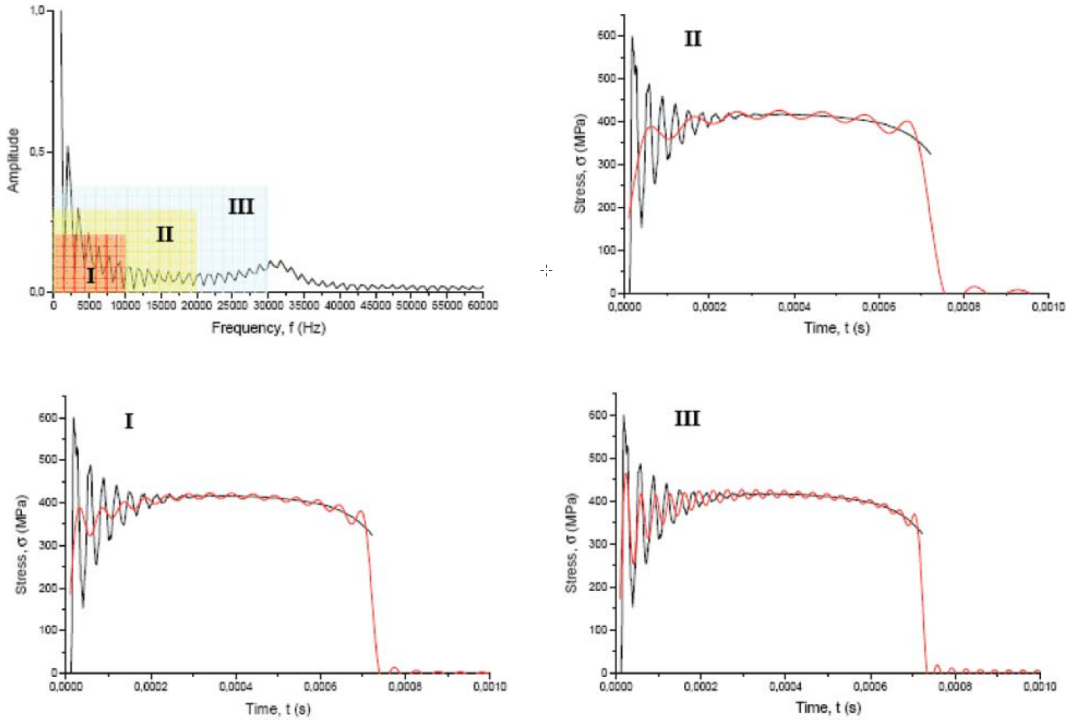

Figure 1.2: Data filtered using different cut-off frequency domains (Source: Rusinek et al. (2008))

Yang et al. (2014) demonstrate this with two strain gauges at opposite sides of a specimen, illustrated in figure 1.3a. The measurement data shows that the strain oscillations are actually caused by bending waves. Another measurement that shows oscillations which are very similar in nature to these is found in the work by Alabi et al. (2018). Alabi et al. (2018) use digital image correlation in combination with a load cell. The stress measured by the load cell oscillates significantly, as can be seen in figure 1.4. These oscillations are attributed to "an imbalance between internal and external forces at high strain rates" and a moving average is employed to remove the oscillations in the measurements. One could conclude that the setup used was insufficient in this case. Possibly, taking measurements on two sides of the specimen and the assumption of linearity trough the thickness could have solved this issue, as was the case for Yang et al. (2014). Furthermore, the work by Yang et al. (2014), as presented in figure 1.3, also illustrates that the use of a moving average to remove oscillations would result in a significant error in the measured material data and should be avoided at all cost.

The second method for intermediate strain rate tests is the dropped-weight method. This method is mostly used for compression tests, but some have investigated its use in tensional tests. One of these is the work by Chan (2009), who investigated two different setups and two different measurement methods. In the first setup a weight is dropped on a horizontal I-beam suspended by two dogbone specimens, as illustrated in figure 1.5a. The second setup has a U-shaped specimen with a dogbone in each vertical side, where a weight is dropped in the middle as illustrated in figure 1.5b. The first measurement method measures the force introduced by a force sensor integrated in the drophead, while the second measurement method employs strain gauges on the specimen to determine the force from the measured strains by assuming linear elastic material behaviour in the grip section. A comparison between the setups reveals

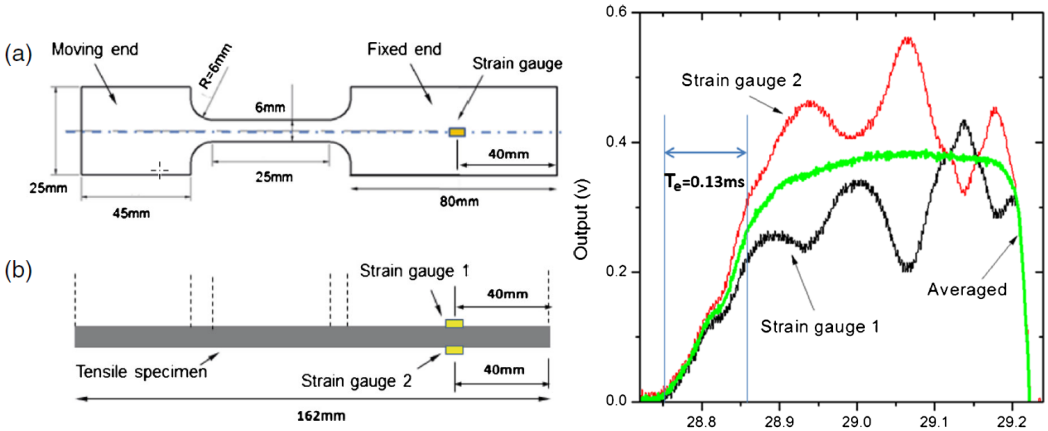

(a) Specimen and placement of strain gauges

(b) Effect of bending on ringing artifact

Figure 1.3: Specimen and measurements on two sides of a specimen to determine the effect of bending on ringing (Source: Yang et al. (2014))

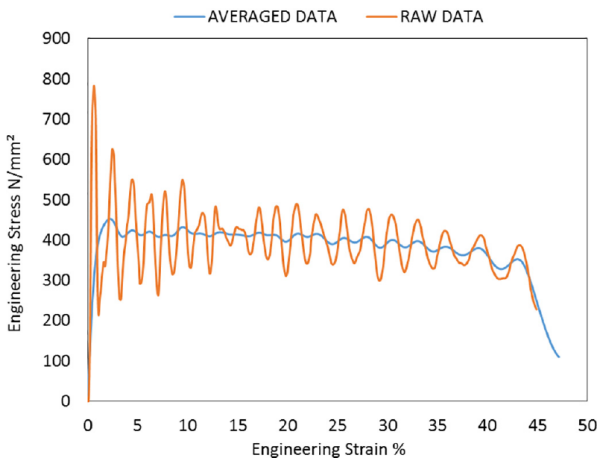

Figure 1.4: Measurement data of Alabi et al. (2018)

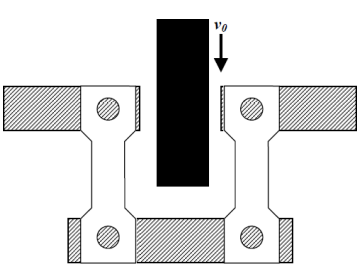

(a) I-beam test setup by Chan (2009)

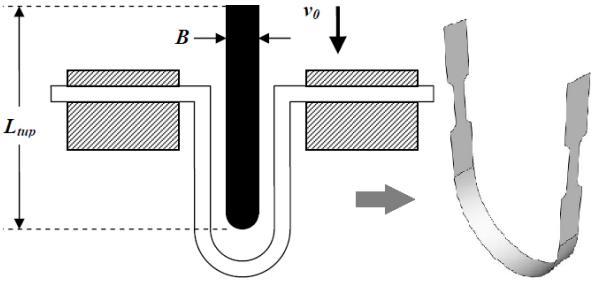

(b) U-shaped test specimen setup by Chan (2009) (Adapted from: Chan (2009))

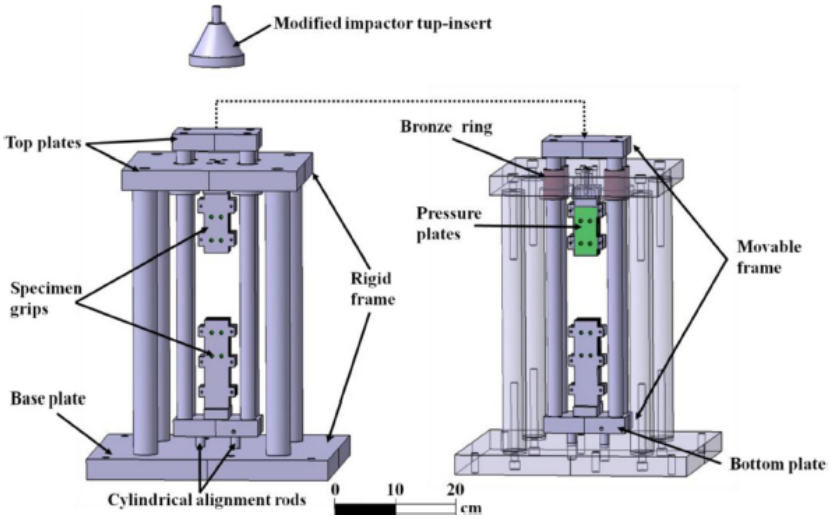

(c) Test setup of Perogamvros et al. (2016)

Figure 1.5: Various setups for dropped weight experiments

that high frequency oscillations (ringing) in the I-beam of the first setup renders those results useless, while results using the U-shaped specimen proved useful. But, there is still plenty of room for improvement, for example, on filtering of stresses due to bending waves from the results. Perogamvros et al. (2016) also proposes the use of a droptower, but rather than dropping the weight directly on a specimen, it is dropped on a moveable frame, as is illustrated in figure 1.5c. A specimen is attached on one side to a movable frame and on the other side to a fixed frame. When the movable frame is hit by the drophead, the specimen will stretch. A load cell in the drophead is used to record the force in the setup. The impact needed to reach the desired strain rate, however, leads to a force overload in the load cell. Moreover, since the load cell is used at high strain rates, high frequency measurements are required, thus introducing noise in the measurements. Lastly, ringing of the frame adds another source of noise, but a thick rubber absorber was placed between the drophead and the frame to successfully combat this. Two different types of material were tested: metallic and composite. A comparison between numerical calculations and experimental data given in figure 1.6, however, shows the complexity of predicting material behaviour by numerical simulations in this setup and hence potentially incorrect material data is obtained from the measurements.

Strain rates higher than 500 s^{-1} are typically tested using a Split-Hopkinson bar (SHB),

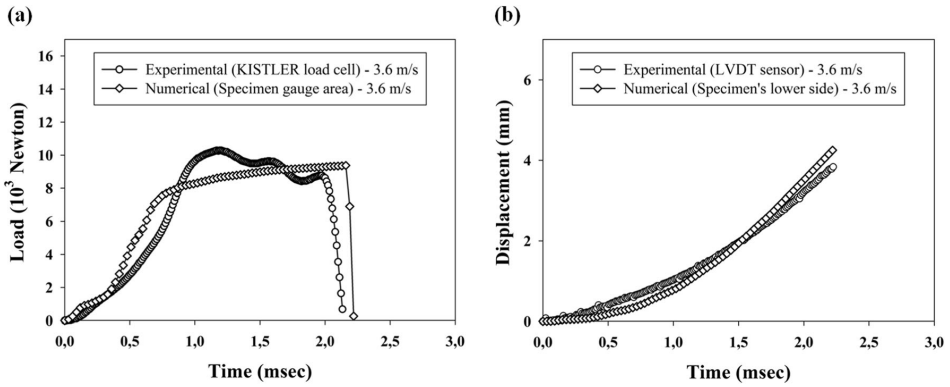

Figure 1.6: Measurement data of Perogamvros et al. (2016)

which is illustrated in figure 1.7. This setup consists of two straight (horizontal) bars, as indicated in blue in the figure, with a specimen in between, as indicated in yellow. The first bar is impacted such that a stress wave (purple) is created. This stress wave propagates through the first bar and when it reaches the specimen, the wave breaks up in a reflected wave (pink) that travels back through the first bar and a transmitted wave through the specimen (blue). This transmitted wave causes the specimen to strain and is then partly transmitted to the second bar. As explained by Spronk (2018), strain gauges (orange rectangles) are used to measure the initial and reflected wave in both bars and the setup should, thus, be such that these do not interfere. A low wave velocity and long way to travel aid in decreasing the likelihood of interference. The wave velocity is the square root of the Young's modulus divided by the density and is, therefore, dependent on the material use for the bars. Furthermore, dynamic equilibrium should be reached within the specimen before the impact ends to ensure a valid measurement. Dynamic equilibrium is reached when the stress wave has travelled at least three times back and forth according to Gray (2000). Therefore, having a short specimen and high stress wave velocity are beneficial to reach dynamic equilibrium quickly. The force in the specimen is determined by multiplication of the strain in the bar, the cross-sectional area and the Young's modulus. Spronk (2018) concludes that: "For low strain rates, one thus wants a bar with a large radius to produce enough force with the small amount of strain. Using a bar with a very high stiffness would namely imply the need for a very long bar as the speed of sound would also rise." SHB made from materials with a lower speed of sound have also been explored as a means to test lower strain rates. Shim and Mohr (2009), among others, use nylon for the horizontal bars. This setup, however, cannot practically be used to measure the material behaviour of steel specimens, since nylon bars would yield before a steel specimen does.

As shown, there is limited research on intermediate strain rate effects and, furthermore, what stands out is the wide range of testing and measurement methods used. Starting with test methods, each has its advantages and disadvantages, and unlike the UTM for low strain rate and the SHB for high strain rates, there is no generally accepted best test method for intermediate strain rates. Fast servo-hydraulic machines are often used but suffer from ringing problems and might have limited availability. Dropped-weight methods mainly suffer from lack of research, but also from ringing. Having to build a big device, which still rings, is not appealing. Meanwhile, dropping a weight directly on to a specimen is promising, but needs much more research. Furthermore, the use of a droptower is convenient, but other ways of

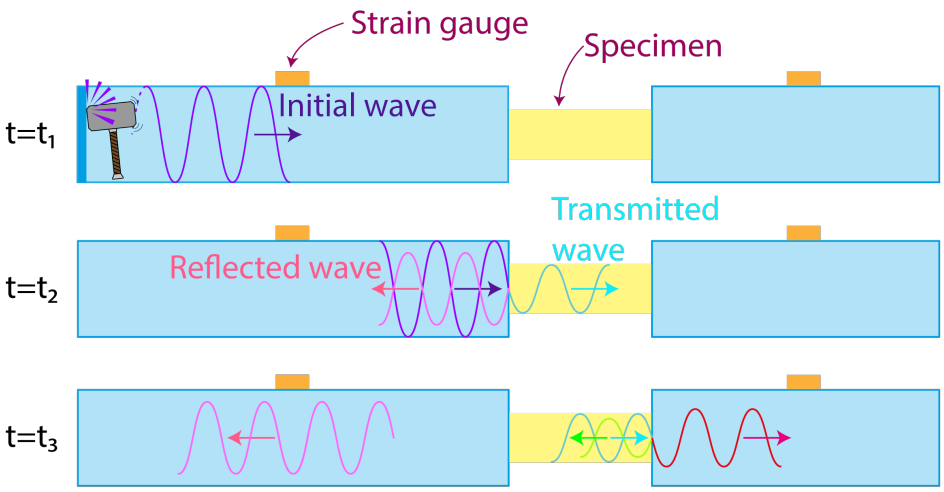

Figure 1.7: Schematic representation of a Split-Hopkinson Bar

dropping a weight from a certain height precisely onto a target are also sufficient, which makes this method very accessible.

When looking at measurement methods, classical strain gauges, piezoelectric sensors and optical measurement methods (i.e. digital image correlation) have been used. Piezoelectric sensors often prove to be too sensitive, especially when ringing is involved, while strain gauges only measure the strain in a single location. Optical methods and digital image correlation (DIC) on the other hand are unobtrusive and provide insight in the distribution of strain over the recorded area, whereas covering the entire area with strain gauges is both inconvenient and subject to error. When using multiple types of sensors on a single experiment, the signals need to be synchronised, which can be difficult. DIC can record the complete specimen on a single device, so synchronisation of different sensors is no longer required. The absence of other sensors also means that the impactor can be just a piece of material in the right shape.

1.2 Research question

The previous section indicates the need for a reliable test method for intermediate strain rate testing. The goal of this thesis is to provide a design guide for a reliable experiment that measures the effect of strain rate, in the range 10-100 s^{-1}, on the tensile stress-strain curve of a material. Therefore the main question guiding the research presented in this thesis is:

> *How can the effect of strain rate on the tensile stress-strain curve at intermediate strain rates of 10-100 s^{-1} be measured by means of DIC?*

In order to answer this question, a test method is presented which is assessed with analytical mechanics and numerical simulations.

1.3 Definitions

Most of the terms and definitions used in this report are considered to be general knowledge for engineers. To prevent confusion, however, a quick overview of the most used definitions in this report can be found here. The meaning of all symbols and abbreviations used in this report can also be found in the nomenclature.

1.3.1 Stress

Stress is load divided by cross-sectional area. For engineering stress, the stress is defined with respect to the initial cross-sectional area:

$$\sigma_e(t) = \frac{F(t)}{A_0} \tag{1.1}$$

where $\sigma_e(t)$ is the engineering stress at time t due to load $F(t)$ in a cross section with initial cross-sectional area A_0. True stress on the other hand defines the stress with respect to the actual cross-sectional area at time, t:

$$\sigma_t(t) = \frac{F(t)}{A(t)} \tag{1.2}$$

where $\sigma_t(t)$ is the true stress at time t due to load $F(t)$ in a cross section with corresponding cross-sectional area $A(t)$. For a uniaxial stress state, the change in cross-sectional area is defined by the Poisson's ratio of the material, which is different for linear elastic material behaviour and plastic material behaviour. The Poisson's ratio for mild steel is 0.3 in case of linear elastic behaviour and 0.5 (constant volume) in case of plasticity. In case of a uniaxial stress state, the deformed area thus becomes:

$$A = A_0(1 - \nu \cdot \varepsilon_t)^2 \tag{1.3}$$

in which the cross-sectional area, A, is a function of the Poisson's ratio, ν, and the true strain normal to the cross-section, ε_t.

1.3.2 Strain

Two types of strain are used; true and engineering strain. Engineering strain is defined as the relative elongation:

$$\varepsilon_e(t) = \frac{L(t) - L_0}{L_0} \tag{1.4}$$

where $\varepsilon_e(t)$ is the strain at time t, $L(t)$ is the length at time t and L_0 is the initial length.

The true or logarithmic strain is related to the engineering strain by:

$$\varepsilon_t(t) = \ln(1 + \varepsilon_e(t)) = \ln\left(\frac{L(t)}{L_0}\right) \tag{1.5}$$

1.3.3 Strain rate

Similar to the strain, two definitions of strain rate can be recognised: the engineering strain rate and the true strain rate. The engineering strain rate is the time derivative of engineering strain:

$$\dot{\varepsilon}_e(t) = \frac{\mathrm{d}\varepsilon_e(t)}{\mathrm{d}t} = \frac{\mathrm{d}}{\mathrm{d}t}\left(\frac{L(t) - L_0}{L_0}\right) = \frac{v(t)}{L_0} \tag{1.6}$$

where $\dot{\varepsilon}(t)$ is the strain rate at time t, ε is the strain at time t, $L(t)$ is the length at time t, L_0 is the initial length and $v(t)$ is the velocity at one end of $L(t)$ relative to the other end.

True strain rate is the time derivative of the true strain and can be related to engineering strain and engineering strain rate by:

$$\dot{\varepsilon}_t(t) = \frac{\mathrm{d}\varepsilon_t(t)}{\mathrm{d}t} = \frac{\mathrm{d}}{\mathrm{d}t}\ln\left(\frac{L(t)}{L_0}\right) = \frac{\dot{\varepsilon}_e(t)}{1 + \varepsilon_e(t)} \tag{1.7}$$

1.3.4 Stress-strain curve

The stress-strain curve describes the relation between stress and strain in a material. Figure 1.8 indicates some important points in a stress strain curve:

$\boldsymbol{\sigma_y}$ is the yield stress. After this point, the material will plastically deform.

$\boldsymbol{\sigma_u}$ is the ultimate stress. After this point, the material starts necking.

$\boldsymbol{\varepsilon_y}$ is the yield strain.

$\boldsymbol{\varepsilon_u}$ is the ultimate strain.

In order to describe the plastic behaviour up to the ultimate stress in a true stress-strain curve, a power law is commonly used for metals, starting at σ_y:

$$\sigma_t = K\varepsilon_t^n \tag{1.8}$$

where the coefficients K and n can be determined by a curve fit through measurement data.

1.4 Strain rate effects on stress-strain curve

The stress-strain curve of metals is dependent on the strain rate at which the strain is introduced. Jones (2012) provides a comprehensive overview of research done on material

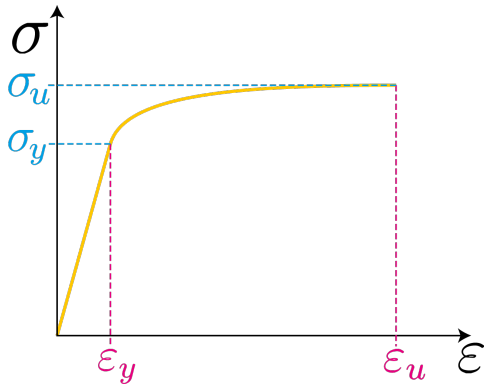

Figure 1.8: Definitions regarding the stress-strain curve

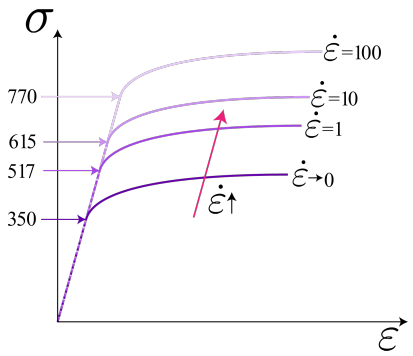

Figure 1.9: Scaling of a stress-strain curve for mild steel using the Cowper-Symonds relation

characteristics of strain-rate-sensitive behaviour of materials. The yield stress and ultimate tensile stress both increase when the strain-rate increases. In order to simulate these effects, the material model introduced by Cowper and Symonds (1957) is commonly used, who introduced the following equation for strain rate sensitivity:

$$\sigma_{t,d} = \sigma_{t,s}\left(1 + \left(\frac{\dot{\varepsilon}_t}{D}\right)^{1/q}\right) \tag{1.9}$$

where $\sigma_{t,d}$ is the dynamic tensile true yield stress at uniaxial true strain rate $\dot{\varepsilon}_t$, $\sigma_{t,s}$ is the quasi static true yield stress and D and q are material specific constants.

It should be noted, however, that, as Jones (2012) also described, a decrease in fracture strain and overall shortening of the stress-strain curve is observed when the strain-rate increases. These effects are not relevant for the measurements simulated in this thesis, but it is important to remember that these effects will manifest in a real sample of material. An example of the scaling of a stress-strain curve, as defined by equation 1.9, is shown in figure 1.9 for various strain rates.

1.5 Digital image correlation

This section provides some background information on the use of a camera for measurements. These are just the basic working principles, needed to understand the current thesis. More details on DIC can be found in the work by Sutton et al. (2009). First a small introduction is given into the fundamentals of DIC. Followed by how and why some factors affect the accuracy of DIC measurements, and some unique challenges posed by working with cameras.

1.5.1 Basic working principles

DIC uses a digital camera to take a series of photos of a specimen while it is tested, or, in this case, stretched. Then the difference between two consecutive photos is used to determine what changed in the meantime. Usually a speckle pattern is applied on the specimen, which is used for the detection of changes between two images. Four steps in this process are given below and illustrated in figure 1.10 for a 1D example:

Step 1: Take at least two pictures The first picture will be the baseline, to which the next is compared. In figure 1.10 blue illustrates the first image and purple the second.

Step 2: Select a subset from the first picture The subset is a small piece of the first picture, of which the location will be tracked from the first to the second picture and so on.

Step 3: Interpolate the subset The discrete pixels of the subset are interpolated to create a grey-level intensity pattern. This is such that the pattern can be tracked from the first to the second picture. When one would try to match the discrete pixels of the subset, the area of the subset could, for example, be stretched, so it would be impossible to find the exact pixel pattern in the second picture. With the intensity pattern, only the pattern needs to match.

Step 4: Match the subset in the second picture Use the grey-level intensity pattern to locate the subset in the second picture.

Multiple subsets combined give a complete displacement field. The difference in distance between two subsets can then be used to calculate the strain with a spatial derivative. When a single camera is used to record the specimen, it can only provide data in 2D, which is called 2D DIC. For 3D DIC, at least two cameras are required that are synchronised to take their photos at the exact same moment.

1.5.2 Accuracy

Measurements are preferably as accurate as possible, so it is vital to know the accuracy of a measurement method. Unfortunately, since DIC systems are commercial products, little verified information is available on this. Sutton et al. (2009) provide an engineering approach to determine the accuracy of a 2D DIC measurement:

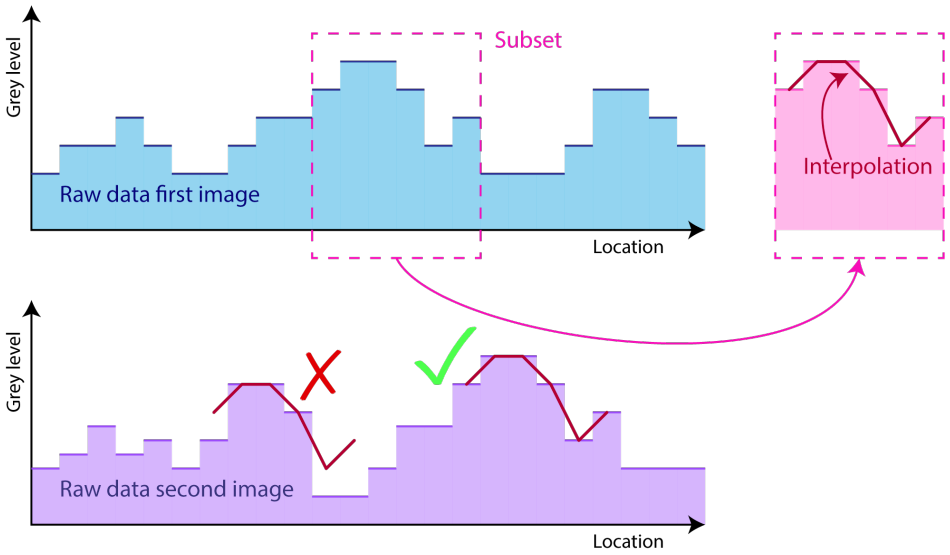

Figure 1.10: schematic representation of matching a subset from one image to the next

$$\beta_0 = \frac{L_{FoV}}{N} \cdot \beta_1 \tag{1.10}$$

in which the object displacement accuracy β_0 is a function of the length of the field of view L_{FoV}, the recording resolution N and the image displacement accuracy β_1, which is typically 0.01 px.

A minimum level of image plane oversampling is needed for accurate matching: "For accurate matching, image plane speckles should be sampled by at least a 3 by 3 pixel array to ensure minimal oversampling and reasonable intensity pattern reconstruction via interpolation." Furthermore, there is a minimum for the number of speckles in a subset: "Each image plane subset of size N by N should contain at least 3 by 3 speckles to ensure reasonable accuracy and isotropy in the subset matching process." (Source: Sutton et al. (2009))

1.5.3 Factors influencing accuracy

For the most accurate measurements, it helps to know what influence various factors have on the accuracy of measurements. Reedlunn et al. (2013) provide helpful insight with tips and tricks on the use of DIC in experiments. They listed the main parameters that affect the accuracy of a measurement. The ones relevant for this thesis are:

Speckle patern The best speckle pattern has a random, fluctuating grey-scale. It is matte, rather than glossy and has a high contrast. Also, speckles should not fracture when changing shape.

Camera, lens and environment The experiment should be clearly visible trough the lens of the camera. Many of the following points are general rules of good camera use:

Exposure The exposure is the amount of light that enters the camera, this determines

how bright the specimen is recorded, too much light blinds (overexposure) the sensor but too little (underexposure) results in a dark image.

Lighting of experiment Related to the exposure, the setup needs to be well lit, not too bright but certainly not too dark. Diffuse rather than focused lighting is recommended.

Field of view The complete area of interest has to be captured by the camera, this is the field of view.

Depth of field Blurred images can't be used for measurements, so the area of interest has to be fully in focus. A shallow depth of field means that only a small part of the image is in focus.

Direct line of sight A direct line of sight often provides the best results. Distortions or changes in light might be introduced by any medium in the line of sight between a lens and its object.

The fish-eye effect Another possible source of distortions is the fish-eye effect. The fish-eye effect is always present when using a lens, it is most prevalent at the edges of the frame and when the lens of the camera is too close to the specimen.

Image spatial resolution versus speckle size The sensor in the camera used for DIC has a certain spatial resolution. This means that a continuous image is converted to a discrete number of pixels. A single speckle in the pattern should be comprised of at least 3 pixels. When this is not the case, either speckles should be made larger or resolution has to increase. This does not mean that bigger speckles are always better, a speckle should not be so big that it makes a subset impossible to match. This could happen for example when an entire subset is the same shade of grey.

Frame rate The number of photos taken in one second is defined as the frame rate. A higher frame rate improves the accuracy of the measurements, since more data points are available. When too many photos are taken, one can always remove the surplus. When too few photos are taken, it is impossible to add any while maintaining the measurement's integrity.

Out-of-plane displacements This point is only applicable when using 2D DIC. Since 2D DIC can only register displacements in two dimensions, out-of-plane displacements are interpreted by the system as biaxial strain. When these are present, it can lead to errors in matching of the subset.

Field of view This point is only applicable when using 3D DIC. The use of two cameras to capture the same (piece of) specimen usually means that one or both do not have the optimal view. For measuring out-of-plane displacements, an angle between both cameras is needed. When this causes a camera to have less optimal view, it might result in a worse overall field of view.

1.5.4 Camera considerations

The perfect DIC camera has an infinite frame rate, spatial resolution and depth of field. There is no fish-eye effect, no noise from the sensor and the camera itself is free. Unfortunately we live in the real world, so some trade-offs have to be made.

The first is price, frame rate and spatial resolution. Cameras that combine a high frame rate with a high spatial resolution are very expensive. A less expensive camera might have lower frame rate, which is no problem for (quasi)static experiments. But a high frame rate is preferred in experiments with a medium to high strain rate. An optimum should be found between the spatial resolution and frame rate needed to capture experiment. Do note that the measured areas should not take up the full frame. The fish-eye effect is most prevalent at the edges of the frame, so measurements should not be taken there.

The second is sensor sensitivity, aperture and exposure time. Higher sensor sensitivity means less light is needed for the same exposure, but also an increase in noise on the image. Aperture is the size of the opening through which light enters a camera. A bigger opening lets in more light but also leads to a more shallow depth of field. Exposure time expresses the time the camera sensor records an image. Longer time lets in more light, but it also leaves time for the specimen to move while the image is recorded, creating a blur. Blurred images cannot be used for measurements. If the desired exposure cannot be reached, adding extra lighting might help.

Chapter 2

Test method

The research question posed in the first chapter identified the need for a measurement method to determine the effect of strain rate on the tensile stress strain curve by means of DIC. This chapter presents a method for such a test. First, a broad overview of the proposed test method is given, after which the setup for each part of the test method is discussed. Finally, the design of the corresponding test specimens for mild steel are discussed.

2.1 Overview of the method

The proposed test method consists of two parts. The first part is a test using a universal testing machine to determine material behaviour at low strain rates of 0.001-10 s^{-1}, as was done by Bruce et al. (2004) and Huh et al. (2008) among others. This provides the material data to design specimens for the second part. The second part is a drop test based on the work by Chan (2009). Material behaviour at higher strain rates of 10-100 s^{-1} is tested by the impact of a drophead on a specimen, causing it to strain.

The specimens for the universal testing machine are regular dogbone specimens with a longer grip section. Figure 2.1a illustrates one such specimen. The specimens for higher strain rates are U-shaped strips with a dogbone at either side, as illustrated in figure 2.1b. In both cases the displacements of the material in the dogbone are recorded by a (high speed) camera. The area that is captured on camera is indicated in figure 2.1 by dots on both specimen types.

The displacement field of the specimens is determined using DIC as discussed in section 1.5. Recorded displacements are then converted to strains by the software from the DIC system. The specimens need to be designed such that the strain field in the grip section of the dogbone stays within the linear elastic domain, such that Hooke's law can be used to convert that strain field into a stress field. The ratio between the cross-sectional areas of the grip and gauge section is then used to convert the stress from grip to gauge section. Combined with the strains recorded in the gauge section, a stress-strain curve for a certain strain rate can be constructed.

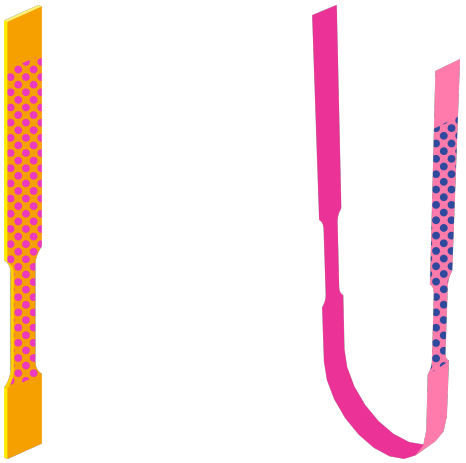

(a) Low strain rates **(b)** Intermediate strain rates

Figure 2.1: Specimens for the proposed method

2.2 Universal testing machine setup

The experimental setup for the universal testing machine is illustrated in figure 2.2a. This setup is used for tests at strain rates in the range of 0.001-10 s^{-1} (ASTM E8, 2016). A specimen is clamped in the machine, the grip on one side is stationary while the other moves with a velocity v, straining the specimen. The velocity is assumed to be as constant as possible over the duration of the experiment, resulting in a constant strain rate. The first test is carried out at a low strain rate, e.g. 0.001 s^{-1}. This is used to determine a quasi-static stress-strain curve. Then subsequent tests are performed with strain rates of 1 and 10 s^{-1}. The tests for each strain rate are carried out at least three times to reduce the chances of experimental or measurement mistakes (ASTM E8, 2016). Bending waves are not expected in these low-velocity, uniaxial strain tests, so a 2D DIC system is sufficient for the recording of deformations in the specimen during the experiment.

Table 2.1: Characteristics for mild steel used for the specimens

Parameter		Value	
Young's modulus	E	210	GPa
Density	ρ	7800	kg/m^3
Poisson's ratio (linear elastic)	ν	0.3	
Poisson's ratio (after yield)	ν	0.5	
Yield stress	σ_y	350	MPa
Yield strain	ε_y	50	
Ultimate stress	σ_u	500	MPa
Ultimate strain	ε_u	150	

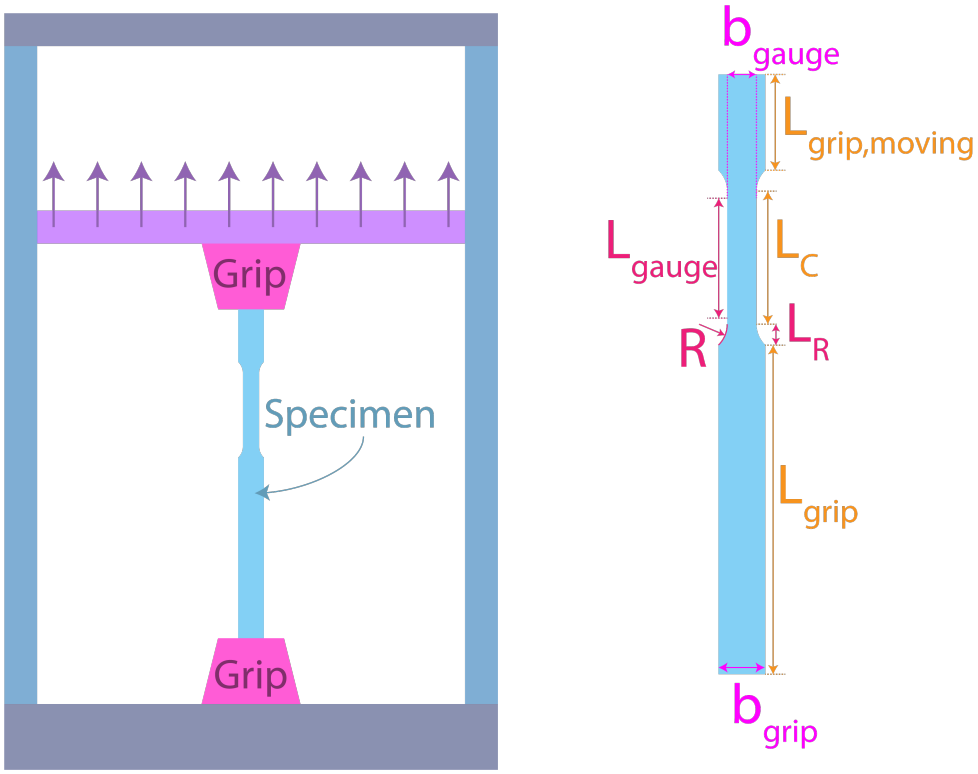

(a) Test setup for universal testing machine

(b) Dimensions of specimen for universal testing machine

Figure 2.2: UTM test

Table 2.2: Dimensions of UTM specimen

Parameter		Value	
Thickness	h	2	mm
Width grip section	b_{grip}	20	mm
Width gauge section	b_{gauge}	12.5	mm
Parallel length gauge section	L_c	57	mm
Length gauge section	L_{gauge}	50	mm
Length radius	L_R	9	mm
Length moving grip section	$L_{grip,moving}$	50	mm
Length clamped grip section	L_{grip}	150	mm
Radius gauge section	R	12.5	mm
Velocity grip	v	very low, 0.05, 0.5	m/s

2.2.1 UTM specimen design

In this section, the specimen design for the low strain rate tests is discussed. The design is based on the guidelines provided by ISO 6892-1 (2016) and ASTM E8 (2016) on tensile testing. First the dimensions of the specimen are discussed, followed by deviations from the standard design. Lastly, since the ISO and ASTM standards are defined for quasi-static tests, several studies are discussed that investigated the effect of some of the parameters on strain rate testing.

Mild steel is used as an example in the development of this method. The characteristics of which are given in table 2.1. The specimen dimensions are given in table 2.2 using the parameters as defined in figure 2.2b.

The thickness of the specimen, h, is chosen such that the stress distribution over the thickness is constant. This means inhomogeneous material behaviour at grain level should be avoided so the thickness should be significantly larger than the grain size of the material. This is for mild steel in the order of 10-20 μm as given by ASTM E112-13 (2013). Furthermore, the desire for membrane behaviour rather than bending along with practical considerations such as storage and the mass needed to strain the specimen lead to the thickness of the specimen being chosen as 2 mm.

With the thickness determined, the rest of the parameters are the ones given by the sheet-type standard specimen of the ASTM, except for the grip length, L_{grip}. DIC measurements require that the grip length is longer than the length specified by the guideline, in order to have a sufficient part of the grip section in view of the camera.

Finally, as can be noted in figure 2.2b, a distinction is made between the gauge length and the parallel length. This distinction accounts for the fact that at the start of the parallel section, the stresses are still influenced by the narrowing of the specimen and, hence, a non-uniaxial stress state is obtained. Therefore, a minimum parallel length is required such that the localized strains do not invalidate measurement in the gauge length. For this purpose, Huh et al. (2008) used a servo hydraulic machine for tests of specimens with varying parallel length to determine the best gauge length at strain rates ranging from 0.003 to 200 s^{-1}. The ratio of strain in a certain gauge length to strain over a longer length is compared for different gauge lengths to determine the best gauge length for that parallel length. A careful investigation of their results shows that for all specimens the best gauge length is the parallel length minus 8 mm indicating a zone of influence on each end of 4 mm. Furthermore, as can be observed from figure 2.3, all specimens fail at the same location: 5 mm from either end of the parallel section. This leads to the conclusion that, as long as a sufficiently long gauge length is used, the location of necking is not a function of gauge length. Variation of the gauge length is, therefore, not considered useful. A longer grip section, however, does contribute, since it lowers the ringing amplitude significantly, as was shown by Yang et al. (2014), who investigated ringing in servo-hydraulic machines for strain rates between 10^{-5} and 500 s^{-1}.

2.3 Impact test setup

The experimental setup for the impact test is illustrated in figure 2.4. Strain rates in the range of 10-100 s^{-1} are tested using this setup. A drophead with mass m_d impacts a U-

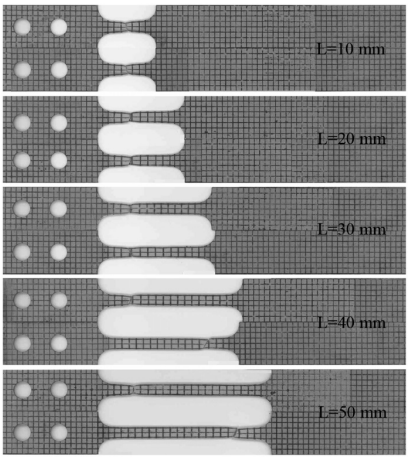

Figure 2.3: Specimens with a variation in gauge section after tensile tests (Source: Huh et al. (2008))

shaped specimen with an initial velocity of v_0, causing the specimen to strain. The specimen is clamped at both ends and the drophead hits the middle section of the specimen. Deformations of the specimen are captured by a 3D DIC system.

2.3.1 Specimen design impact test

While the specimen design for the UTM is defined by standards, this is not the case for the impact test. Furthermore, the proposed test method of testing strain rate using impact tests is not widely used, so limited literature is available. Combine that with strain measurements using Digital Image Correlation (DIC), and the consequence is that no standardised specimen is available and a new specimen design needs to be created. Starting from the design by Chan (2009) and the specimen for the UTM, this section presents the beginnings of a design guide for an impact testing specimen. The specimen design illustrated in figure 2.5 uses the dimensions given in table 2.3.

A thickness h of 2 mm is maintained from the UTM specimen (see table 2.3), along with the values for L_{gauge}, L_c, b_{gauge} and R. Initially, the width of the grip section, which would render the measurement invalid. b_{grip}, was also maintained, but this had to be increased due to plasticity in the grip section. The rest of the dimensions will be used in a parametric study to determine what effect each of them has on the accuracy of the measurements. Parameters which are indicated to be used in the parameter study are still assigned a default value, which is used when that parameter is not varied.

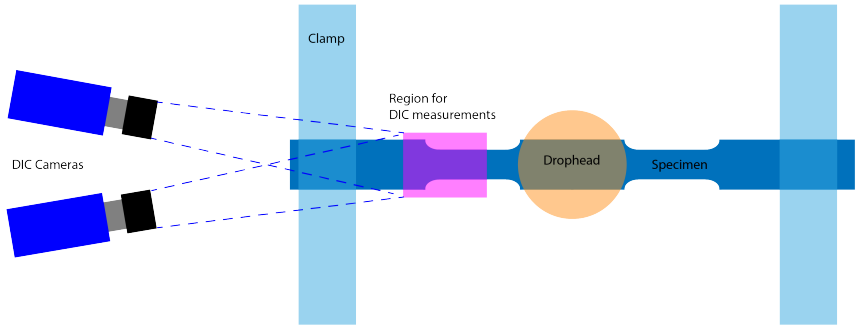

(a) Top-view

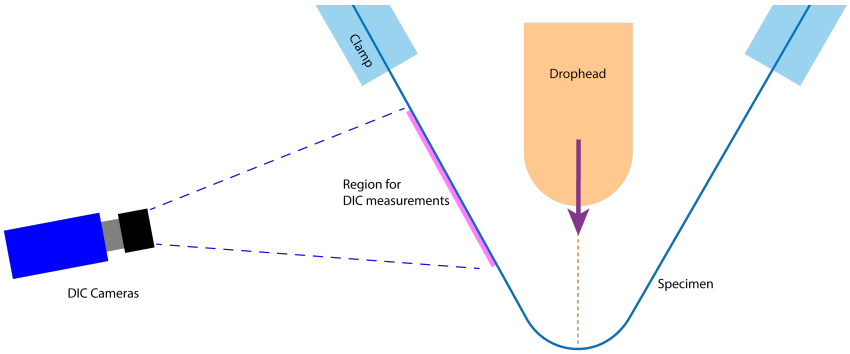

(b) Side-view

Figure 2.4: Impact test setup

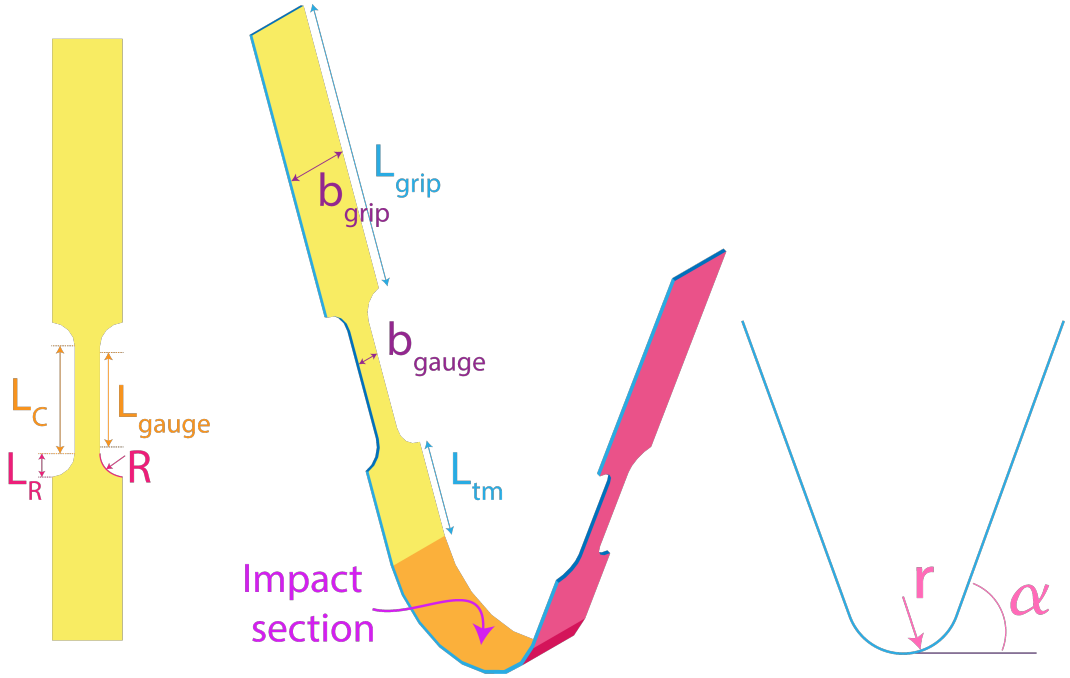

Figure 2.5: Impact test specimen

Table 2.3: Dimensions of impact specimen and drophead

Parameter		Value		Varied?	Range
Specimen					
Thickness	h	2	mm	No	
Width grip section	b_{grip}	35	mm	Yes	20-40
Width gauge section	b_{gauge}	12.5	mm	No	
Parallel length gauge section	L_c	57	mm	No	
Length gauge section	L_{gauge}	50	mm	No	
Length radius	L_R	9	mm	No	
Length toward middle section	L_{tm}	50	mm	Yes	0-450
Length grip section	L_{grip}	150	mm	Yes	50-500
Radius gauge section	R	12.5	mm	No	
Inner radius specimen	r	50	mm	Yes	50-58
Angle dogbone part	α	90	°	Yes	45-90
Drophead					
Mass	m_d	30	kg	Yes	3-50
Radius drophead	r_d	50	mm	No	
Height	L_d	456.4	mm	*	
Velocity on impact	v_0	1.7	m/s	Yes	1.5-6
Position of drophead	dy	0	mm	Yes	0-8

*L_d varies with the mass of the drophead

Chapter 3

Analytical model

An analytical solution can be used as an easy and fast approach to provide a first estimate of the expected stress and strain behaviour in the specimen. It also provides a check for the numerical model in the next chapter. First the approximation of the material model for mild steel is discussed, followed by the analytical models for the UTM setup and the impact test setup. For each setup, the assumptions and simplifications applied to that setup are discussed. Then an analytical equation is given to describe the strain, strain rate and stress in the specimen, which are subsequently used to construct a strain-rate dependent stress-strain curve. The complete derivation of these equations can be found in appendix A. Finally an example is given for each setup.

3.1 Material models

The material of the specimens is mild steel. Figure 3.1a shows the stress-strain curve for the quasi-static case. For the analytical estimate, material model is simplified using two different models. The first considers a perfectly plastic material model neglecting the contribution of the linear elastic part and simplifying the plastic regime to a constant flow stress for all strains. The flow stress, σ_0, is taken as the average of the yield stress and the ultimate stress. The second expands the first model with using a linear plastic material model to account for the effect of strain hardening under the assumption of a linear stress strain curve in the plastic regime between the yield stress and the ultimate stress. The corresponding stress-strain curves are shown in figure 3.1b and figure 3.1c for the perfectly plastic and linear plastic model, respectively. In all cases, the effect of strain rate on the stress-strain curve is accounted for by the Cowper-Symonds relation, as given by equation 1.9.

3.2 Flat specimen

The first case to consider is the setup for the universal testing machine. A regular flat dogbone is clamped on one end and is given a velocity $v(t)$ on the other. For the analytical model, the dogbone specimen is simplified to three rectangles, as is illustrated in figure 3.2. The two

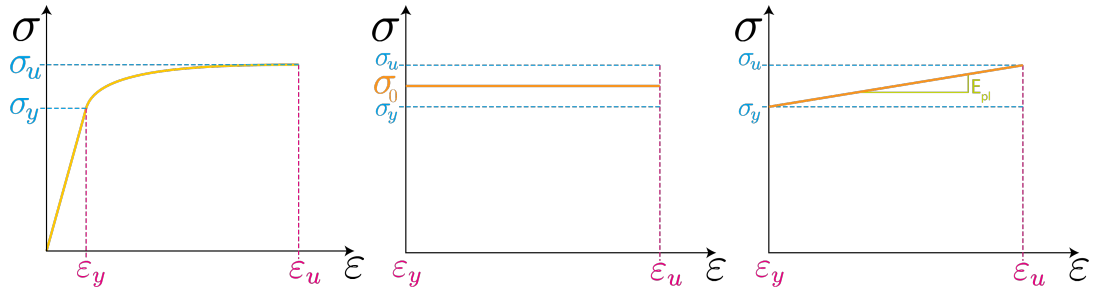

(a) Original **(b)** Perfectly plastic **(c)** Linear plastic

Figure 3.1: Stress-strain curves of material models at $\dot{\varepsilon} \to 0$

grip sections are assumed to be rigid, since the linear elastic strain in these sections is small compared to the plastic strain in the parallel section, L_c.

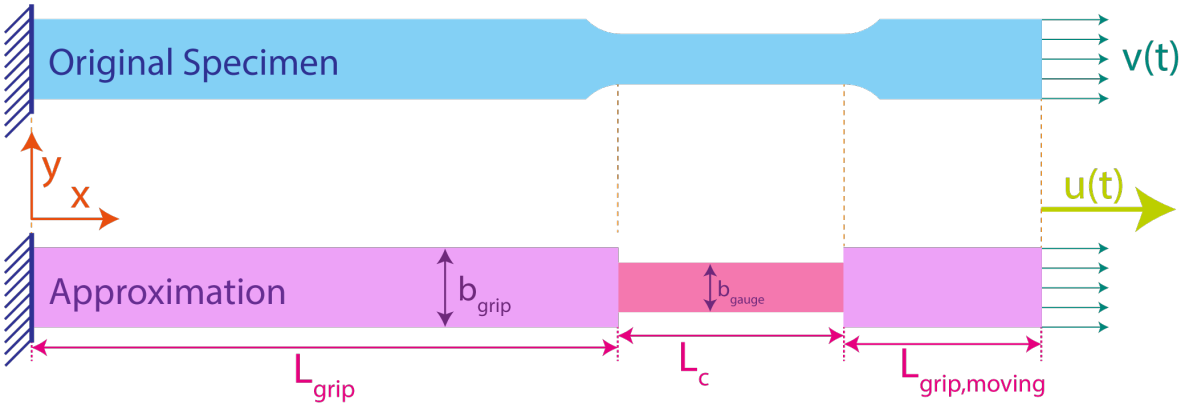

Figure 3.2: Definitions flat specimen

3.2.1 Strain and strain rate

Engineering strain in the parallel section is given by equation 1.4. Since the two grip sections are assumed to be rigid, the difference in length of the parallel section is equal to the displacement of the moving end. The displacement $u(t)$ of the moving end is given by:

$$u(t) = \int v(t)\ \mathrm{d}t \tag{3.1}$$

Where the displacement $u(t)$ in x-direction is the time integral of velocity $v(t)$. The engineering strain is then given by:

$$\varepsilon_e(t) = \frac{u(t)}{L_{c,0}} = \frac{\int v(t)\ \mathrm{d}t}{L_{c,0}} \tag{3.2}$$

in which $\varepsilon_e(t)$ is the engineering strain, $u(t)$ is the displacement of the moving end and $L_{c,0}$ is the initial length of the parallel length. Next, equation 1.5 is used to convert the engineering strain to the true strain. Using equation 1.6, the engineering strain rate is given by:

$$\dot{\varepsilon_e}(t) = \frac{v(t)}{L_{c,0}} \tag{3.3}$$

The engineering strain rate, which is then converted to true strain rate by using equation 1.7.

3.2.2 Stress

After computing the strain, the engineering stress in the gauge section is determined using the perfectly plastic and linear plastic material model, as presented in section 3.1.

Perfectly plastic

In case of a perfectly plastic material model ignoring the effect of strain rate, the engineering stress in the gauge section is always equal to the flow stress, σ_0. However, once equation 1.2 is used to convert the engineering stress to the true and the effect of strain rate is accounted for using the Cowper-Symonds law in equation 1.9, a non-constant stress is obtained, as presented in figure 3.3c and further discussed in section 3.2.3.

Linear plastic

Assuming linear plasticity and ignoring the effects of strain rate, the engineering stress in the parallel section increases linearly with strain:

$$\sigma_e(t) = E_{pl} \cdot \varepsilon_e(t) = E_{pl} \cdot \frac{\int v(t)\ \mathrm{d}t}{L_{c,0}} \tag{3.4}$$

in which σ_e is the engineering stress, E_{pl} is the plastic Young's modulus, $\varepsilon_e(t)$ is the engineering strain and $L_{c,0}$ is the initial length of the parallel length. Similar to the perfectly plastic material model, equation 1.2 is then used to convert the engineering stress to true stress, after which the Cowper-Symonds law in equation 1.9 is used to account for the effect of strain rate.

3.2.3 Example

Figure 3.3 shows an example of the analytical solution for a flat specimen using the parameters given in table 3.1. The engineering and true strain in figure 3.3a show that, as expected, the engineering strain increases linearly, while the true strain deviates slightly. As shown in 3.3b, this is also reflected in the strain rate showing a constant engineering strain rate, because of the constant velocity. The true strain rate, however, decreases as the length of the specimen increases resulting in a lower relative velocity.

The corresponding stress curves for the perfectly plastic and linear plastic analytical solutions are shown in figure 3.3c. As explained, all stress curves are scaled using the Cowper-Symonds law for strain rate. Based on a constant engineering strain rate and perfectly plastic material

behaviour, one would expect the perfectly plastic engineering stress to remain constant. However, the perfectly plastic engineering stress actually decreases slightly as time progresses, as can be seen when comparing the perfectly plastic engineering stress to the constant reference curve. This can be explained by the fact that the Cowper-Symonds law is actually based on the true strain rate instead of the engineering strain rate. Therefore, the decreasing true strain rate in figure 3.3b results in a decreasing perfectly plastic engineering stress.

Furthermore, as can be seen, the difference between the engineering and true stress increases as time progresses. This can be explained by the decreasing cross-sectional area that is accounted for in the true stress and, thus, results in a higher true stress than engineering stress. A similar trend is also shown in the stress-strain curves in figure 3.3d.

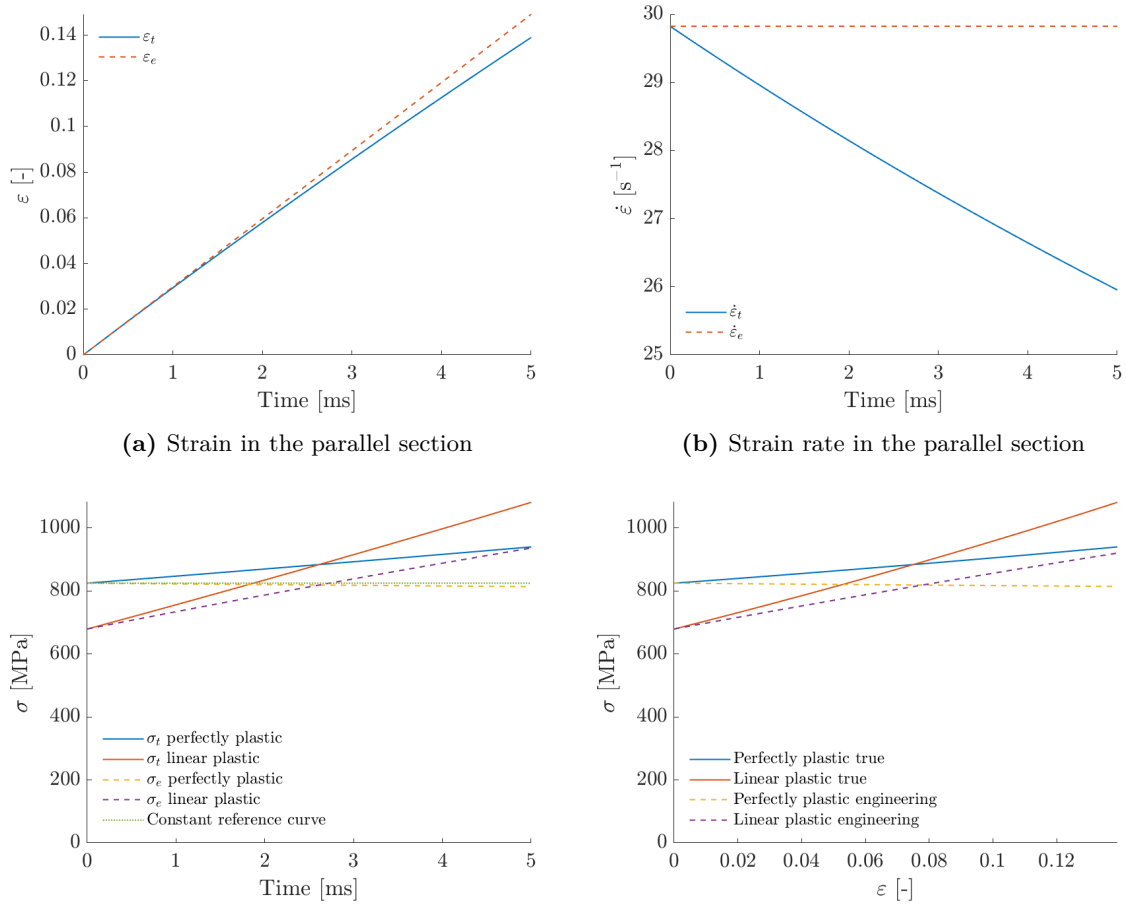

(a) Strain in the parallel section

(b) Strain rate in the parallel section

(c) Stress in the parallel section

(d) Stress-strain curve

Figure 3.3: Plots of flat specimen example

Table 3.1: Parameters used in the analytical solution of a flat specimen

Parameter		Value	
Thickness	h	2	mm
Width grip section	b_{grip}	35	mm
Width gauge section	b_{gauge}	12.5	mm
Length parallel section	$L_{c,0}$	57	mm
Length moving grip section	$L_{grip,moving}$	62	mm
Length clamped grip section	L_{grip}	162	mm
Velocity grip	v	1.7	m/s
Yield stress	σ_y	350	MPa
Ultimate stress	σ_u	500	MPa
Flow stress	σ_0	425	MPa
Plastic Young's modulus	E_{pl}	1000	MPa

3.3 Impact specimen

The setup of the impact test is described in section 2.3. Figure 3.4 illustrates the setup and simplifications for the analytical computations. The top of the specimen is clamped and the middle section (yellow) is impacted by the drophead (green). The dogbone part (blue) is simplified to three rectangles, of which the grip section, L_{grip}, and section towards the middle, L_{tm}, are assumed to be rigid, while the gauge section deforms plastically, similar to the assumptions for the analytical model of the flat specimen. Next, the middle section is also assumed to be rigid such that the displacement of the two dogbones is directly given by the displacement of the drophead, $u_d(t)$, and the angle α. Finally, since the strain is small compared to the total length, the angle α is assumed to stay constant during the deformation.

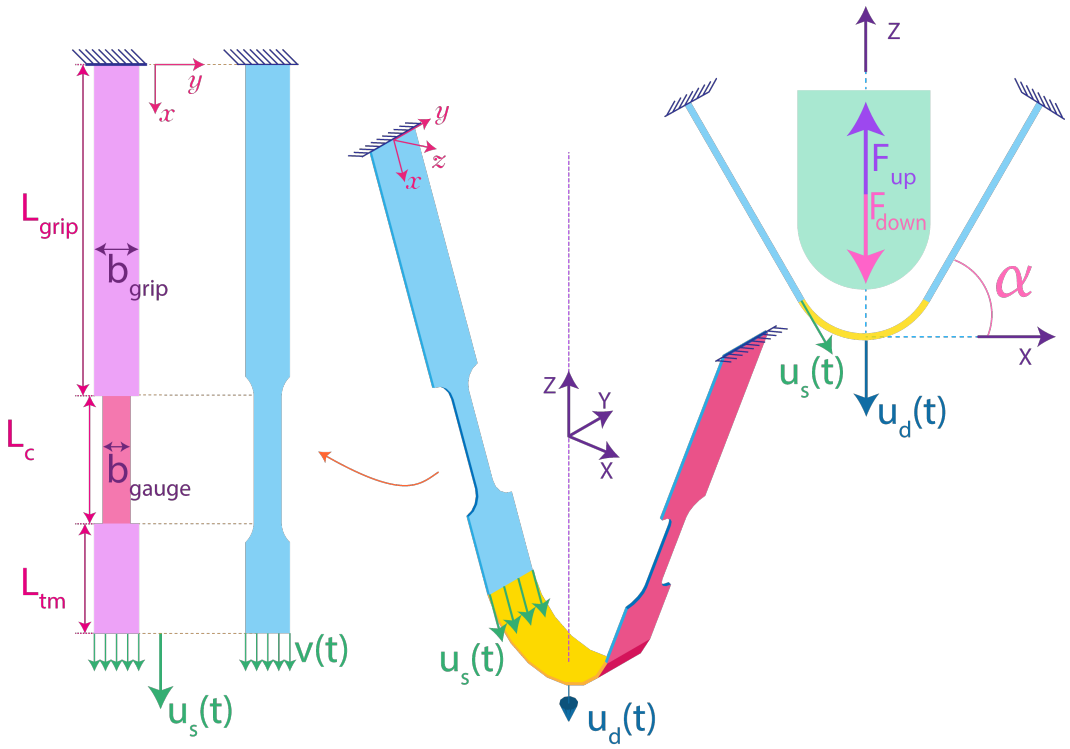

Figure 3.4: Definitions of impact test specimen for analytical model

3.3.1 General equations

For the impact specimen, the displacement of the drophead is linked to the strain of the specimen. Starting with Newton's section law of motion for the drophead:

$$\Sigma F_Z = m_d \cdot \frac{\mathrm{d}^2 u_d(t)}{\mathrm{d}t^2} \tag{3.5}$$

in which ΣF_Z is the sum of the forces in Z-direction, m_d is the mass of the drophead and $u_d(t)$ is the displacement of the drophead in time. Starting the approximations from the

moment the drophead hits the specimen, the effect of gravity is neglected, since its effect on the dynamic behaviour is expected to be small, resulting in:

$$F_{down} = 0 \tag{3.6}$$

That leaves force exerted by the specimen on the drophead:

$$F_{up} = 2 \cdot \sigma_e(t) \cdot A_0 \cdot \sin(\alpha) \tag{3.7}$$

in which F_{up} is the force exerted by the specimen on the drophead, $\sigma_e(t)$ is the engineering stress in the gauge section, A_0 is the initial cross-sectional area in the gauge section of a single dogbone and α is the angle of the dogbone part of the specimen. Combining equations 3.5 and 3.7 relates the stress in the gauge section to the displacement of the drophead:

$$-2 \cdot \sigma_e(t) \cdot A_0 \cdot \sin(\alpha) = m_d \cdot \frac{\mathrm{d}^2 u_d(t)}{\mathrm{d}t^2} \tag{3.8}$$

Stress and strain, and therefore displacement, are related via the material models described in section 3.1.

3.3.2 Perfectly plastic

Integrating equation 3.8 twice, the engineering strain in the gauge section for the perfectly plastic case is given by:

$$\varepsilon_e(t) = -\frac{\sigma_0 \cdot A_0 \cdot t^2}{m_d \cdot L_{c,0}} + \frac{v_0}{L_{c,0} \cdot \sin(\alpha)} \cdot t \tag{3.9}$$

in which $\varepsilon_e(t)$ is the engineering strain, σ_0 is the flow stress, A_0 is the initial cross-sectional area in the gauge section of a single dogbone, α is the angle of the dogbone part of the specimen, $L_{c,0}$ is the initial parallel length of the gauge section, m_d is the mass of the drophead, t is time and v_0 is the impact velocity of the drophead. The complete derivation of this equation is given in appendix A.1. Equation 1.5 is then used to convert the engineering strain to the true strain. Using equation 1.6, the engineering strain rate is given by:

$$\dot{\varepsilon}_e(t) = -\frac{2 \cdot \sigma_0 \cdot A_0 \cdot t}{m_d \cdot L_{c,0}} + \frac{v_0}{L_{c,0} \cdot \sin(\alpha)} \tag{3.10}$$

which can be converted to the true strain rate using equation 1.7. The engineering stress is determined similar to the flat specimen, as was presented in section 3.2.2. Equation 1.2 is then used to convert the engineering stress to true stress, after which the Cowper-Symonds law in equation 1.9 is used to account for the effect of strain rate.

3.3.3 Linear plastic

The engineering strain in the gauge section for the linear plastic case is given by:

$$\varepsilon_e(t) = -\frac{\sigma_y}{E_{pl}} + \frac{v_0 \cdot \sqrt{m_d}}{\sin(\alpha) \cdot \sqrt{L_{c,0} \cdot E_{pl} \cdot 2 \cdot A_0}} \sin\left(\sqrt{\frac{E_{pl} \cdot 2 \cdot A_0}{L_{c,0} \cdot m_d}} \cdot t\right) + \frac{\sigma_y}{E_{pl}} \cos\left(\sqrt{\frac{E_{pl} \cdot 2 \cdot A_0}{L_{c,0} \cdot m_d}} \cdot t\right) \tag{3.11}$$

in which $\varepsilon_e(t)$ is the engineering strain, σ_y is the yield stress, E_{pl} is the plastic Young's modulus, v_0 is the impact velocity of the drophead, $L_{c,0}$ is the initial parallel length of the gauge section, A_0 is the initial cross-sectional area in the gauge section of a single dogbone, α is the angle of the dogbone part of the specimen, m_d is the mass of the drophead and t is time. The complete derivation of this equation is given in appendix A.1. Equation 1.5 is then used to convert the engineering strain to the true strain. Using equation 1.6, the engineering strain rate is given by:

$$\dot{\varepsilon}_e(t) = \frac{v_0}{L_{c,0} \cdot \sin(\alpha)} \cos\left(\sqrt{\frac{2 \cdot E_{pl} \cdot A_0}{L_{c,0} \cdot m_d}} \cdot t\right) - \frac{\sigma_y}{\sqrt{E_{pl}}} \sqrt{\frac{2 \cdot A_0}{L_{c,0} \cdot m_d}} \sin\left(\sqrt{\frac{2 \cdot E_{pl} \cdot A_0}{L_{c,0} \cdot m_d}} \cdot t\right) \tag{3.12}$$

which can be converted to the true strain rate using equation 1.7. The engineering stress is determined similar to the flat specimen, as was presented in section 3.2.2. Finally, equation 1.2 is then used to convert the engineering stress to true stress, after which the Cowper-Symonds law in equation 1.9 is used to account for the effect of strain rate.

3.3.4 Example

Figure 3.5 shows an example of the analytical solution for an impact specimen using the parameters given in table 3.2. First of all, it can be seen that unlike the example of the flat specimen, the true and engineering curves are almost equal. This can be explained by the decreasing velocity of the drophead as time progresses, as shown in figure 3.5a, resulting in a significantly smaller strain in the specimen and, thus, a smaller difference between engineering and true strain. A similar conclusion can be drawn when looking at the strain rate in figure 3.5c, showing an almost equal true and engineering strain rate.

Furthermore, velocity and strain rate decrease faster for the perfectly plastic solution, because the force exerted on the drophead by the specimen is initially larger than for the linear plastic solution. This can be explained by the definition of the perfectly plastic stress, σ_0, in the perfectly plastic material model, which is larger than the yield stress of the material, thus resulting in a larger exerted initial force. However, as expected, as time progresses, the difference between the perfectly plastic and linear plastic solution reduces, because of the strain hardening present in the linear plastic model.

This also explains the difference in the stress and stress-strain curves shown in figure 3.5d and figure 3.5e. The perfectly plastic solution initially shows a higher stress after which the difference decreases, because of the strain hardening in the linear plastic solution. Note that both solutions show a decreasing stress related to a decrease in strain rate.

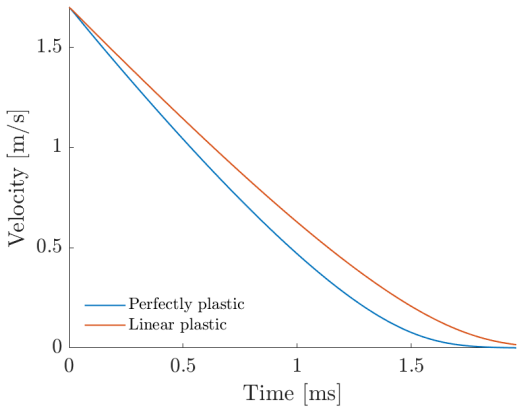

(a) Velocity of the drophead

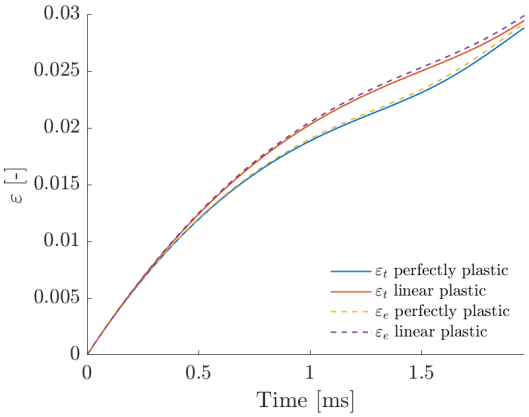

(b) Strain in the parallel section

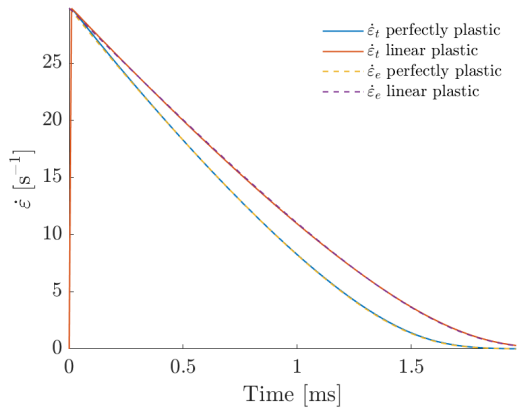

(c) Strain rate in the parallel section

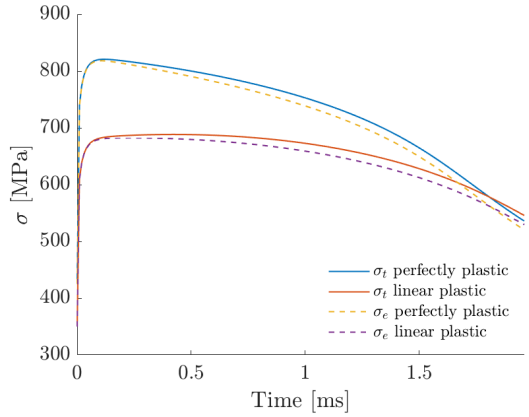

(d) Stress in the parallel section

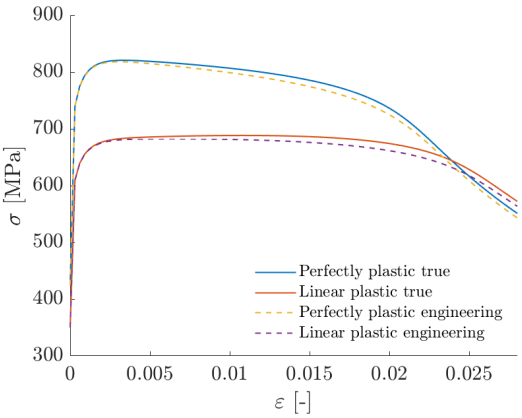

(e) Stress-strain curve in the parallel section

Figure 3.5: Plots of impact specimen

Table 3.2: Parameters used in the analytical solution of an impact specimen

Parameter		Value	
Thickness	h	2	mm
Width grip section	b_{grip}	35	mm
Width gauge section	b_{gauge}	12.5	mm
Total cross-sectional area gauge section	A_0	50	mm^2
Parallel length gauge section	$L_{c,0}$	57	mm
Length grip section	L_{grip}	150	mm
Length toward middle section	L_{tm}	50	mm
Angle dogbone part	α	90	°
Mass of drophead	m_d	30	kg
Velocity on impact	v_0	1.7	m/s
Yield stress	σ_y	350	MPa
Ultimate stress	σ_u	500	MPa
Flow stress	σ_0	425	MPa
Plastic Young's modulus	E_{pl}	1000	MPa

Chapter 4

Finite element analysis

In the analytical model from the previous chapter, some assumptions were made to simplify the calculations. These include a simplified material model, which does not take linear elasticity into account, the assumption of rigid grip and impact sections, and the assumption of homogeneous stress and strain fields in the specimen. In reality though, these simplifications do not hold. To accurately predict the experiment, numerical simulations are used. In this chapter, a numerical simulation of the impact test using the finite element method (FEM) is described. The chapter consists of four parts. The first describes what type of analysis is used. The second describes the actual modelling of the experiment in the finite element package Abaqus, followed by the explanation of the post-processing of the numerical results in the third section. Finally, the fourth addresses some modelling considerations in the definition of the FE model.

4.1 Type of analysis

Numerical modelling of the experiment is done using the program Abaqus 2018. To determine what type of analysis is typically used for these types of problems, the following aspects are taken into account: elastic and plastic behaviour with a strain rate dependency in the material model lead to material non-linearity. Contact non-linearity is caused by the impact of the drophead on the specimen. The last type of non-linearity is geometric, because large deformations are present. Given the short timespan of the impact, an explicit analysis is used for a stable solution. Finally, the presence of vibrations caused by the impact requires a dynamic analysis. All in all, this experiment requires an explicit, dynamic, non-linear impact analysis.

4.2 Modelling

The creation of an FEA model in Abaqus and corresponding modelling considerations are discussed in this section. Since the analysis is used to run a parametric study, a large number of models is required. Python scripts are employed to generate models and input files for

the parametric study. An example of one of the scripts can be found in appendix B and an example of an input file can be found in appendix C.

4.2.1 Specimen

The specimen is modelled using thin shell elements (S4R), since transverse shear effects are expected to be small, because of the small thickness of the specimen. According to the Abaqus manual (Dassault Systèmes Simulia Corp, 2017): "S4R is a 4-node, quadrilateral, stress/displacement shell element with reduced integration and a large-strain formulation." This means element type S4R can handle large strains and reduced integration saves running time, while maintaining accuracy, provided that the elements are not loaded in in-plane bending, which is not to be expected for the proposed test method. The shells are given a shell thickness, h, with the middle as reference surface. This means that the radius of the curved middle part of the specimen needs to be modelled as $r + h/2$ instead of only the specimen inner radius, r. This is illustrated in figure 4.1 with the purple arrow indicating r and the magenta indicating $r + h/2$.

A mesh convergence study on stress, strain and strain rate to determine the number of elements across the width of the specimen was done, resulting in 16 elements across the width of the specimen. The mesh for one of the specimens is given in figure 4.2. Also indicated in this figure are the reference nodes (in red), two in the grip section and two in the gauge section. For these nodes, displacements are recorded which are post-processed as if they were DIC measurements. The exact procedure of this is discussed in section 4.3. Right in the middle of a nodes pair is a node, that is part of four elements (in blue), for which strain, strain rate and stress are recorded. These are later used for comparison to the post-processed displacements.

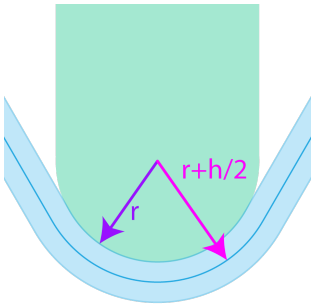

Figure 4.1: Shell thickness and the radius of the specimen

4.2.2 Drophead

The drophead is a solid steel hemisphere with a cylinder on top, both with a radius of r_d. In order to investigate the simplification of modelling the drophead as a rigid, two options have been investigated: an analytical rigid and a 3D deformable drophead. The corresponding results are presented and discussed in section 4.4.2.

The analytical rigid is illustrated in figure 4.3a. A reference point P_d is created on the

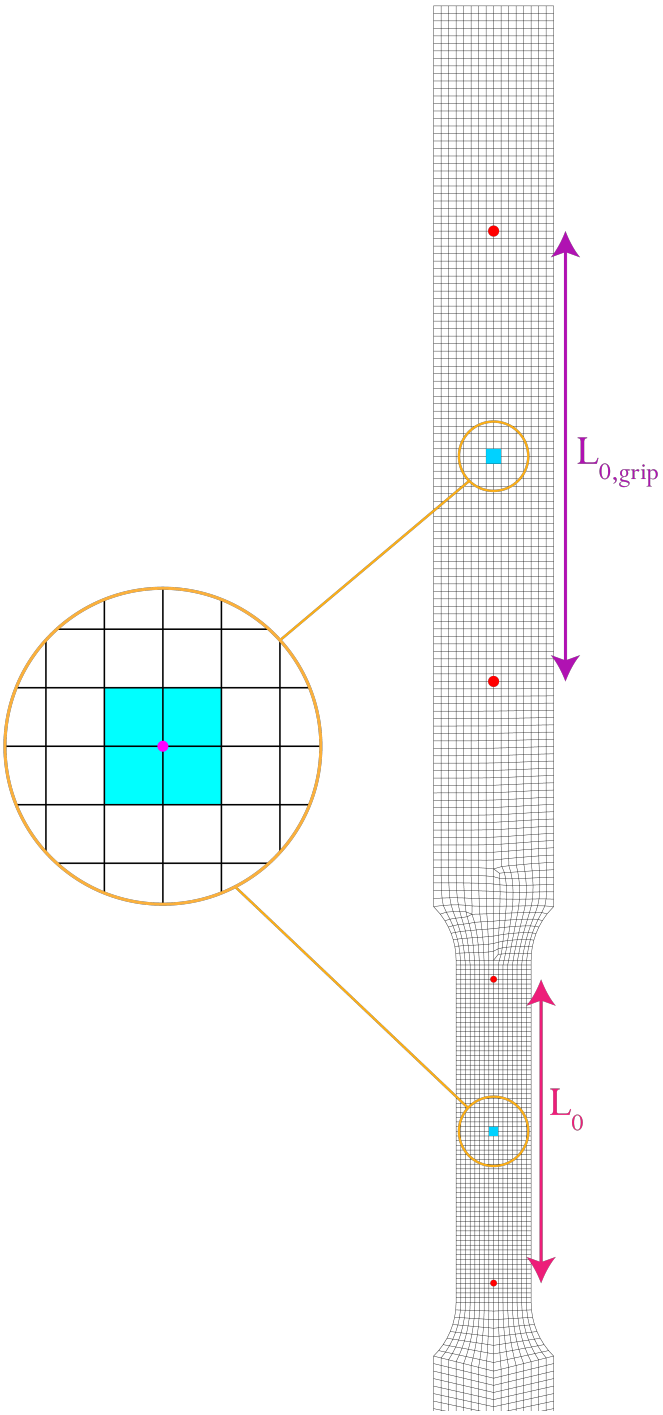

Figure 4.2: Specimen mesh with reference nodes (red) and middle elements (blue) around the middle node (pink)

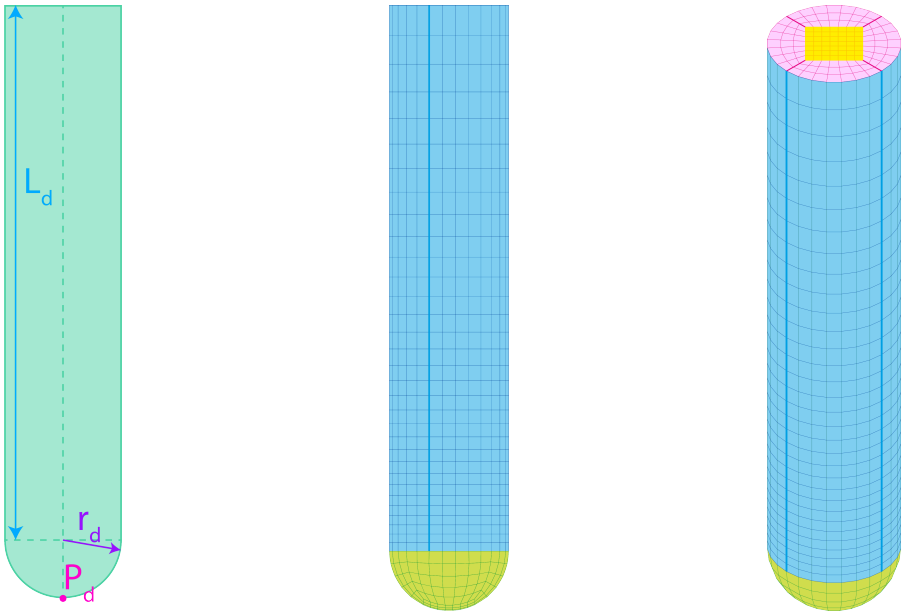

(a) Rigid drophead **(b)** Deformable drophead **(c)** Deformable drophead

Figure 4.3: FEA model of the drophead

bottom to record the movements and control the placement on the specimen. The mass of the drophead m_d is assigned as a point mass in this reference point. Combined with the density and radius, the mass is used to determine the height of the drophead, L_d. This formulation for the drophead is used in the entire thesis unless explicitly stated otherwise.

The same geometry is used to create the deformable drophead using solid 8-node linear brick elements (C3D8), which is illustrated in figure 4.3b. The material of the drophead is the same mild steel as the specimen. A mesh convergence study to determine the mesh size was done on displacement of the drophead and stress, strain and strain rate in the specimen. This resulted in the mesh shown in figures 4.3b and 4.3c for a drophead with a radius of 50 mm and weight of 30 kg. Note that the mesh size varies along the blue lines, from a fine mesh close to the specimen to a coarse mesh towards the top of the drophead.

4.2.3 Complete setup

The complete setup combines the drophead and specimen in to a single setup with boundary conditions, as is illustrated in figure 4.4a. The boundary conditions are taken from the experimental setup. Indicated in orange is the top of the specimen that is clamped at both sides. Rotation of the drophead is constrained in all directions and translation is constricted in x- and y-direction such that the drophead can only translate in z-direction, which is indicated in magenta. Gravity is not modelled, as this is a static load and does not affect the dynamic behaviour of the specimen. The drophead is given an initial velocity v_0 and is positioned on such short distance from the specimen that the effect of gravity on the velocity is negligible. The position of the drophead relative to the specimen is illustrated in figure 4.4b, in which dy is the horizontal and dz is vertical distance from the centre of the specimen.

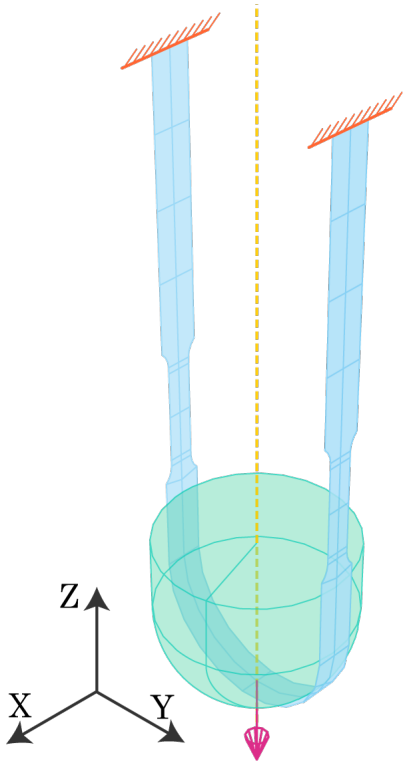

(a) FEA model with boundary conditions

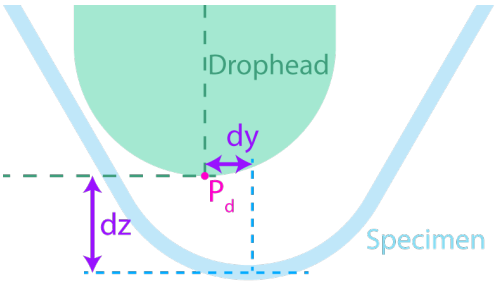

(b) Drophead alignment relative to the specimen

Figure 4.4: Complete setup in FEA

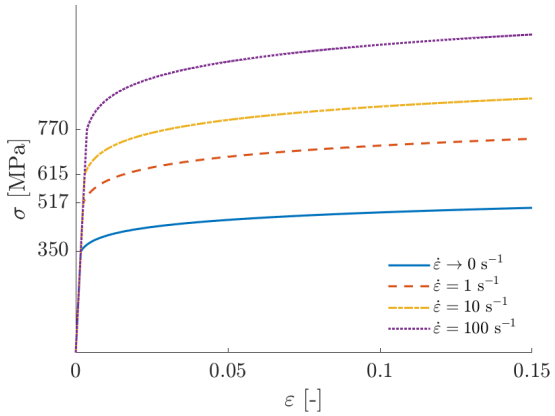

Figure 4.5: Stress-strain curves used as input for FEA

4.2.4 Material model

The material model for steel is the source of two non-linearities, plasticity and strain rate dependency. The plastic behaviour is based on the power law approximation mentioned in section 1.3.4. The input stress-strain curve given in figure 4.5 is a curve-fit through $\sigma_y = 350$ MPa and $\sigma_u = 500$ MPa at $\varepsilon_u = 0.15$. The strain rate dependency is implemented with Cowper-Symonds coefficients, as mentioned in section 1.4. For steel: $D = 40.4$ s^{-1} and $q = 5$ (Cowper and Symonds, 1957). Furthermore, a Young's modulus of 210 GPa is used and a density of 7800 kg/m^3. Note that this material model does not account for failure.

Strain rate factor

Strain rate dependency in the material model might introduce "non-physical high-frequency oscillations in an explicit dynamic analysis" (Dassault Systèmes Simulia Corp, 2017). In Abaqus, this is overcome by calculating the plastic strain rate in the current time step according to Dassault Systèmes Simulia Corp (2017):

$$\dot{\bar{\varepsilon}}_{pl}\big|_{t+\Delta t} = \omega \frac{\Delta \bar{\varepsilon}_{pl}}{\Delta t} + (1-\omega)\, \dot{\bar{\varepsilon}}_{pl}\big|_{t} \tag{4.1}$$

Where the $\Delta\bar{\varepsilon}_{pl}$ is the incremental change in equivalent plastic strain during the time increment Δt and $\dot{\bar{\varepsilon}}_{pl}\big|_t$ and $\dot{\bar{\varepsilon}}_{pl}\big|_{t+\Delta t}$ are the strain rates at the beginning and end of the increment, respectively. The factor ω $(0 < \omega \leq 1)$ facilitates filtering high-frequency oscillations associated with strain-rate-dependent material behaviour. After parametric study on strain rate using strain rate factors from 0.1 to 0.9 in steps of 0.1, the strain rate factor ω is determined at 0.3. Determination of the strain rate factor is in further detail discussed in chapter 4.4.1.

4.2.5 Contact

Since the drophead impacts the specimen, a contact definition is needed. It stipulates that the drophead can deform the specimen, but not vice versa in the case of the analytical rigid.

Furthermore, the drophead will not stick to the specimen, which means it will move back up after impact. Finite sliding is used to force the software to constantly check which part of the drophead interacts with which nodes of the specimen. Normal contact behaviour is included by using the 'hard' contact formulation in Abaqus (equivalent to an infinite penalty stiffness). Tangential contact behaviour, i.e. friction, can be added in the form of penalty friction with a friction coefficient, f_c. The assumption is that the static friction is overcome by the impact such that the friction coefficient represents the sliding friction. Typical values of steel on steel sliding friction coefficients are approximately 0.4 for dry surfaces and 0.05 for greasy surfaces, but these values may vary greatly depending on the situation (Meriam et al., 2003). The effect of the friction coefficient is discussed in further detail in section 4.4.3.

When using the deformable drophead, care should be taken with the mesh size of the drophead compared to the mesh size of the specimen in the area of contact. In the current implementation in Abaqus, the drophead was selected as master surface and the specimen as slave surface. As a consequence the drophead should have a larger mesh size than the specimen. Otherwise the master-slave relation should be reversed.

4.2.6 Output

The output given for each simulation consists of displacements of the points indicated in section 4.2.1. Furthermore, strains, strain rate and in-plane axial stresses are recorded for the middle elements. Each of the two sets of middle elements share a single node in the middle of the set. The average of the recorded data in all four elements represents the data in that middle node. The strain, strain rate and stress of this node are then compared to the post-processed displacement. As mentioned in the previous section, non-physical high frequency oscillations might occur in the strain rate. An anti-aliasing filter on the strain rate output smooths the data by excluding these high frequency data. In this case the cut-off frequency is the history output frequency of 10^5 Hz. This is the highest frequency where the cut-off frequency hardly affect the measurement data but only smooths it. The rest of the data does not require the anti-aliasing filter, so it is not used.

4.3 Post-processing

Post-processing of the numerical simulations is done in three steps. First the relevant part of the experiment has to be determined. Then strain, strain rate and stress are calculated using the displacements found by the FE software as if it were DIC measurement data. Finally, these 'measurement data' are compared to the corresponding output data from Abaqus to assess their accuracy. The base specimen from section 2.3.1 is used as an example to show the post-processed results. Results of the parameter study are discussed in the results chapter.

4.3.1 Measurement time

Measurement time is the timespan of the relevant part of the experiment. That is when the gauge starts straining until drophead reaches zero velocity. The same total time has been

used for each numerical simulation, but a different velocity or mass of the drophead will result in zero velocity at a different time, so the measurement time needs to be determined in post-processing. Figure 4.6, for example, shows the different measurement times for two simulations. The blue dotted line shows the complete simulation time and the red line shows the measurement time. The beginning is marked with the magenta arrow and the end is marked with the green arrow. The simulations with a shorter measurement time will, as a result, have less data points than simulations with a longer measurement time. The measurement time is used in linking stress to strain for the stress-strain curve, for the determination of the average strain rate, to determine whether the specimen can reach dynamic equilibrium and to estimate the requirements on DIC systems.

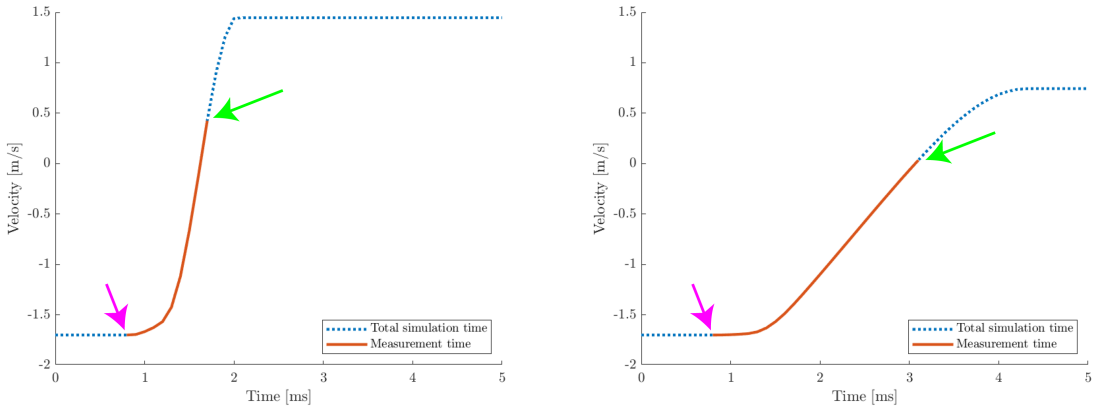

(a) $v_0 = 1.7$ m/s and $m_d = 3$ kg **(b)** $v_0 = 1.7$ m/s and $m_d = 30$ kg

Figure 4.6: Differences in measurement times for different experiments

4.3.2 Strain

The relative distance between two reference points is used to determine the strain. At time t, the engineering strain ε_e between points p at $(x_p(t), y_p(t))$ and q at $(x_q(t), y_q(t))$ in the x-y-plane is given by:

$$\varepsilon_e(t) = \frac{L(t) - L_0}{L_0} = \frac{\sqrt{\left(x_p(t) - x_q(t)\right)^2 + \left(y_p(t) - y_q(t)\right)^2} - \sqrt{\left(x_p(0) - x_q(0)\right)^2 + \left(y_p(0) - y_q(0)\right)^2}}{\sqrt{\left(x_p(0) - x_q(0)\right)^2 + \left(y_p(0) - y_q(0)\right)^2}} \tag{4.2}$$

in which the engineering strain ε_e is a function of the distance $L(t)$ between the points at time t, and L_0, the initial distance. Both are given by the location (x, y) of each point. The engineering strain is then converted to true strain by using equation 1.5.

Displacements of the reference points in the grip and gauge section are used to determine the strain in those sections. In figure 4.7, an example of the measurements compared to the in-plane membrane strain given by FEA is given for both grip and gauge section. In principle,

these should of course be equal, but when they are not, it indicates a non-uniform strain in either the grip or gauge section depending on which shows the error. This can, for example, be caused by bending waves, stress waves, or necking.

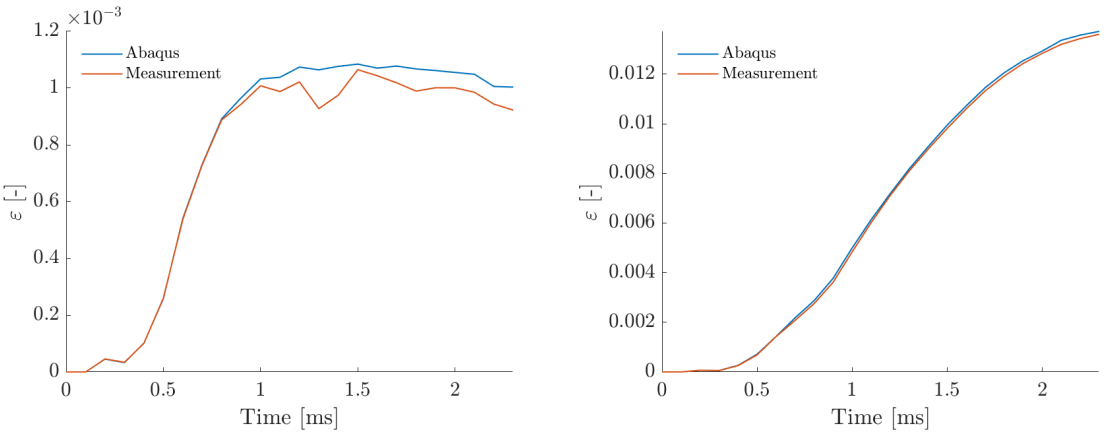

(a) Grip section **(b)** Gauge section

Figure 4.7: True strain comparison for $v_0 = 1.7$ m/s and $m_d = 30$ kg

4.3.3 Strain rate

Once the strain has been determined as described above, the strain rate is calculated by taking the numerical derivative. The central difference method is used to take the numerical derivative:

$$\dot{\varepsilon}_e(t) = \frac{\varepsilon(t + \delta t) - \varepsilon(t - \delta t)}{2\delta t} \tag{4.3}$$

in which the strain rate $\dot{\varepsilon}$ at time t is a function of time step δt and the strain ε at times $(t + \delta t)$, and $(t - \delta t)$. The engineering strain rate is then converted to true strain rate by using equation 1.7.

The average strain rate over the measurement time is also determined such that a stress-strain curve with an assumed constant strain rate can be constructed, which can be compared to the measured stress-strain curve. The average is taken from the strain rate as given in the Abaqus output. Figure 4.8 depicts an example of these three strain rates: the numerical derivative as 'Measurement', strain rate as given in the Abaqus output as 'Abaqus' and the average of the latter as 'Abaqus average'.

4.3.4 Stress

Grip

Engineering stress in the grip section is determined in four ways. One uses the stress as directly obtained from Abaqus (represented by 'Abaqus' in figure 4.9a), two apply Hooke's

law and one applies force equilibrium. Note that for comparison to FE results, all engineering stresses are converted to true stress using equation 1.2.

For Hooke's law to apply, the grip section should stay within the linear elastic regime. If that is the case, strain can directly be converted to stress. The strain in the grip section is available through the measurements and directly as Abaqus output, as previously mentioned. This results in two different methods to determine the stress in the grip section, which are shown as 'Measurement' and 'Abaqus ε' respectively in figure 4.9a. In principle these should of course be equal, so when they are not, this is an indication that the strains obtained through the measurements and directly as Abaqus output are not equal and one should further investigate the difference in strain, as discussed in section 4.3.2.

The last method to determine stress assumes force equilibrium in the grip section and an even stress distribution in the gauge section. This method is described by Rusinek et al. (2008), where it is used as measure for the global material behaviour in the comparison of local to global material behaviour to determine the best location for a strain gauge. The nominal stress σ is determined by dividing force F in the cross section over the cross-sectional area A_0, as given in equation 1.1, where F is determined by the sum of the nodal reaction forces at the top of the specimen in the direction of the specimen. This stress is shown as 'Abaqus F' in figure 4.9.

In case 'Abaqus ε' is not equal to 'Abaqus', Hooke's law apparently no longer applies, thus indicating plasticity in the grip section. In case 'Abaqus F' is not equal to 'Abaqus', the nominal stress in the grip section differs from the local stress in the middle of the grip section. This can either indicate a stress concentration is present or dynamic equilibrium has not been reached.

Gauge

Similar to the stress in the grip section, the engineering stress in the gauge section is also determined in four ways. First of all, the stress is directly obtained from Abaqus, as represented by 'Abaqus' in figure 4.9b. Secondly, three different methods of force equilibrium are used, since the presence of plasticity in the gauge section makes direct conversion of strain into stress by Hooke's law invalid, while force equilibrium still holds. For comparison to FE results, all engineering stresses are converted to true stress using equation 1.2.

The first method of applying force equilibrium scales the stress in the gauge section from the stress in the grip section, as given by the following equation:

$$\sigma_{gauge} = \frac{\sigma_{grip} b_{grip}}{b_{gauge}} \tag{4.4}$$

in which σ is the stress and b is the width in the indicated section. Since the stress in the grip section is available for both the measurements and directly from the Abaqus output, this yields two results for the stress in the gauge section, as shown by 'Measurement' and 'Abaqus σ_{grip}', respectively, in figure 4.9b. In principle, these should of course be equal, so when they are not, it is an indication that the two results for stress in the grip are not equal and the investigation should be continued in the grip section.

Finally, 'Abaqus F' is determined using the same method as for the grip section, but using the cross-sectional area of the gauge section.

In case 'Abaqus F' is not equal to 'Abaqus', the same holds as for the grip section; the nominal stress in the grip section differs from the local stress in the middle of the gauge section, thus indicating either a stress concentration or that dynamic equilibrium has not been reached.

4.3.5 Stress-strain curve

The stress-strain curves given in figure 4.10 as 'Measurement' are a combination of the stress and strain in the gauge section found by measurement. The same holds for the curve called 'Abaqus', which is comprised of the stress and strain in the gauge section as obtained directly from the Abaqus output. The two curves called 'Reference' scale the input stress-strain curve from the material model using the Cowper-Symonds law given in equation 1.9. The expectation is that one of these can be reconstructed by combining stress and strain to a stress-strain curve. 'Reference $\dot{\varepsilon} = \mathrm{C}$' uses the average strain rate to scale the entire curve at once and 'Reference $\dot{\varepsilon} \neq \mathrm{C}$' uses the measured strain rate to determine the scaling for each data point.

4.3.6 Objective functions

This section will explain the criteria that are used to evaluate parameters in the parameter study. An objective function is a single parameter that helps in judging the accuracy of a model. In the case of strain and stress, the difference between measurements and FEA output is used to determine accuracy of the measurements. It is important to know that, although FEA is treated as giving true results, it is still a simulation. This means that FEA can also be wrong and results should be treated with caution.

That said, the objective function for strain and stress in time, given in equation 4.5, is defined by average deviation of the measurement from the FEA output given in %. The objective functions in equation 4.5 require the number of data points to be taken at the exact same points in time.

$$\varsigma_\sigma[\%] = \frac{\sum_{i=1}^{N} \left(\left| \sigma_m(t(i)) - \sigma_{abq}(t(i)) \right| \right)}{\sum_{i=1}^{N} \sigma_{abq}(t(i))} \cdot 100\% \tag{4.5}$$

$$\varsigma_\varepsilon[\%] = \frac{\sum_{i=1}^{N} \left(\left| \varepsilon_m(t(i)) - \varepsilon_{abq}(t(i)) \right| \right)}{\sum_{i=1}^{N} \varepsilon_{abq}(t(i))} \cdot 100\%$$

in which the average deviation ς_σ is a percentage, N is the number of data points, ε_m and

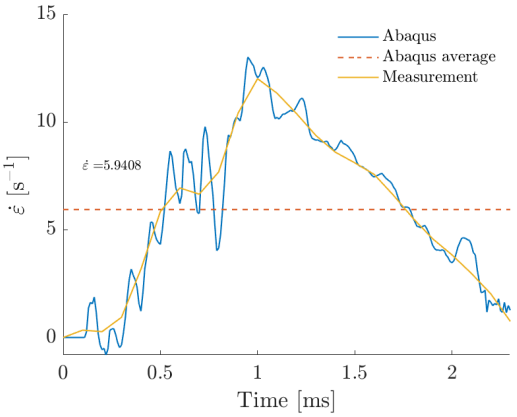

Figure 4.8: Strain rate comparison in the gauge section for $v_0 = 1.7$ m/s and $m_d = 30$ kg

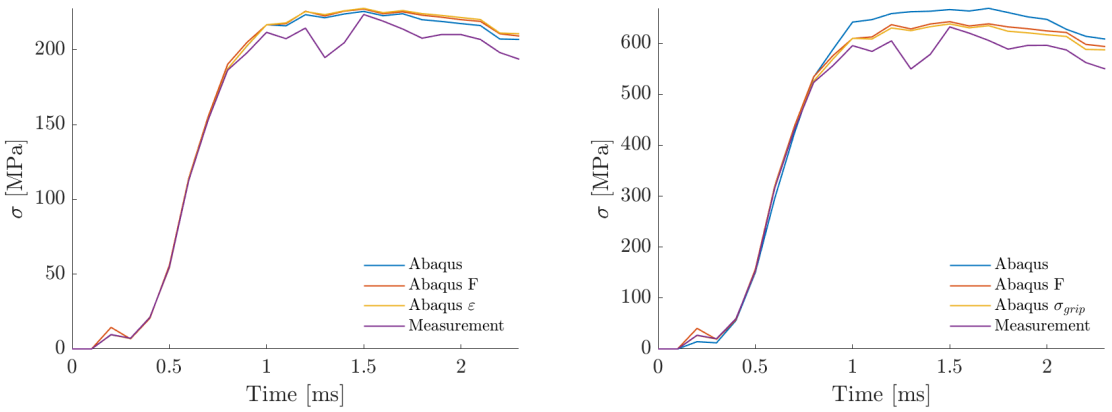

(a) Grip section **(b)** Gauge section

Figure 4.9: Stress comparison for $v_0 = 1.7$ m/s and $m_d = 30$ kg

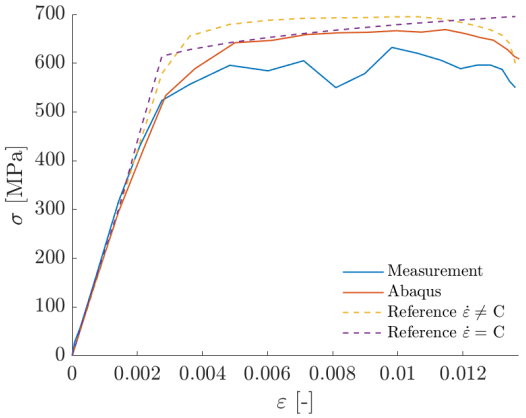

Figure 4.10: Stress strain curve comparison for $v_0 = 1.7$ m/s and $m_d = 30$ kg

σ_m are the measurement strain and stress and, ε_{abq} and σ_{abq} are the in-plane strain and membrane stress from Abaqus.

The first objective function for the stress-strain curve, given in equation 4.6, combines the objective functions for stress and strain in the gauge section to determine the best overall specimen. In order to mitigate the effect an outlier might have, the squared difference is added to the sum of these two objective functions squared.

$$\varsigma_{abq}[\%] = \sqrt{\varsigma_\sigma^2 + \varsigma_\varepsilon^2} \tag{4.6}$$

The second objective relates the measured stress-strain curve to the input curve. Two stress-strain curves are constructed at the exact same strain intervals as the measured stress-strain curve, as mentioned in the previous section. The deviation is determined accordingly for both of these curves using the same method as stress and strain:

$$\varsigma_{\sigma\varepsilon}[\%] = \frac{\sum_{i=1}^{N} \left(\left| \sigma_m(\varepsilon_m(i)) - \sigma_{\dot{\varepsilon}}(\varepsilon_m(i)) \right| \right)}{\sum_{i=1}^{N} \sigma_{\dot{\varepsilon}}(\varepsilon_m(i))} \cdot 100\% \tag{4.7}$$

in which the average deviation $\varsigma_{\sigma\varepsilon}$ is a percentage, N is the number of data points, $\sigma_m(i)$ is the stress at strain $\varepsilon_m(i)$ and $\sigma_{\dot{\varepsilon}}(i)$ is the stress of the input curve ($\dot{\varepsilon} \neq$ C) at the same $\varepsilon_m(i)$.

4.4 Modelling considerations

This section discusses several modelling considerations and parameter choices that were made in creating the finite element model for the impact test and their impact on the results.

4.4.1 Determination of the strain rate factor

As discussed in section 4.2.4, the strain rate factor is a factor used by Abaqus to combat non-physical high-frequency oscillations introduced by the numerical simulation of strain rate dependency in the material. The default strain rate factor used by Abaqus is 0.9. This is, for example, used in the simulation results shown in figure 4.11a, in which the stress-strain curve obtained directly from Abaqus is compared to the input material data at various strain rates. In this case and for every other simulation with a strain rate factor of 0.9 in a set of varying specimen dimensions, drophead mass and drophead velocity, the stress-strain curve matches the case of the quasi-static input curve, marked as 'Reference $\dot{\varepsilon} \rightarrow 0$', indicating that the strain rate dependency of the material model is not properly accounted for in the simulation. Based on the non-zero strain rate curve in figure 4.11b, the stress-strain curve from Abaqus should be close to the stress-strain curve obtained from the material model for either the average strain rate, marked as 'Reference, $\dot{\varepsilon} = C$' or the instantaneous strain rate, marked as 'Reference, $\dot{\varepsilon} \neq C$'.

In order to investigate the influence of the strain rate factor on this error, various simulations have been done for strain rate factors ranging from 0.1 to 0.9 in steps of 0.1. An example of the resulting stress-strain curves at various strain rate factors is shown in figure 4.12, which shows that lower strain rate factors indeed result in a better match between the scaled input curves and the stress-strain curve.

The next step is to determine what strain rate factor should be used for the simulations in the parametric study. To this end, the analytical model from the previous section for the narrow gauge section is used. The resulting comparison for various strain rate factors is shown in figure 4.13. As can be seen, the best match is found for strain rate factors in the range of 0.1-0.5. In order to narrow down this range, finally, a strain rate convergence study is done. Figure 4.14a shows an example of the strain rate as determined by Abaqus for a single experiment at various strain rate factors, while figure 4.14b shows a plot of the average strain rate versus strain rate factor for various experiments. Based on these results 0.3 is determined to be the best strain rate factor to use in the simulations.

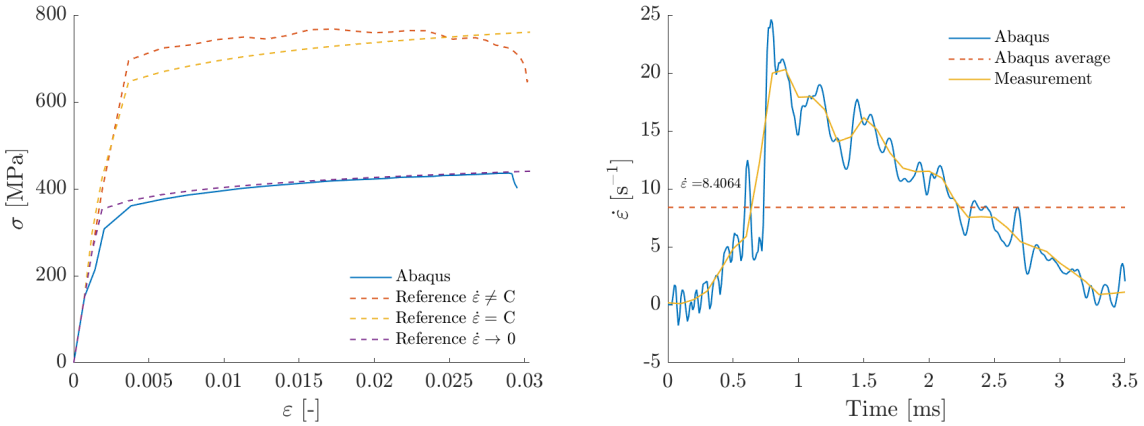

(a) Stress-strain curve **(b)** Strain rate curve

Figure 4.11: Stress-strain curve and strain rate curve for a strain rate factor of 0.9, where $v_0 = 1.5$ m/s and $m_d = 40$ kg

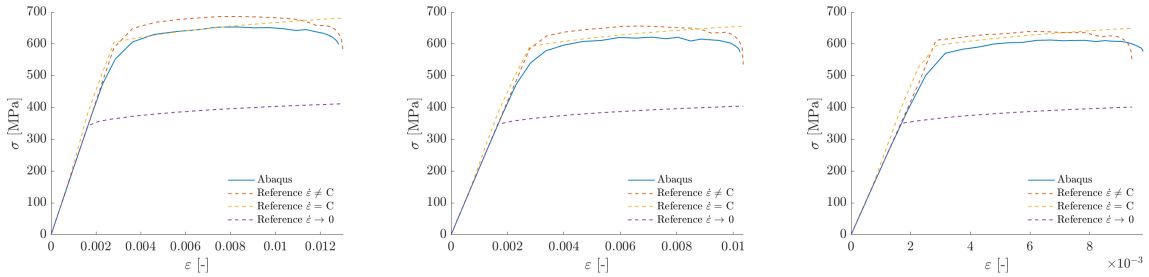

(a) Strain rate factor = 0.1 **(b)** Strain rate factor = 0.2 **(c)** Strain rate factor = 0.3

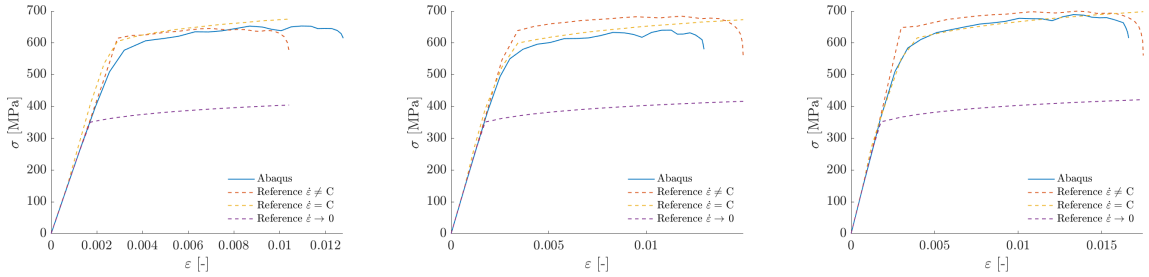

(d) Strain rate factor = 0.4 **(e)** Strain rate factor = 0.5 **(f)** Strain rate factor = 0.6

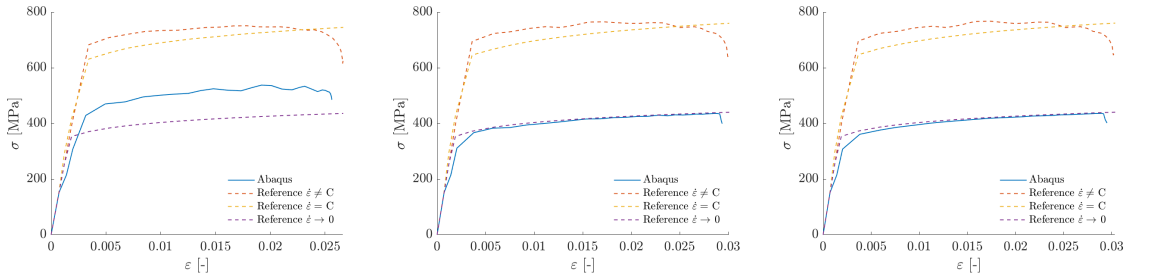

(g) Strain rate factor = 0.7 **(h)** Strain rate factor = 0.8 **(i)** Strain rate factor = 0.9

Figure 4.12: Stress-strain curves for various strain rate factors where $v_0 = 1.5$ m/s and $m_d = 40$ kg

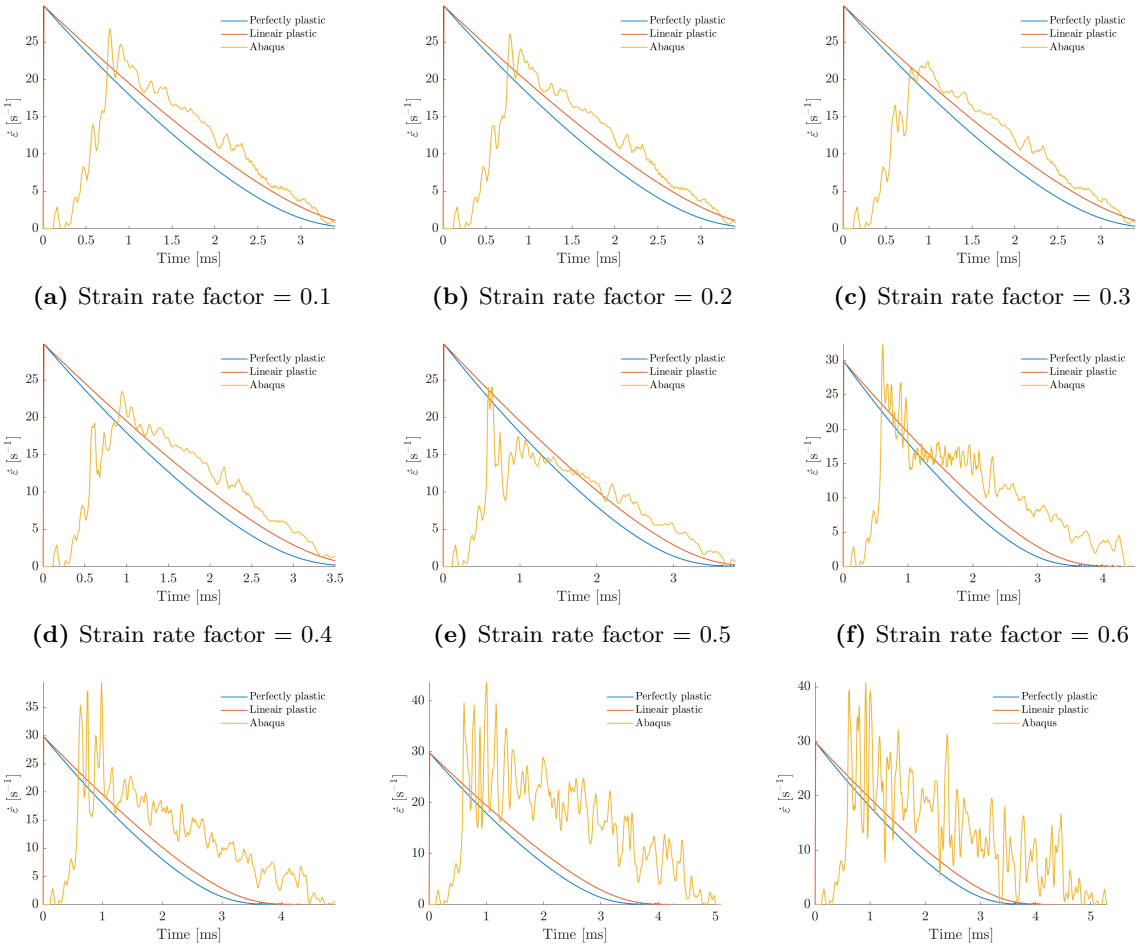

(a) Strain rate factor = 0.1 **(b)** Strain rate factor = 0.2 **(c)** Strain rate factor = 0.3

(d) Strain rate factor = 0.4 **(e)** Strain rate factor = 0.5 **(f)** Strain rate factor = 0.6

(g) Strain rate factor = 0.7 **(h)** Strain rate factor = 0.8 **(i)** Strain rate factor = 0.9

Figure 4.13: Strain rate curves for various strain rate factors where $v_0 = 1.7$ m/s and $m_d = 30$ kg

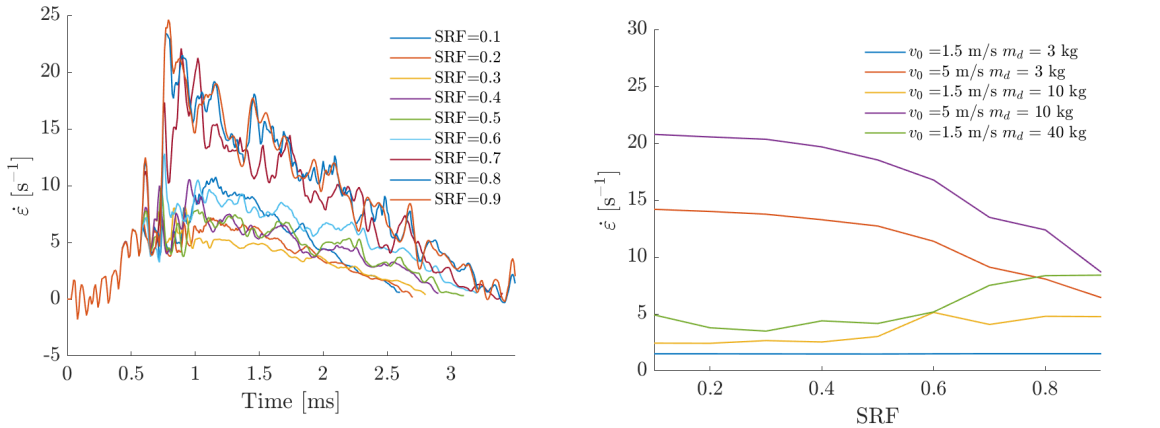

(a) Strain rate for various strain rate factors where $v_0 = 1.5$ m/s and $m_d = 40$ kg **(b)** Average strain rate for various strain rate factors

Figure 4.14: Strain rate for various strain rate factors

4.4.2 Rigid and deformable drophead

As discussed in section 4.2.2, two options for modelling the drophead have been investigated: as an analytical rigid and as a deformable body. A comparison of strain and strain rate in the gauge section for both formulations can be seen in figure 4.15. The two formulations show very similar results in the beginning but start to diverge after that. The cause for this divergence can be found in the difference in shape between the analytical rigid and the deformable drophead. The analytical rigid is a perfect hemisphere whereas the deformable is a discretized hemisphere, as is illustrated in figure 4.16. As a consequence of the discretization, the specimen slips away from under the drophead, since the contact has been defined as frictionless. The specimen slipping away from the drophead is illustrated in figure 4.17, where where both the deformed and undeformed specimen are shown to illustrate the sideways movement of the deformed specimen. This slipping of the specimen leads to inhomogeneous stress- and strain fields in the specimen and is therefore undesirable. Friction will, of course, have an impact of these results. This will be addressed in the next section.

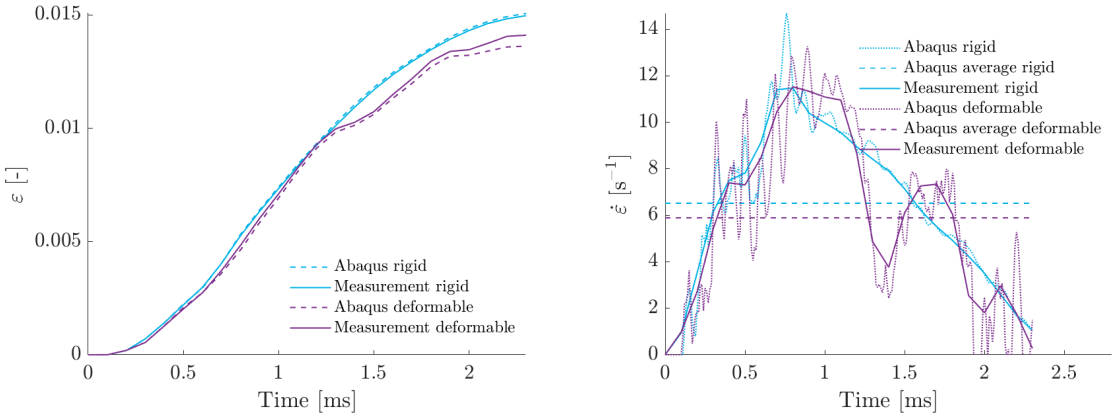

(a) Strain in the gauge section **(b)** Strain rate in the gauge section

Figure 4.15: Comparison of rigid and deformable drophead where $v_0 = 1.7$ m/s, $m_d = 30$ kg and $\alpha = 60°$

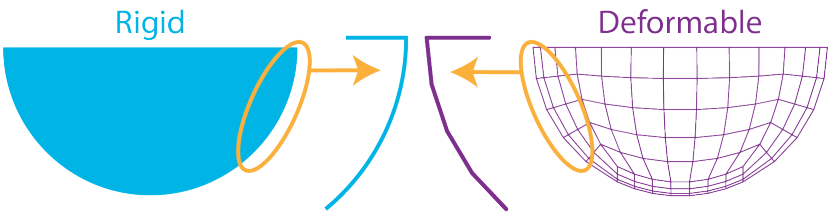

Figure 4.16: Difference in shape between rigid and deformable drophead

4.4.3 Effect of friction

So far, all tangential contact between the specimen and drophead has been assumed to be frictionless. In reality, some amount of friction will always be present between the specimen and drophead. In order to investigate the impact of friction on the results, friction between

Figure 4.17: The specimen slips away from under the deformable drophead

the specimen and drophead is included for both the rigid and deformable drophead in the form of a friction coefficient, f_c, as mentioned in section 4.2.5. The corresponding results for the average strain rate and measurement accuracy are shown in figure 4.18.

It can be observed that the strain rate increases as more friction is present. This can be explained by the fact that more friction between the specimen and drophead allows for more energy to be transferred from the drophead to the specimen, resulting in a higher strain rate. This trend is also reflected by the detailed strain rate curves in figure 4.19. The strain rate curves also show that in case of a deformable drophead more fluctuations are observed the strain rate than for the assumption of a rigid drophead. This can be attributed to stress waves in the drophead itself. Finally, it is interesting to note that the rigid and deformable drophead initially show a similar strain rate curve, but as time progresses the deformable drophead shows higher strain rates than the assumption of a rigid drophead.

Furthermore, as can be concluded from figure 4.20, a little friction is beneficial for the measurement accuracy of the experiment, but once sufficient friction is present, no further impact on measurement accuracy is observed. In conclusion, although friction has some influence on the strain rate and measurement accuracy, the overall impact on the experiment is expected to be small.

In a practical sense, these results indicate that it is desirable to have sufficient friction between the specimen and drophead and avoid an extremely smooth interface.

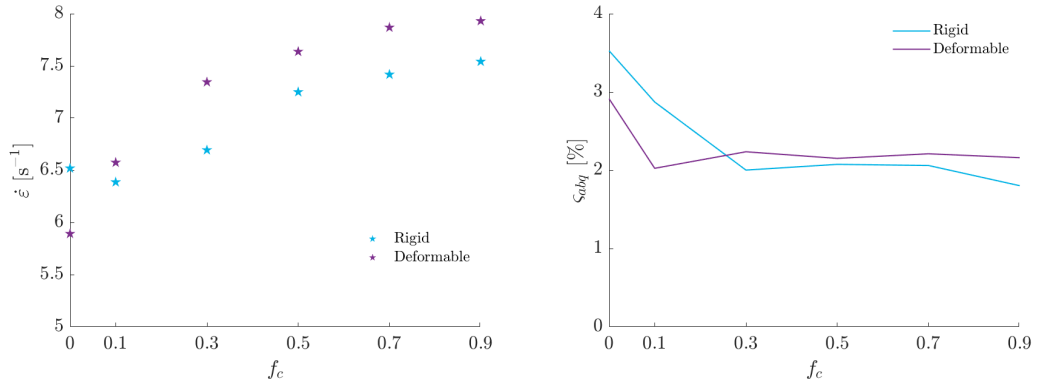

(a) On average strain rate in gauge section **(b)** On measurement accuracy

Figure 4.18: Effect of friction on rigid and deformable drophead where $v_0 = 1.7$ m/s, $m_d = 30$ kg and $\alpha = 60°$

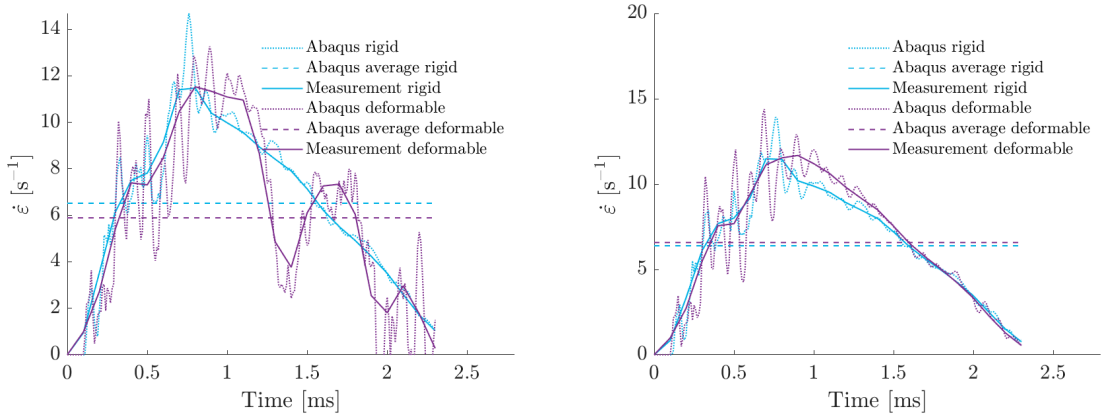

(a) Frictionless **(b)** $f_c = 0.1$

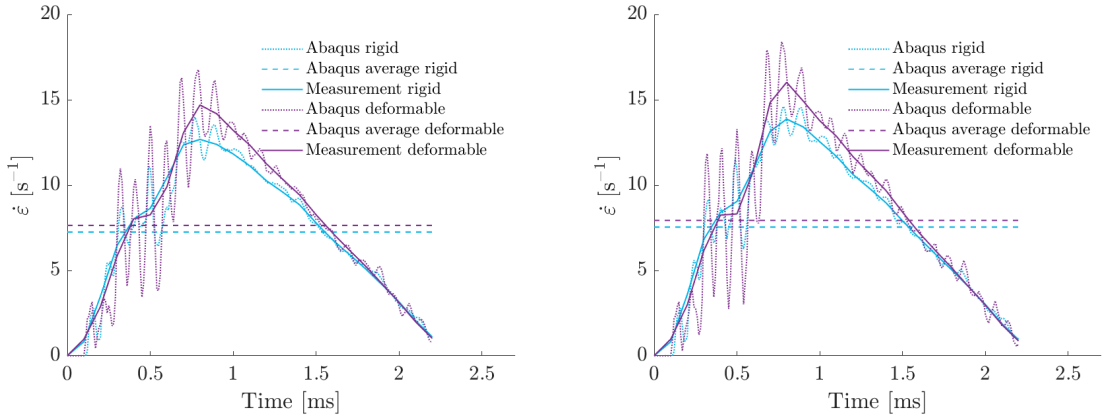

(c) $f_c = 0.5$ **(d)** $f_c = 0.9$

Figure 4.19: Comparison of the strain rate in the gauge section for rigid and deformable drophead where $v_0 = 1.7$ m/s, $m_d = 30$ kg and $\alpha = 60°$

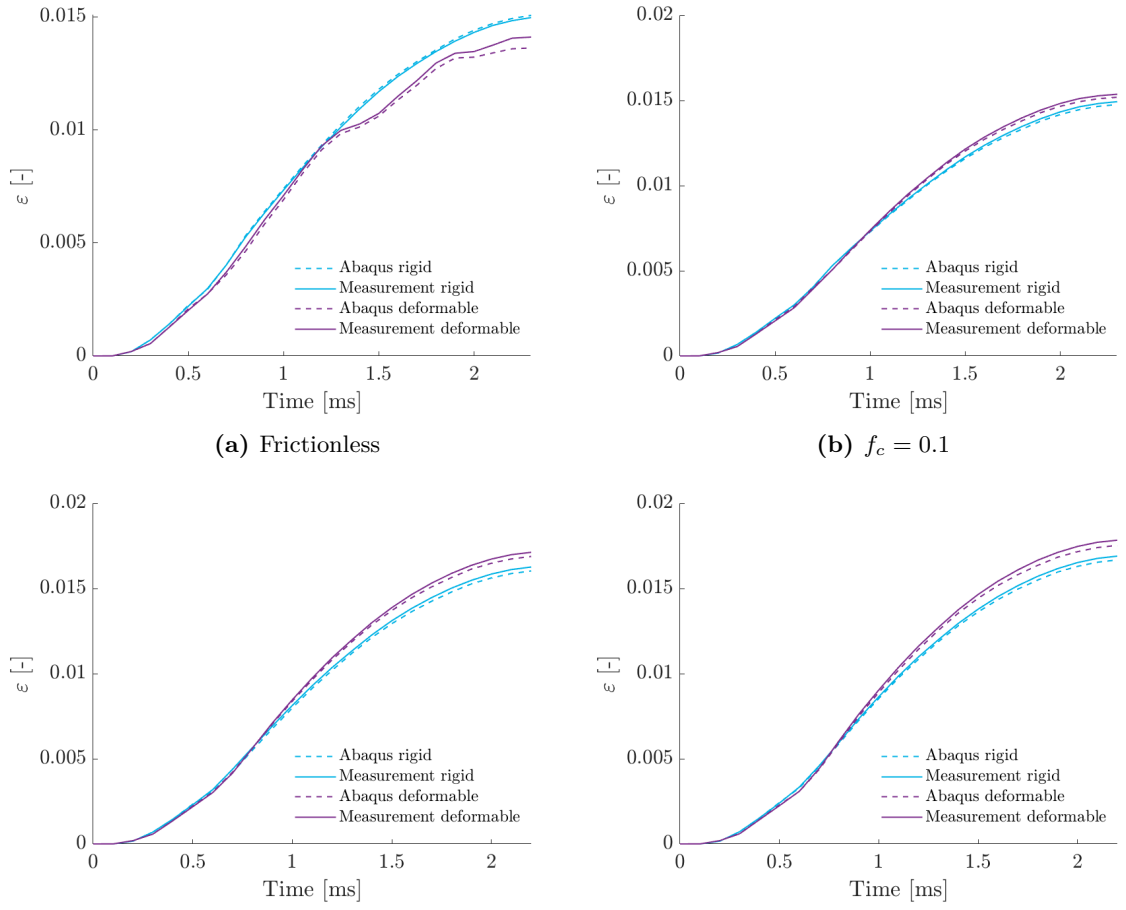

(a) Frictionless

(b) $f_c = 0.1$

(c) $f_c = 0.5$

(d) $f_c = 0.9$

Figure 4.20: Comparison of the strain in the gauge section for rigid and deformable drophead where $v_0 = 1.7$ m/s, $m_d = 30$ kg and $\alpha = 60°$

Chapter 5

Results

First, in order to investigate the validity of the analytical solution and verify the FEA simulations, section 5.1 presents the results of a comparison between the analytical model from chapter 3 and the numerical simulations from chapter 4. Furthermore, as already concluded in chapter 4, the strain rate factor used as a parameter in the FEA solutions needs to be determined, as is presented in section 4.4.1.

Finally, after the validity of the FEA simulations has been determined, section 5.2 presents several parametric studies that have been carried out to investigate the influence of various parameters on the strain rate and accuracy of the experiment.

5.1 Comparison analytical model and FEA

In order to assess the validity of the analytical solutions presented in chapter 3 and verify the results of the FEA simulations, this section presents a comparison between both solutions. Note that, as presented in chapter 2, two experiments are carried out, so two sets of comparison have been done: one for the flat specimen used in the universal test machine and one for the impact specimen used in the impact test.

5.1.1 Flat specimen

The example given in section 3.2.3 of a flat specimen that can be used in a UTM, is compared to a finite element model of the same specimen. The dimensions can be found in table 5.1. The material model is the same as in the other FE simulations, as discussed in section 4.2.4. The FE model is fixed on side, while a constant velocity is applied to the other side. The resulting comparison between the analytical solutions and the FE analysis is shown in figure 5.1.

A comparison between the true strain as given by the analytical model and strain directly from the Abaqus output in figure 5.1a indicates that the analytical model overestimates the strain with respect to Abaqus. This can be explained by the energy that is absorbed by strain in linear elastic regime and in the grip section, both of which are not taken into account

by the analytical model. Consequently this energy has to be absorbed by plasticity in the gauge section resulting in higher strains. Therefore, initially the two curves diverge but as time progresses, Abaqus and the analytical solution show a similar slope, since the relative contribution of elastic strain to the strain in the FE model reduces as time progresses.

This is also reflected by the strain rate in figure 5.1b. The initial large oscillations of the Abaqus strain rate are non-physical, numerical artefacts, as explained in section 4.2.4. The curve marked as 'measurement', which is constructed as described in section 4.3.3, more accurately represents the initial strain rate. As explained, since the analytical model does not account for the linear elastic regime and for any strain in the grip section, the analytical strain rate is initially overestimated with respect to 'measurement' but, as plasticity in the gauge section becomes dominant, both curves converge as time progresses.

The stress in figure 5.1c and stress-strain curve in figure 5.1d show that both the perfectly plastic and linear plastic material models initially overestimate the stress in the gauge section, since neither takes linear elastic material behaviour into account. However, as can be seen, both analytical solutions and the Abaqus solution show stresses in the same order of magnitude, thereby verifying the Abaqus solution. The near perfect match of the perfectly plastic stress in the second half of figure 5.1c is most likely a coincidence, where the errors caused by the assumptions in the analytical material model negate the errors caused by the overestimated strain rate. Furthermore, when looking at the stress-strain curve in figure 5.1d, it is clear that both the perfectly plastic and linear plastic models show decent agreement with the Abaqus results, thereby verifying the Abaqus solution.

Table 5.1: Specimen dimension for the flat specimen used in the comparison between analytical model and FEA

Parameter		Value	
Thickness	h	2	mm
Width grip section	b_{grip}	35	mm
Width gauge section	b_{gauge}	12.5	mm
Length parallel section	$L_{c,0}$	57	mm
Length moving grip section	$L_{grip,moving}$	62	mm
Length clamped grip section	L_{grip}	162	mm
Velocity grip	v	1.7	m/s

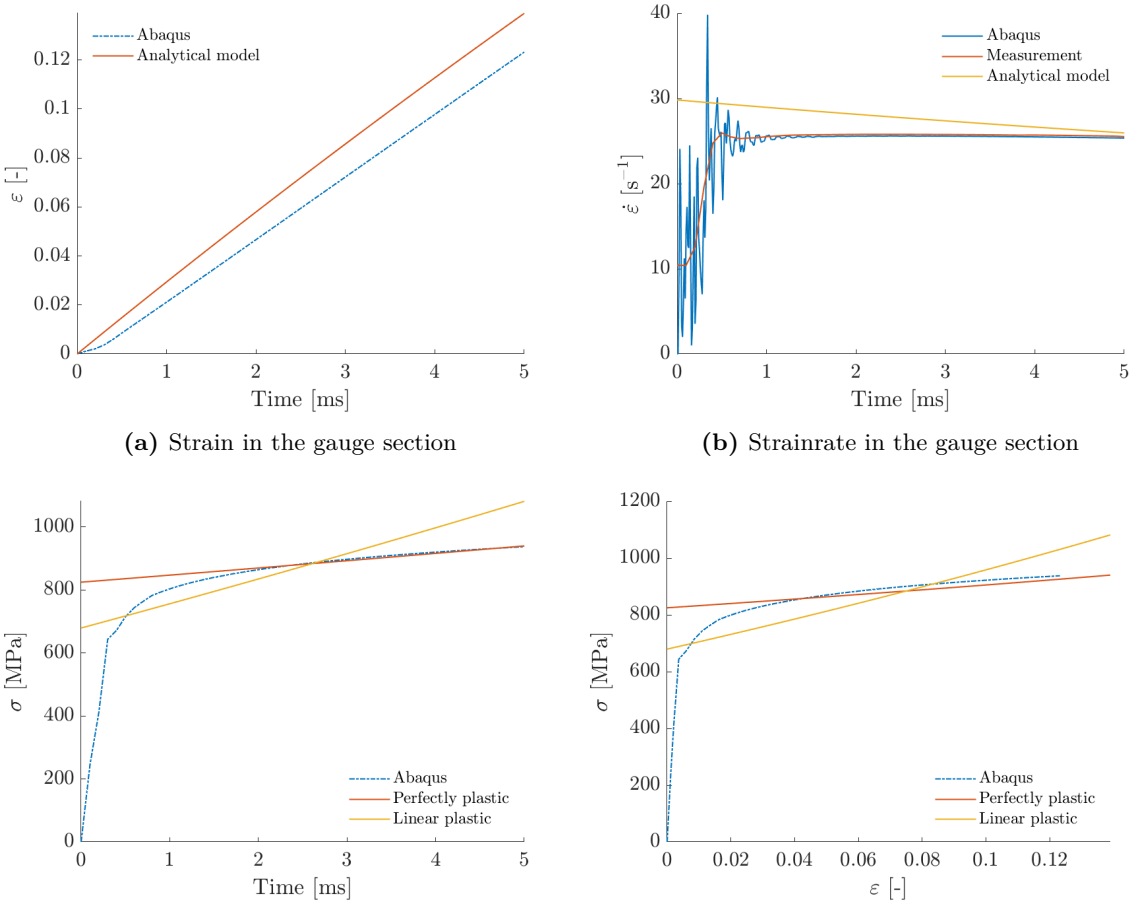

(a) Strain in the gauge section

(b) Strainrate in the gauge section

(c) Stress in the gauge section

(d) Stress-strain curve

Figure 5.1: Comparison between analytical approach and FEA results for a flat specimen

5.1.2 Impact specimen

The example given in section 3.3.4 of a specimen that be used for the higher strain rate impact test is compared to a finite element model of the same specimen. The dimensions are given in table 3.2. The setup of the FE model is discussed in chapter 4. In order to investigate the influence of the impact section on the overall results, models were created for three different widths of the gauge section: 6.25 mm, 12.5 mm, and 25 mm.

As can be seen in figure 5.2a, the match between the analytical solution and the FEA results improves when the gauge section is more narrow. This can be explained by a combination of two factors. First of all, as the gauge section becomes more narrow, it reaches plasticity easier such that less energy is absorbed by the impact section and elastic deformation of the grips. Second of all, since the assumption of a rigid impact section in the analytical model implies no energy is absorbed by the impact section, the match between the analytical solution and the FEA results should improve as the impact section and grips absorb less energy in the FE analysis and, thus, as the gauge section becomes more narrow. This is also confirmed by the stress distribution in figure 5.3, which shows the Von Mises stress distribution in the specimen when the stress in the gauge section is at its peak. For the specimen with a narrow gauge section, the highest stress and all plasticity is observed in the gauge section, while for the specimen with the widest gauge section, no plasticity is observed in the gauge section and the highest stresses are actually observed in the impact section. Note that the lag in the FEA strain compared to the analytical solution is caused by the linear elastic deformation, which is not accounted for in the analytical solution.

The strain rate curves in figure 5.4 again confirm the best fit for the model with the most narrow gauge section, which is therefore used for the comparison. The lack of elastic deformation in the analytical model explains the difference in the first part of the strain rate curves. The FEA total strain rate rises slower due to the elastic strain. However, in case of the narrow gauge section, most of the energy of the drophead is absorbed by plasticity in the gauge section resulting in a good match between the analytical solution and the FEA results after the initial linear elastic part. As can be expected, as the drophead slows down, the strain rate decreases, as is shown by both the analytical solutions and the FEA results.

Finally, the stress-strain curves in figure 5.5 show that, for the specimen with the narrow gauge section, the analytical model yields a good approximation of the resulting stress-strain curve. In conclusion, within the assumptions of the analytical solutions, the FEA results and the analytical solution show good agreement, thereby verifying the FEA results. Yet, it should be noted that the FEA results also show that the assumption of a rigid impact section as used in the analytical solutions is not valid for the impact specimens considered in the proposed test method. This, however, has no impact on the final results of the experiment as long as the loss of energy in the middle section and consequently lower strain rate in the gauge section are accounted for in the design of the specimen.

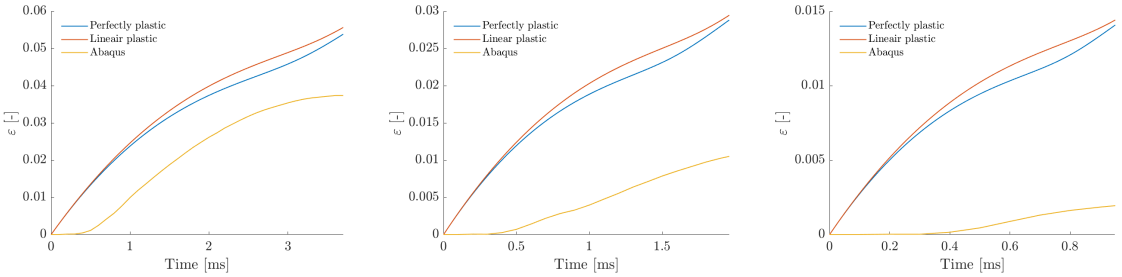

(a) $b_{gauge} = 6.25$ mm **(b)** $b_{gauge} = 12.5$ mm **(c)** $b_{gauge} = 25$ mm

Figure 5.2: Total strain in the gauge section for different widths of the gauge section for the analytical and FE solutions.

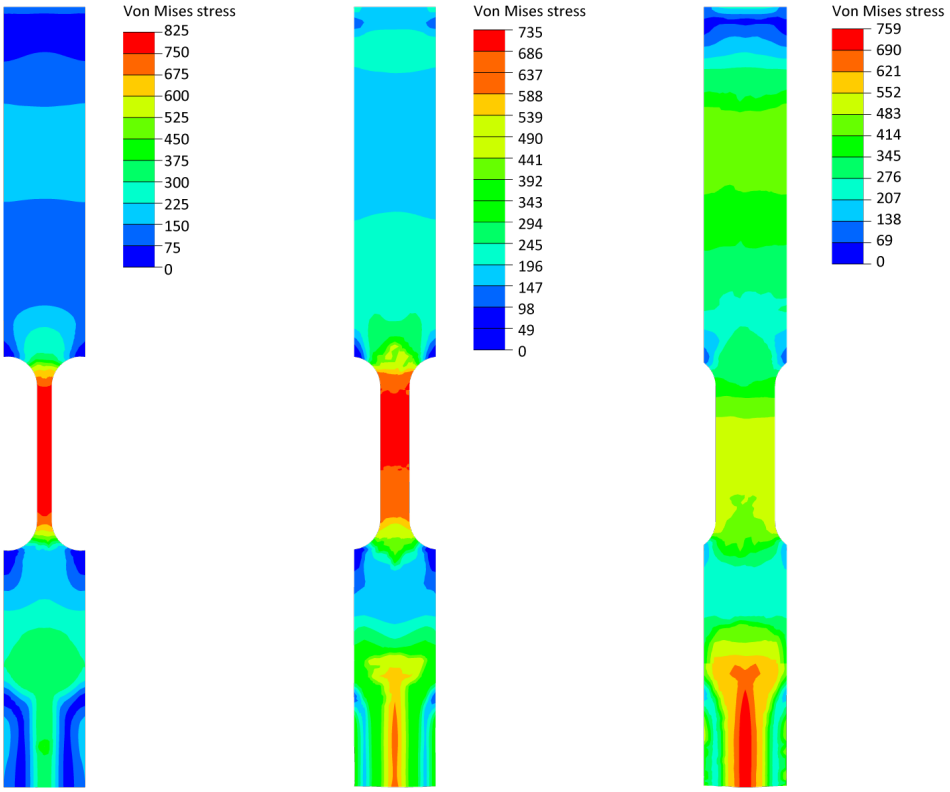

Figure 5.3: Von Mises stress distribution at peak stress in the gauge section for different widths of the gauge section

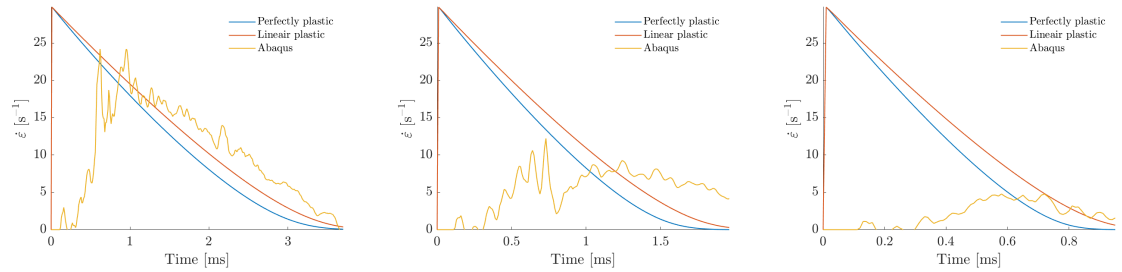

(a) $b_{gauge} = 6.25$ mm **(b)** $b_{gauge} = 12.5$ mm **(c)** $b_{gauge} = 25$ mm

Figure 5.4: Strain rate in the gauge section for different widths of the gauge section for the analytical and FE solutions.

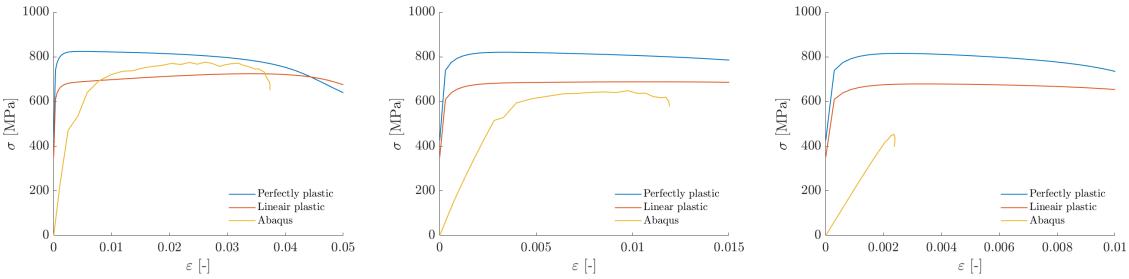

(a) $b_{gauge} = 6.25$ mm **(b)** $b_{gauge} = 12.5$ mm **(c)** $b_{gauge} = 25$ mm

Figure 5.5: Stress-strain curve in the gauge section for different widths of the gauge section for the analytical and FE solutions.

5.2 Parametric study

This section describes the various parametric studies that have been carried out to investigate the effect of different parameters on the experiments. The parametric study to determine the effect of various parameters is described in this section. The following parameters have been investigated:

- Width of the grip section
- Mass and velocity of the drophead
- The effect of bending waves
- Specimen length and position of the gauge section
- Angle of the dogbone section
- Mismatch and misalignment of drophead and specimen

The dimensions of the standard specimen can be found in table 5.2, where the range of variation for each of the varied parameters can be found. The effect of each of these parameters is first discussed separately, focusing on the impact on strain rate and measurement accuracy. After this, section 5.2.7 shows some of the choices that can be made for an example experiment at a given target strain rate.

Note that all measurements have been carried out with a measurement frequency of 10^4 measurements per second or in terms of DIC measurements: the frame rate is 10^4 frames per second. This is not an extremely high frame rate for high speed DIC cameras, which can go up to $2.1{\cdot}10^6$ frames per second (Limess Messtechnik & Software GmbH, 2020).

Table 5.2: Dimensions of impact specimen and drophead

Parameter		Standard value		Varied?	Range
Specimen					
Thickness	h	2	mm	No	
Width grip section	b_{grip}	35	mm	Yes	20-40
Width gauge section	b_{gauge}	12.5	mm	No	
Parallel length gauge section	L_c	57	mm	No	
Length gauge section	L_{gauge}	50	mm	No	
Length radius	L_R	9	mm	No	
Length toward middle section	L_{tm}	50	mm	Yes	0-450
Length grip section	L_{grip}	150	mm	Yes	50-500
Radius gauge section	R	12.5	mm	No	
Inner radius specimen	r	50	mm	Yes	50-58
Angle dogbone section	α	90	°	Yes	45-90
Drophead					
Mass	m_d	30	kg	Yes	3-50
Radius drophead	r_d	50	mm	No	
Velocity on impact	v_0	1.7	m/s	Yes	1.5-6
Position of drophead	dy	0	mm	Yes	0-8

5.2.1 Effect of grip section width

As discussed in chapter 2 on the test method, it is important to ensure linear elastic behaviour in the grip section. Therefore, as a first parameter study, simulations have been done for various widths of the grip section to determine the correct width to be used in the experiment.

On strain rate in gauge section

As can be seen in figure 5.7a, varying the width of the grip section has little effect on the average strain rate. As long as there is no plasticity in the grip section, this is to be expected, since the linear elastic grip section will only absorb a small amount of energy. However, as can be seen, when combining figure 5.6a and figure 5.6b, as soon as the grip section deforms plastically, the strain rate in the gauge section drops, since a significant part of the energy of the drophead is now also absorbed by the grip section. This is, for example, the case for the outlier with a grip section width of 20 mm at $m_d = 40$ m/s and $v_0 = 4$ m/s.

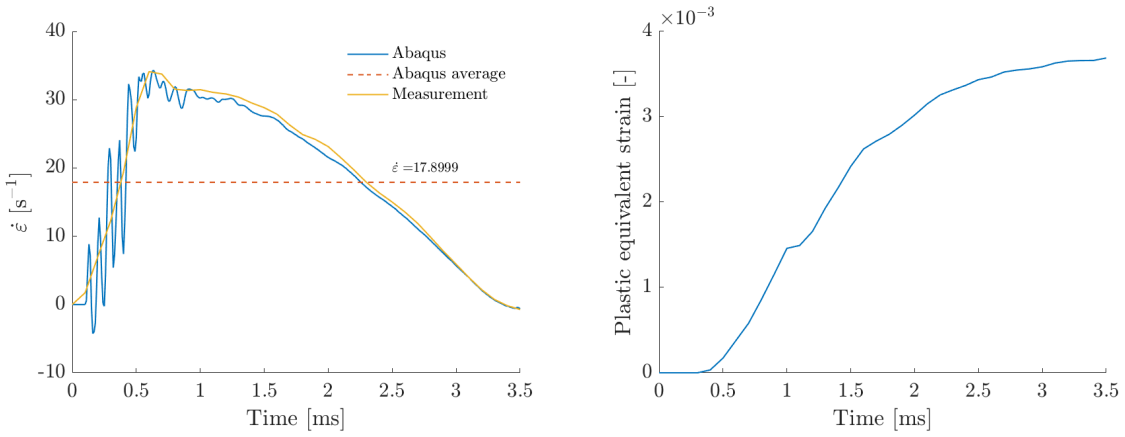

(a) Strain rate in gauge section

(b) Plastic equivalent strain in the grip section

Figure 5.6: Effect of plasticity in the grip section for the case where $v_0 = 4$ m/s, $m_d = 30$ kg and $b_{grip} = 20$ mm

On measurement accuracy

Selecting the correct width of the grip section for the most accurate measurements is trade-off between, on the one hand, selecting a grip section that is wide enough to avoid plasticity, while, on the other hand, keeping it as narrow as possible to avoid measurement inaccuracies resulting from too little strain to be measured.

Furthermore, it should be noted that plasticity in the grip section is more likely to be present at higher strain rates, since a higher strain rate leads to a higher stress in the gauge section because of the strain rate sensitivity of the material. Consequently the gauge section can take a higher load, which in turn means there will be higher stress in the grip section. This is also confirmed by figure 5.7c and, as can be seen in figure 5.7b, consequently the accuracy of the measurement decreases drastically. Figure 5.7b also shows that the accuracy improves significantly for a grip section width of 35 mm or more. Since a more narrow grip section

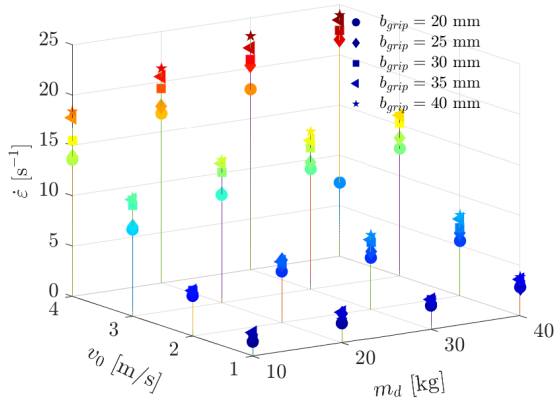

(a) On average strain rate in gauge section

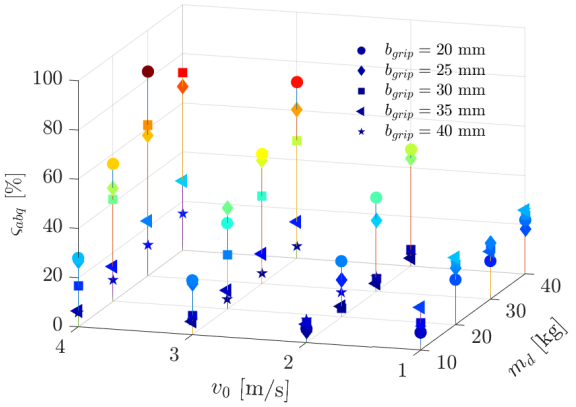

(b) On measurement accuracy

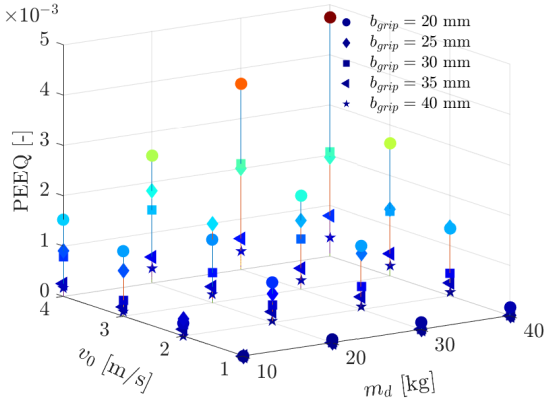

(c) On maximum plastic equivalent strain in the grip section

Figure 5.7: Effect of grip section width, mass and velocity

allows for easier measurements, a grip section width of 35 mm is chosen for the remainder of the simulations.

5.2.2 Effect of drophead mass and impact velocity

The analytical model indicates a strong relation between the strain rate and the mass and impact velocity of the drophead, suggesting a trade-off can be made. Therefore, this section presents a combined discussion on the effect of these parameters on the strain rate and measurement accuracy.

On strain rate in gauge section

Figure 5.8 shows the effect of impact velocity and mass of the drophead on the average strain rate. As can be seen, the average strain rate increases faster with drophead velocity than mass. This can be explained using the analytical model, which predicts, within the assumptions of the model, an initial strain rate, at $t = 0$, that is only dependent on the impact velocity of the drophead and length of the gauge section and independent of the drophead mass, as can seen in equation 3.10 and equation 3.12. The mass mainly affects the duration of the experiment; in other words, a heavier drophead takes longer to slow down. Based on this, it also not surprising that the increase in strain rate due to an increase in drophead mass is less pronounced for low velocity. Similarly, the increase in strain rate due to an increase in velocity is more pronounced when the drophead has a higher mass.

This is also observed in the following example where two cases with approximately the same average strain rate, but different drophead and mass are compared. As is shown in figure 5.9, even though the average strain rate is similar to actual strain rate curve differs significantly. First of all, it can be observed that a higher drophead mass combined with a lower velocity results in a smoother strain rate curve than a higher velocity combined with a lower mass. Secondly, as can be seen when comparing figure 5.9c to figure 5.9d, a higher mass combined with a lower velocity results in more plasticity in the gauge section and hence more material data, which is to be expected, since a higher mass results in a longer duration of the experiment.

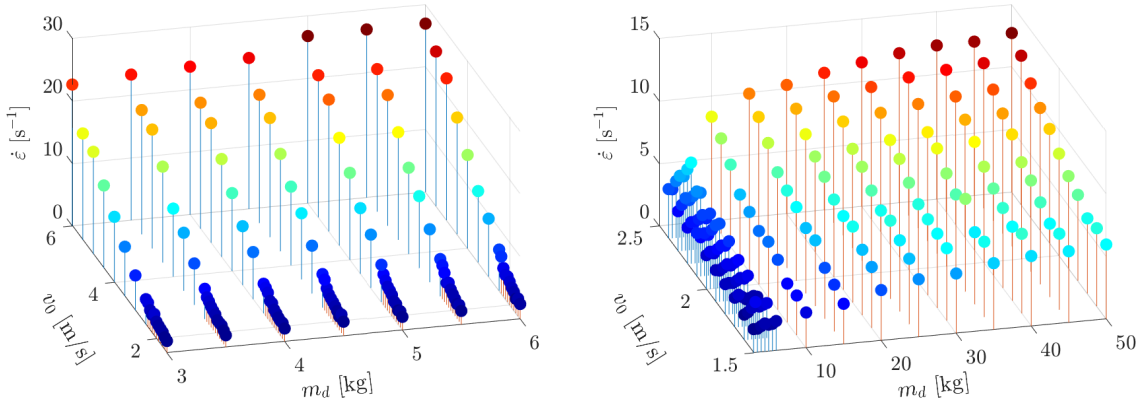

Figure 5.8: Effect of mass and velocity on the average strain rate

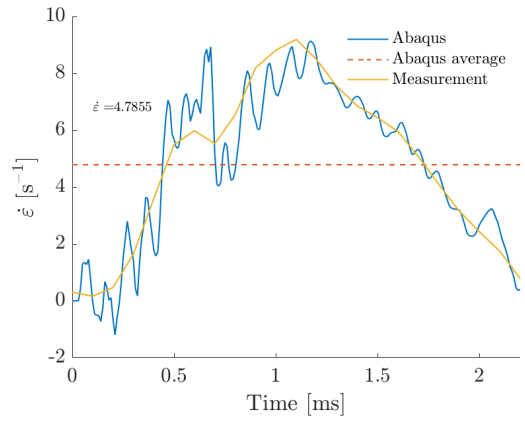

(a) Strain rate for $v_0 = 1.5$ m/s and $m_d = 30$ kg

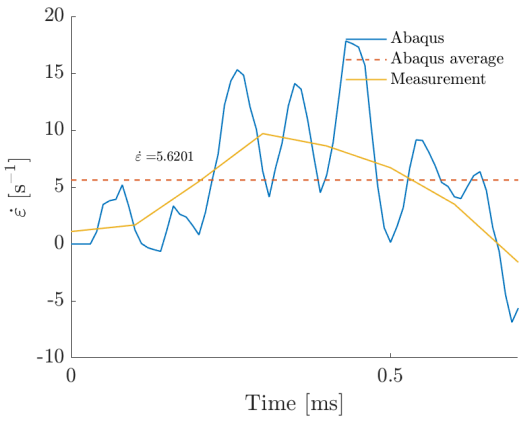

(b) Strain rate for $v_0 = 3$ m/s and $m_d = 3$ kg

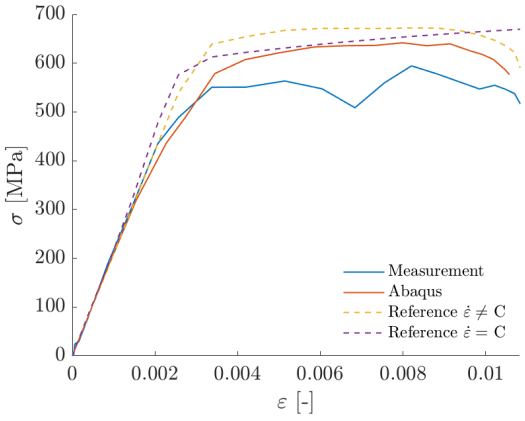

(c) Stress-strain curve for $v_0 = 1.5$ m/s and $m_d = 30$ kg

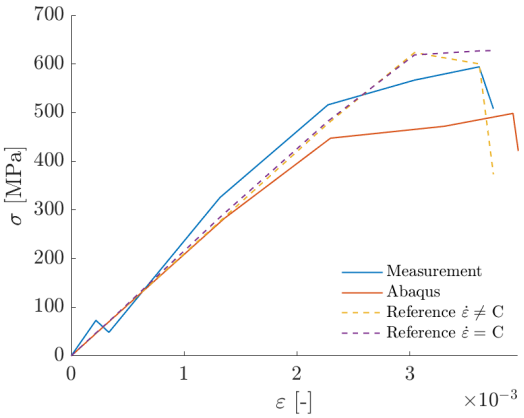

(d) Stress-strain curve for $v_0 = 3$ m/s and $m_d = 3$ kg

Figure 5.9: Effect of mass and velocity on strain rate and the stress-strain curve at a similar average strain rate

On measurement accuracy

The effect of drophead mass and impact velocity on measurement accuracy is shown in figure 5.10. Note that for clarity, the axes have been reversed with respect to figure 5.8. It can be observed in figure 5.10 that measurement accuracy improves as the drophead mass or the impact velocity increases, with an optimum at approximately $v_0 = 2.3$ m/s and $m_d = 50$ kg.

A higher initial velocity results in more accurate measurements because there are less bending waves, as will be discussed in the section 5.2.3 on bending waves. Furthermore, a higher mass ensures a more stable measurement and longer measurement time, which positively affect the measurement accuracy. When the energy from the drophead is too much, it will introduce plasticity in the grip section. But when the energy input is too high, plasticity in the grip section causes less accurate measurements and should be avoided.

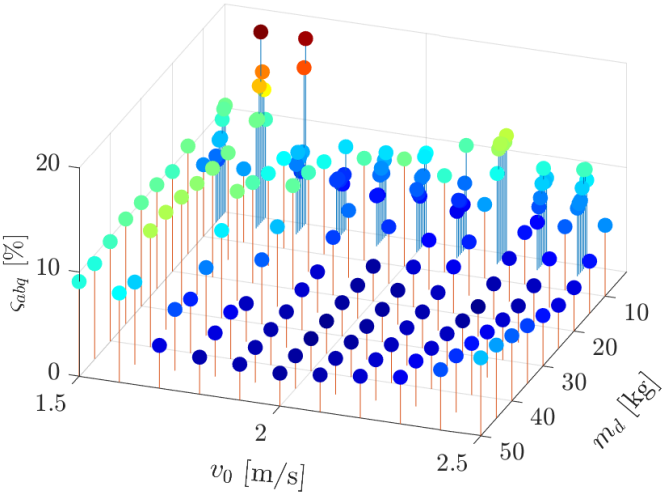

Figure 5.10: Effect of mass and velocity on measurement accuracy

5.2.3 Effect of bending waves

An example of the effect of bending waves on the experiment can be seen in figure 5.9c in the previous section, which shows a significant difference between the measured stress-strain curve and the stress-strain curve directly obtained from Abaqus. This is because the bending waves introduce inhomogeneity in stress and strain fields over the thickness of the material (Yang et al., 2014). In order to further investigate the effect and presence of bending waves on the experiments, an additional FEA model is created in which bending waves are eliminated by means of a constraint. This is achieved by constraining the pink areas of the model in figure 5.11 in their local z-direction, thereby restricting out-of-plane movement and thus eliminating bending waves. Finally, the results of these simulations are compared to the initial simulations, while varying the drophead mass and impact velocity.

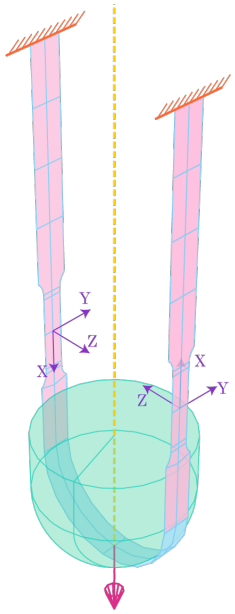

Figure 5.11: FEA model where bending waves are restricted

On strain rate in gauge section

As is to be expected, the absence of bending waves results in a higher average strain rate compared to simulations with bending waves, as can be seen in figure 5.12a. This can be explained by the fact that the energy that previously resulted in bending waves, now results in additional axial strain in the specimen.

On measurement accuracy

Figure 5.12b shows that the accuracy of the measurements improves significantly for the absence of bending waves. This can be seen in detail from the stress-strain curves in figure 5.13, where the case without bending waves has a exact match between the measurement and Abaqus data. Furthermore, bending waves are more prevalent in the grip section, since

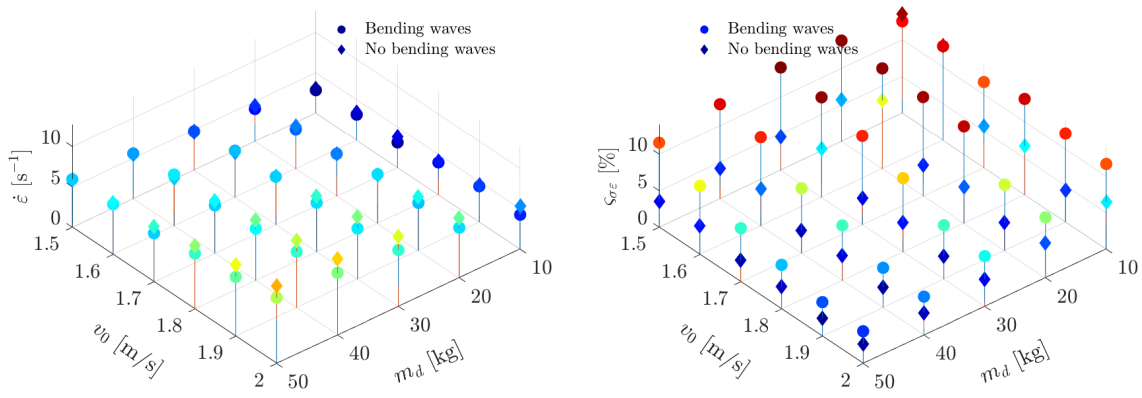

(a) On average strain rate in gauge section **(b)** On measurement accuracy

Figure 5.12: Effect of bending waves

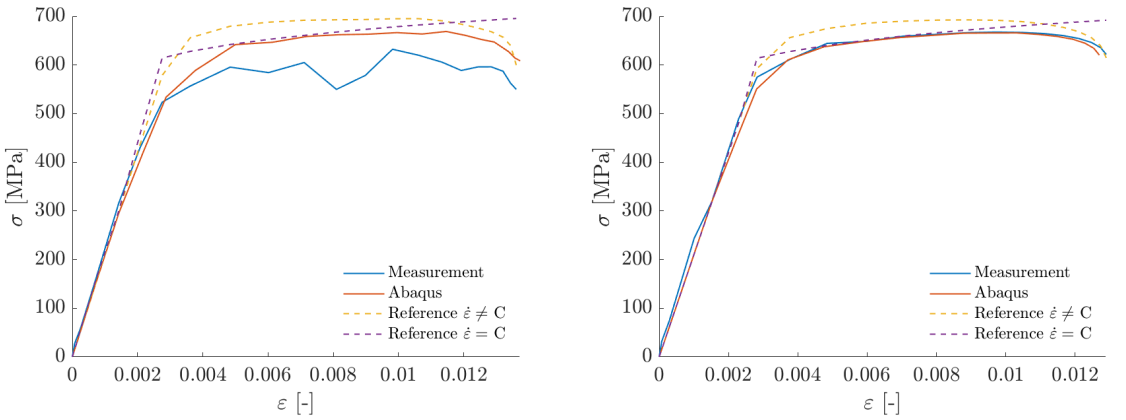

(a) Stress-strain curve with bending waves **(b)** Stress-strain curve without bending waves

Figure 5.13: Effect of bending waves on the stress-strain curve for the case where $v_0 = 1.7$ m/s and $m_d = 30$ kg

the same out-of-plane displacements are relatively bigger in the grip section compared to the gauge section.

When comparing all different simulations, it can be seen that there is less improvement for the cases with higher velocity, for example along the line where $v_0 = 2$ m/s, compared to the cases with a higher mass, for example along the line of $m_d = 40$ kg. This indicates that there are less bending waves present in the specimen when the velocity is higher.

Furthermore, it should be noted that there is hardly any difference between the cases with and without bending waves when the gauge section remains in the linear elastic regime, for example, When $v_0 = 1.5$ m/s and $m_d = 10$ kg.

5.2.4 Effect of specimen length and position of the gauge section

In order to investigate the effects of variation in length, the total length of the specimen is varied along with the position of the gauge section. The position of the gauge section in the specimen is determined by the length of the grip section, L_{grip}, and the length of the section toward the middle, L_{tm}, as illustrated in figure 5.14.

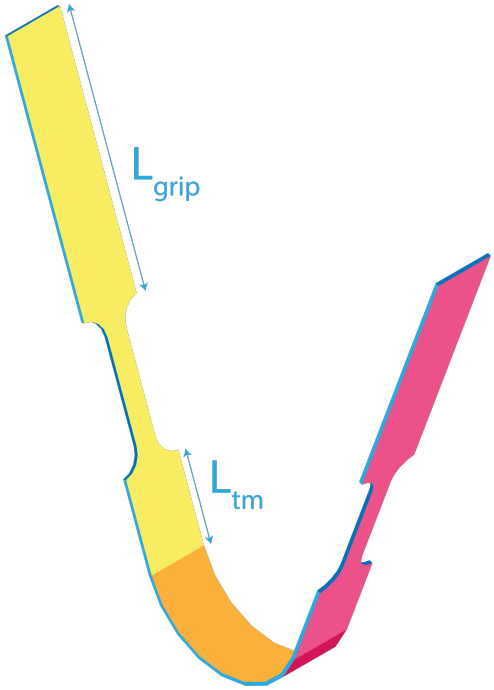

Figure 5.14: Definition of the parameters used to investigate the effect of specimen length and position of the gauge section

On strain rate in gauge section

The effect of the length variations of the specimen on the strain rate is shown in figure 5.15a. It can be observed that a longer specimen results in a lower average strain rate, as expected, since the energy needed for straining the specimen is now distributed over more material. The difference, however, is small, since the majority of the energy is still absorbed by the gauge section.

A special case is the case when L_{tm} is zero, so when the drophead hits the specimen directly next to the gauge section and no buffer zone is present between the impact section and the gauge section. As can be seen, in this case the average strain rate increases irrespective of the specimen length. This can be explained by the fact that the first part of L_{tm}, close to the impact section, in general deforms plastically, thereby taking up some energy of the impact and thus reducing the average strain rate in the gauge section. Consequently, when this sections is removed by setting L_{tm} to zero, the average strain rate in the gauge section increases.

On measurement accuracy

The measurement accuracy in figure 5.15b clearly shows that there is a significantly larger measurement error when L_{tm} is zero. This indicates that a small piece of material is needed as a buffer between the impact zone and the gauge section to absorb bending waves. Furthermore, when looking at the accuracy along the line of $L_{grip} = 50$ mm, the measurements are consistently more accurate, because a larger part of the bending waves is already absorbed by the rest of the specimen. This is also good news for the DIC measurements, because this means that the required field of view becomes smaller, resulting in more accurate measurements, as discussed in section 1.5.

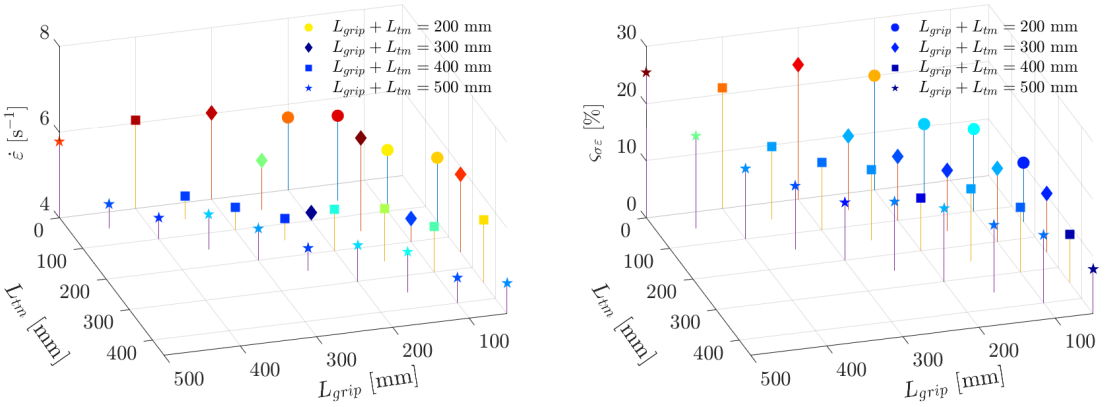

(a) On average strain rate in gauge section

(b) On measurement accuracy

Figure 5.15: Effect of length variation

5.2.5 Effect of angle α

This section presents the effect of the angle of the dogbone section, α, on the strain rate and measurement accuracy to first identify the effect of angle α in a perfect setup where the drophead matches the specimen properly and is dropped exactly in the centre of the specimen. However, as will be shown in section 5.2.6, α becomes especially important when considering an imperfect setup.

On strain rate in gauge section

The strain rate results in figure 5.16a indicate a small change in average strain rate for variation in α, as is also confirmed by the detailed strain rate curves in figure 5.17. The effect of α is similar to that of the drophead mass, in that higher values of α slow down the drophead faster, but the effect is significantly smaller.

On measurement accuracy

The effect of the angle on the measurement accuracy in figure 5.16b shows that as long as a sufficiently small angle α, below 75°, is used, the achieved measurement accuracy is fairly constant and varying angle α has a limited influence on the measurement accuracy. However, when using an angle α above 75° larger bending waves are present, thereby reducing the accuracy of the measurement.

Furthermore, as can be seen, for an angle α of 55° or 70°, a larger measurement error is observed on the strain in the gauge section. As can be seen in figure 5.18, this results from an overestimated strain in the measurements compared to the Abaqus results. A closer investigation of the Abaqus results showed no significant differences between all cases from 45 to 70°, leading to the conclusion that these small differences between experiments are to be expected when a single strain measurement is used. However, it should be noted that these errors will probably be mitigated in reality when DIC is used, because a complete strain field is obtained instead of a single strain measurement.

Finally, the best results are obtained for an angle α of 65°.

Combined effect of α and mass, velocity and length

Now that the best angle is determined to be 65°, it is useful to verify whether the main findings of the previous sections still hold for different values of α. Therefore, the parametric study of angle α is expanded with a variation in drophead mass, impact velocity, specimen length, and position of the gauge section.

The results for the average strain rate in figure 5.19a indicate that the same trends for a variation in drophead mass and impact velocity are found for different angles, which means that the previous conclusions regarding the effect of drophead mass and impact velocity still hold for other values of α. The same conclusions can be drawn when looking at the trends of varying specimen length and gauge position for various angles α, as is shown in figure 5.20a. Finally, it should be noted that in general, α has a small impact on the average strain rate, as was already concluded previously.

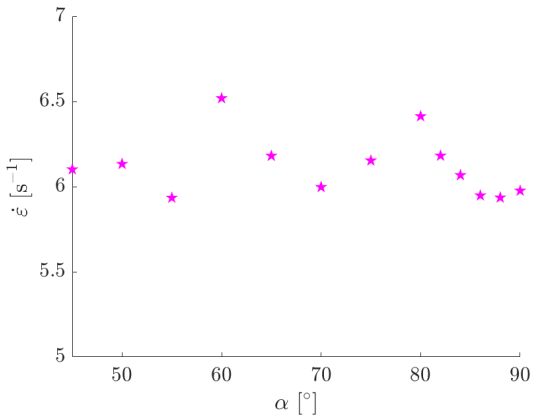

(a) On average strain rate in gauge section

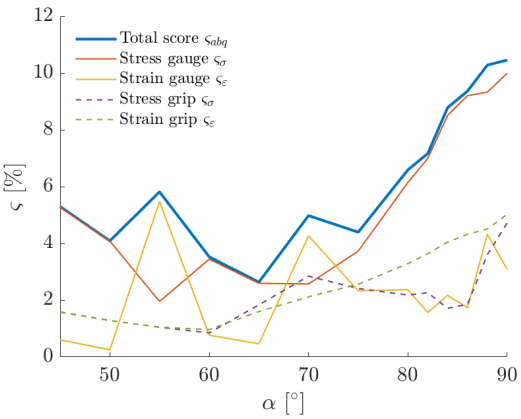

(b) On measurement accuracy

Figure 5.16: Effect of angle α where $v_0 = 1.7$ m/s and $m_d = 30$ kg

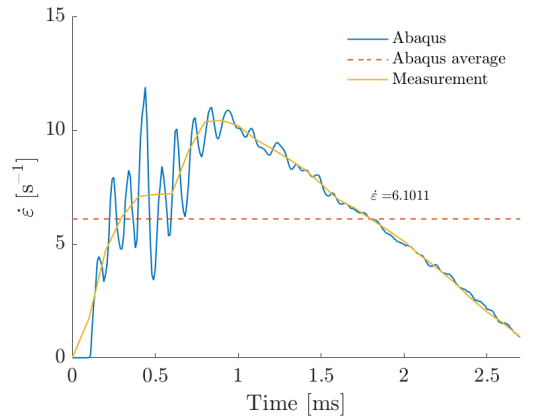

(a) $\alpha = 45°$

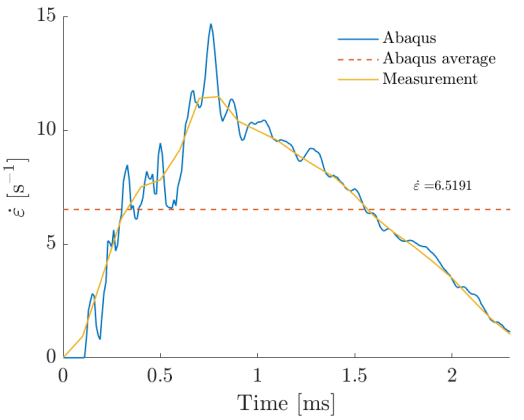

(b) $\alpha = 60°$

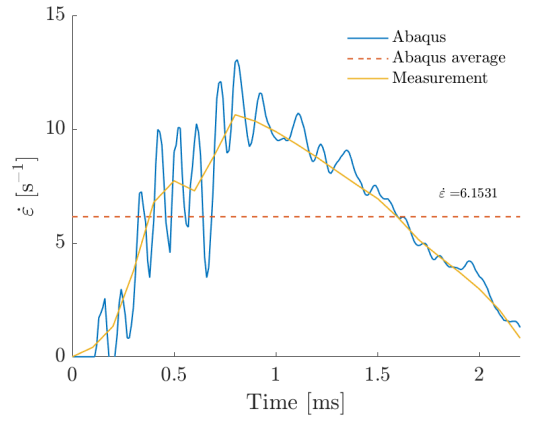

(c) $\alpha = 75°$

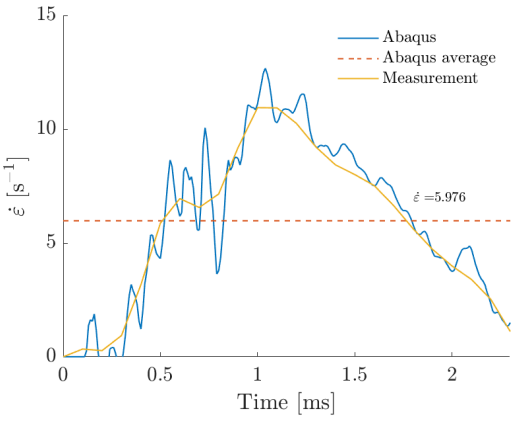

(d) $\alpha = 90°$

Figure 5.17: Detailed strain rate curves for various angles α where $v_0 = 1.7$ m/s and $m_d = 30$ kg

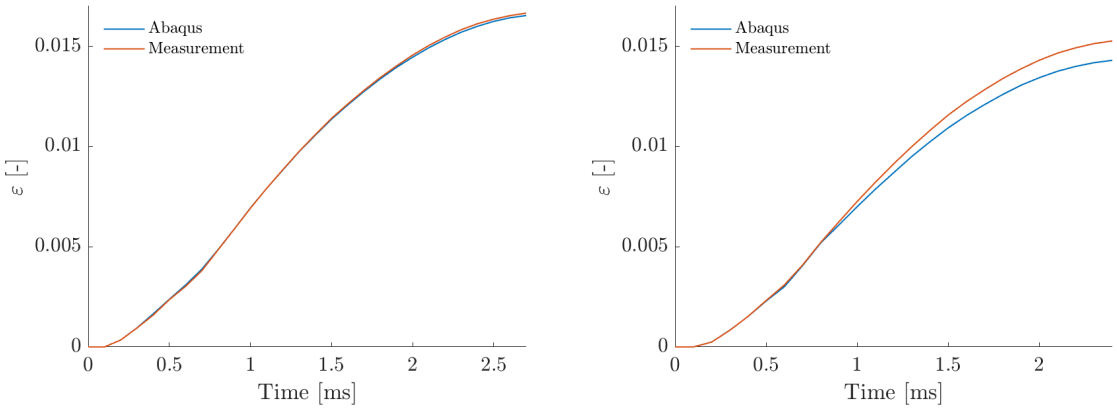

(a) $\alpha = 45°$

(b) $\alpha = 55°$

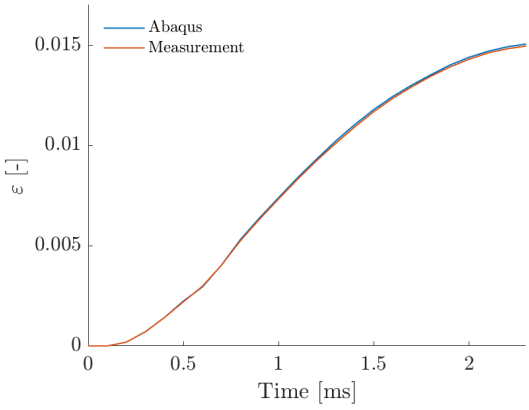

(c) $\alpha = 60°$

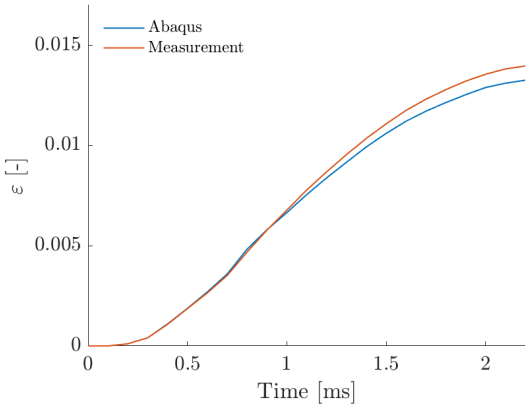

(d) $\alpha = 70°$

Figure 5.18: Effect of α on strain in the gauge section when $v_0 = 1.7$ m/s and $m_d = 30$ kg

The results for the measurement accuracy in figure 5.19b for a variation of drophead mass and impact velocity and figure 5.20b for a variation in specimen length and position of the gauge section indicate that indicate that the same trends in terms of measurement accuracy are found for different angles, which means that the previous conclusions regarding the effect of drophead mass, impact velocity, specimen length, and position of the gauge section still hold for other values of α. Furthermore, the effect of angle α on the measurement accuracy indicates that the smaller angles, of 45° and 60°, yield consistently more accurate results than when α is 90°.

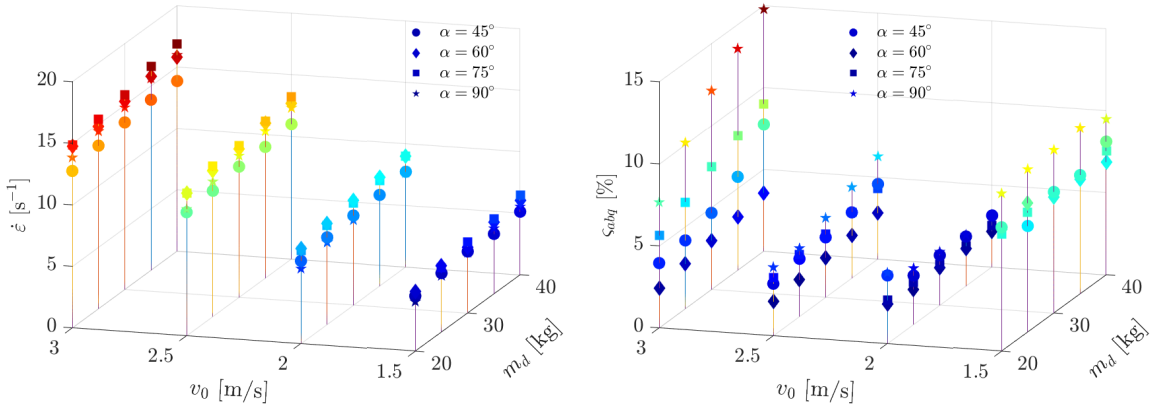

(a) On average strain rate in gauge section **(b)** On measurement accuracy

Figure 5.19: Effect of mass and velocity for various values of α

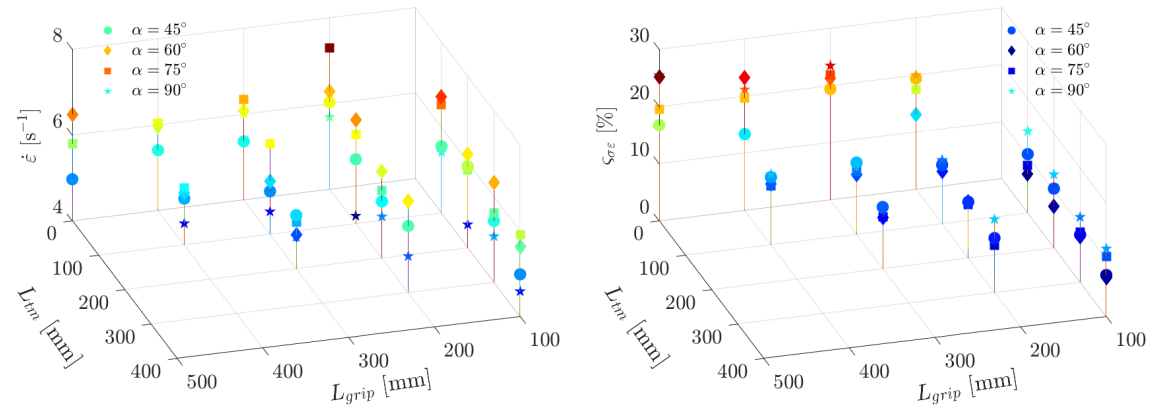

(a) On average strain rate in gauge section **(b)** On measurement accuracy

Figure 5.20: Effect of length for various values of α

5.2.6 Effect of mismatch and misalignment between drophead and specimen

In prior sections, all parametric studies have been carried under the assumption that the experiment is carried out perfectly, in the sense that the drop mass strikes directly in the centre. However, as with all experiments, there is always a possibility that slight errors are made. There might, for example, be a mismatch between the radii of the drophead and the specimen, for example, due to spring back from forming the specimen. Furthermore, the drophead might, for example, not be dropped exactly in the centre of the impact section. Therefore, this section presents the effects of a mismatch and misalignment between the drophead and specimen.

Misalignment is discussed for a mismatched drophead, where the specimen has a larger radius than the drophead. The results in relation to misalignment are discussed with regard to both the horizontal position of the drophead relative to the specimen and the distance of the drophead to the measurement section, which is defined as:

$$distance = (r - r_d) - dy \tag{5.1}$$

where r is the inner radius of the specimen, r_d is the radius of the drophead and dy is the horizontal position of the drophead with respect to the centre of the specimen. Although it might seem counter-intuitive to use this distance as a parameter rather than the position of the drophead, as will be shown, the trends for measurement accuracy appear to be related to this distance instead of the position of the drophead. The relation between distance and drophead are also illustrated in figure 5.21, where they are defined with respect to the measurement area of the specimen, which is marked in yellow. In the current section, three specimens with different radii are discussed. The first is the perfectly matched specimen, where $r = 50$ mm, which is used as a baseline for comparisons of the second and third, with specimen radii of 51 and 52 mm, respectively. The radius of the drophead is kept at 50 mm in all cases.

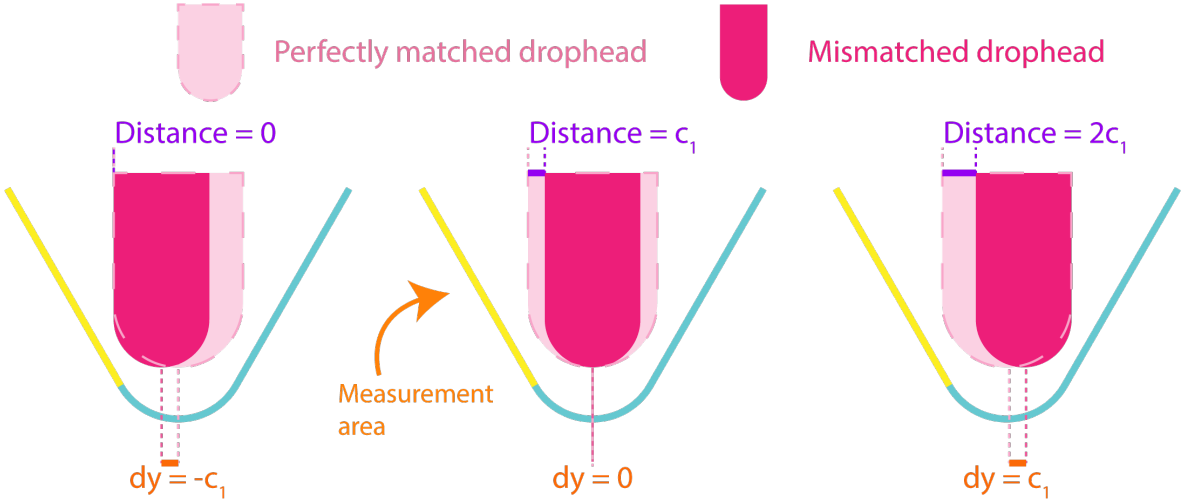

Figure 5.21: Definitions of misalignment

On strain rate in gauge section

Figure 5.22a shows the effect of a mismatch and misalignment between drophead and specimen for various angles α on the average strain rate. It can be observed that the strain rate drops when the drophead is dropped off-centre, independent of the angle α of the specimen. Furthermore, a mismatched drophead and specimen results in an increase in bending waves in the specimen, which leads to a drop in average strain rate also discussed in section 5.2.3 on the effect of bending waves. Finally, a difference can be observed between a horizontal position of, for example, 2 mm and -2 mm. This is related to the fact that dropping the drophead off-centre results in an asymmetric component in the experiment, while measurements are only taken on one side.

On measurement accuracy

The effect of mismatch and misalignment on measurement accuracy is shown in figure 5.22b. Do note that the effect on measurement accuracy in figure 5.22b is shown in relation to the distance of the drophead to the measurement section, in contrast to the position as was used for the effect on strain rate. The first thing to notice is the significant impact of a mismatch between specimen and drophead radii on the measurement accuracy, especially for larger angles α.

In order to investigate this in more detail, figure 5.23 and figure 5.24 show the comparison between the Abaqus and measured strains in the grip section for various mismatches and misalignments, for an angle α of 90° and 60°, respectively. First of all, interestingly, both figures show that, in case there is a mismatch between drophead and specimen radii, it is beneficial for the measurement accuracy to drop the drophead closer to the measured side instead of dropping the drophead in the centre of the impact section. Furthermore, as can be seen, this effect is significantly more pronounced for a large angle α of 90° than for an angle α of 60°, indicating that a smaller angle α results in a more robust measurement compared to using a large angle α. This can be explained when, for example, looking at the out-of-plane displacements of the reference nodes in the grip section, as shown in figure 5.25 and figure 5.26, for α equals 90° and 60° respectively. As can be seen, when the distance between the drophead and measurement section increases, the out-of-plane displacement increases, indicating an increase in bending waves and, thus, a loss of accuracy.

In conclusion, the effect of mismatch and misalignment is strongly dependent on the angle chosen for the specimen, showing more robust measurement for smaller angles α. However, independent of the angle, a perfect match between the radii of the drophead and specimen results in the best measurements.

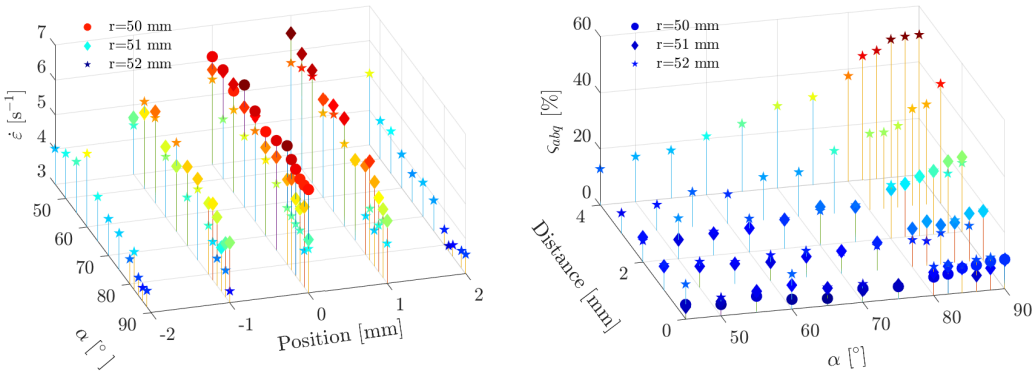

(a) On average strain rate in gauge section **(b)** On measurement accuracy

Figure 5.22: Effect of α, distance and inner radius of the specimen

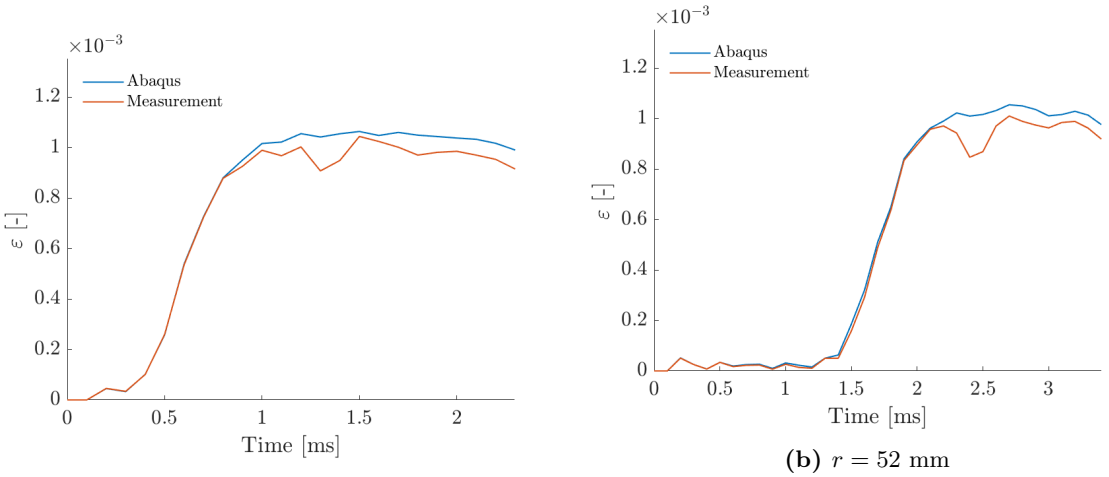

(a) Correctly matched specimen

(b) $r = 52$ mm
horizontal position is -2 mm
distance is 0 mm

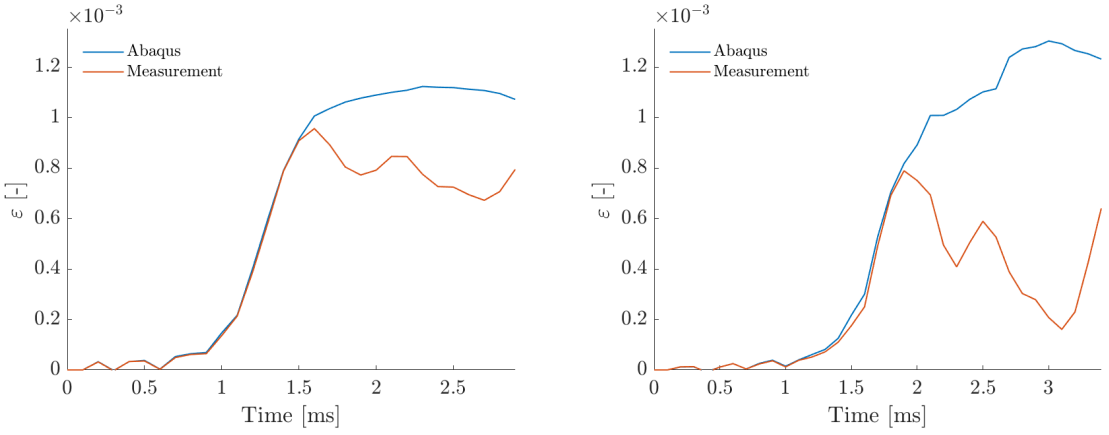

(c) $r = 52$ mm
horizontal position is 0 mm
distance is 2 mm

(d) $r = 52$ mm
horizontal position is 2 mm
distance is 4 mm

Figure 5.23: The difference in strain measurements in the grip section for correctly and incorrectly matched specimens where $\alpha = 90°$, $v_0 = 1.7$ m/s and $m_d = 30$ kg

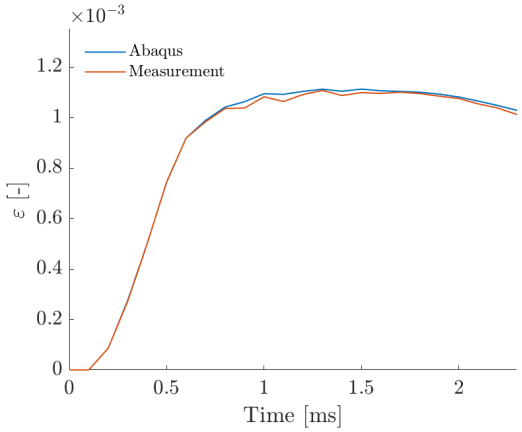

(a) Correctly matched specimen

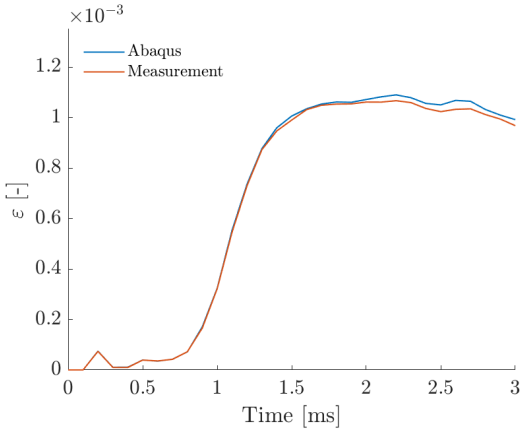

(b) $r = 52$ mm
horizontal position is -2 mm
distance is 0 mm

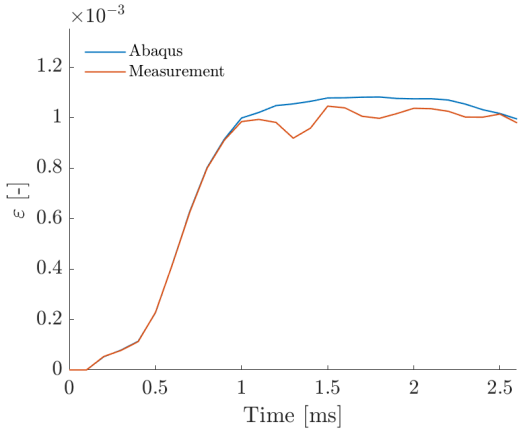

(c) $r = 52$ mm
horizontal position is 0 mm
distance is 2 mm

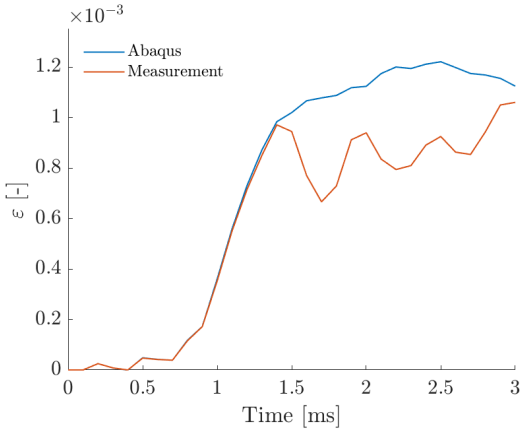

(d) $r = 52$ mm
horizontal position is 2 mm
distance is 4 mm

Figure 5.24: The difference in strain measurements in the grip section for correctly and incorrectly matched specimens where $\alpha = 60°$, $v_0 = 1.7$ m/s and $m_d = 30$ kg

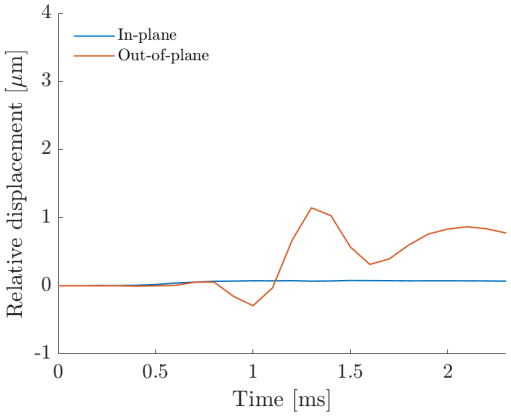

(a) Correctly matched specimen

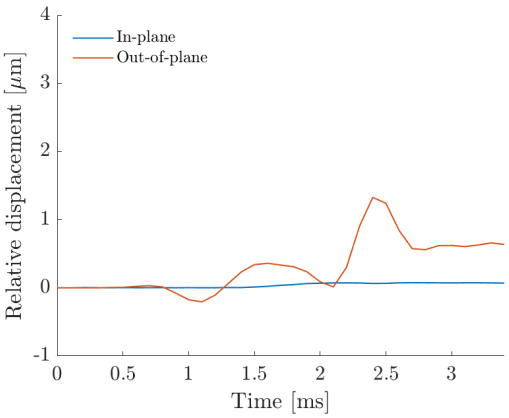

(b) $r = 52$ mm
horizontal position is -2 mm
distance is 0 mm

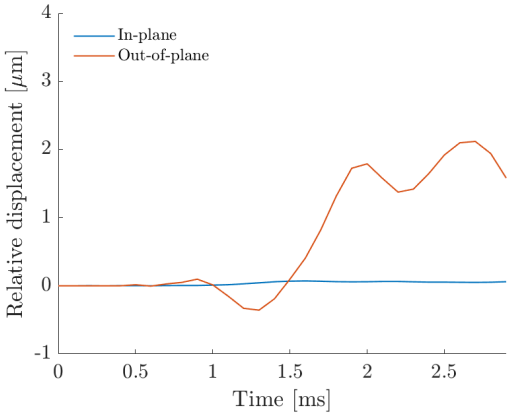

(c) $r = 52$ mm
horizontal position is 0 mm
distance is 2 mm

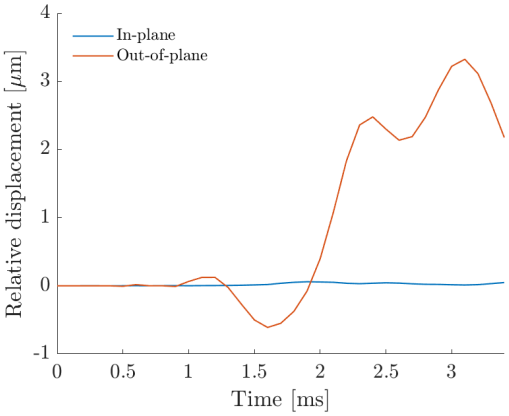

(d) $r = 52$ mm
horizontal position is 2 mm
distance is 4 mm

Figure 5.25: The difference in relative displacements of the reference points in the grip section (location can be found in figure 4.2) for correctly and incorrectly matched specimens where $\alpha = 90°$, $v_0 = 1.7$ m/s and $m_d = 30$ kg

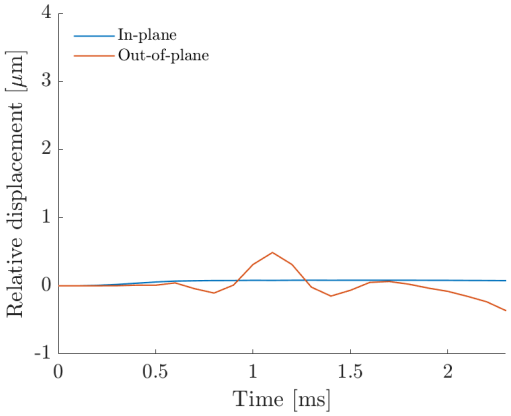

(a) Correctly matched specimen

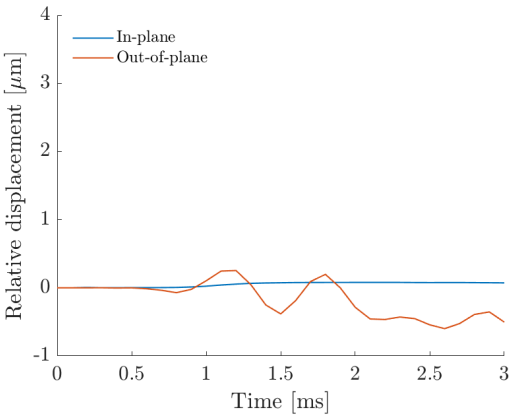

(b) $r = 52$ mm
horizontal position is -2 mm
distance is 0 mm

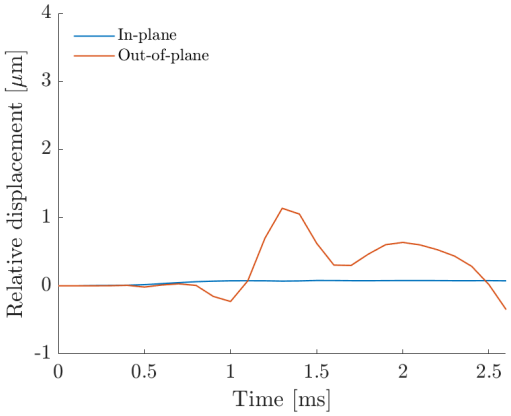

(c) $r = 52$ mm
horizontal position is 0 mm
distance is 2 mm

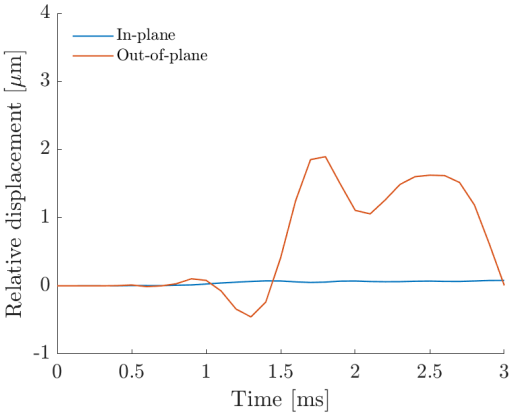

(d) $r = 52$ mm
horizontal position is 2 mm
distance is 4 mm

Figure 5.26: The difference in relative displacements of the reference points in the grip section (location can be found in figure 4.2) for correctly and incorrectly matched specimens where $\alpha = 60°$, $v_0 = 1.7$ m/s and $m_d = 30$ kg

5.2.7 Example experiment

In order to apply the conclusions drawn in the previous sections to an actual experiment and illustrate some of the trade-offs to be made, figure 5.27 and figure 5.28 present the strain rate as a function time and stress-strain curve, respectively, of various experiments that reach the same average strain rate of around 16 s^{-1}, but show significantly different results. For each experiment, it is assumed that the DIC equipment has the same frame rate and thus measurement frequency.

The first experiment has a high velocity of 5 m/s and low mass of 3 kg. As mentioned in section 5.2.2 on the effect of mass and velocity, compared to the other experiments, this case has a shorter duration and therefore less measurement data. This is most pronounced in the stress-strain curve in figure 5.28a, where it is clear that this curve has significantly fewer measurement points than the other experiments and, therefore, provides less material data.

The second experiment has a lower velocity of 3 m/s and higher mass of 40 kg. The first thing to notice in figure 5.27b is an increase of the duration by a factor 5 compared to the previous experiment in figure 5.27a. When looking at figure 5.28b, however, it becomes clear that the measurement curve does not match the Abaqus curve. This is caused by plasticity is in the grip section, thereby invalidating the experiment, as discussed in section 5.2.1 on width of the grip section.

Plasticity in the grip section can, for example, be addressed by a wider grip section, as is done in the third experiment or by a smaller angle α, as is done in the fourth experiment such that, in both cases, plasticity is no longer present in the grip section. The resulting average strain rate is slightly higher in the third experiment, but a comparison between figure 5.27c and figure 5.27d shows there is little difference between the actual strain rate curves, except that reducing the angle alpha has resulted in a smoother strain rate curve with fewer oscillations. This is also reflected in the stress-strain curves in figure 5.28c and figure 5.28d, where the reduced oscillations result in a smoother stress-strain curve.

Furthermore, making the grip section wider results in smaller deformations in the grip section. This is illustrated in figure 5.29, which shows the relative displacements of the reference points in the grip section for the third and fourth experiment. As can be seen, the displacements in the narrow grip section are up to 20% bigger than those in of the wide grip section, which allows for more accurate measurements.

In conclusion, when comparing these four experimental possibilities to achieve an average strain rate of around 16 s^{-1}, the best choice is the fourth experiment with $v_0 = 3$ m/s, $m_d = 40$ kg, $\alpha = 60°$ and $b_{grip} = 35$ mm.

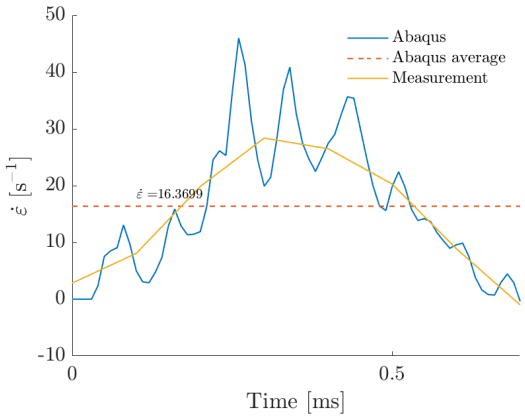

(a) $v_0 = 5$ m/s
$m_d = 3$ kg
$\alpha = 90°$
$b_{grip} = 35$ mm

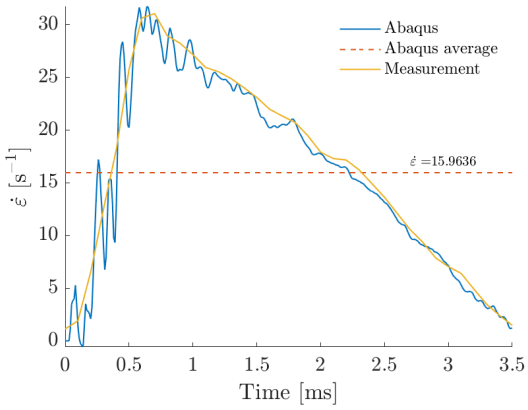

(b) $v_0 = 3$ m/s
$m_d = 40$ kg
$\alpha = 90°$
$b_{grip} = 35$ mm

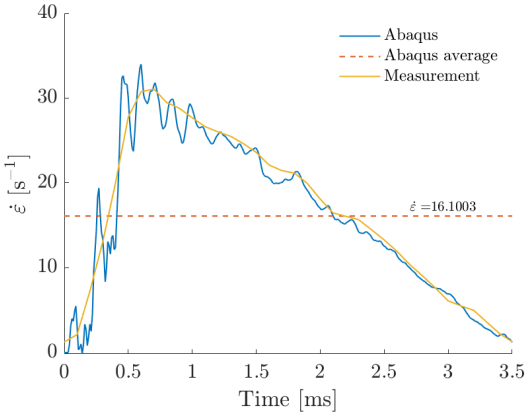

(c) $v_0 = 3$ m/s
$m_d = 40$ kg
$\alpha = 90°$
$b_{grip} = 40$ mm

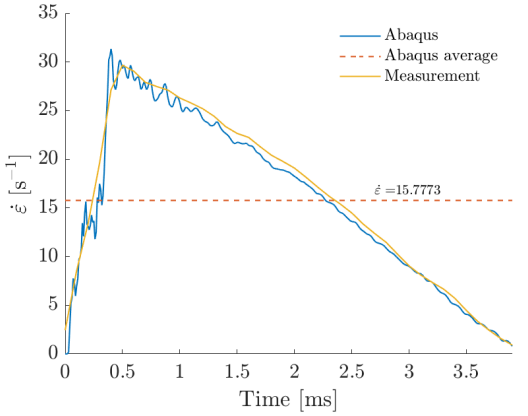

(d) $v_0 = 3$ m/s
$m_d = 40$ kg
$\alpha = 60°$
$b_{grip} = 35$ mm

Figure 5.27: Effect of various parameters on strain rate at a similar average strain rate

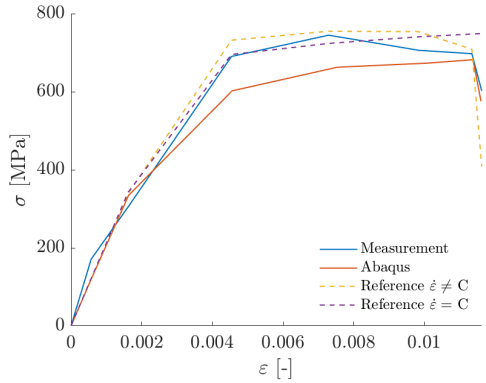

(a) $v_0 = 5$ m/s
$m_d = 3$ kg
$\alpha = 90°$
$b_{grip} = 35$ mm

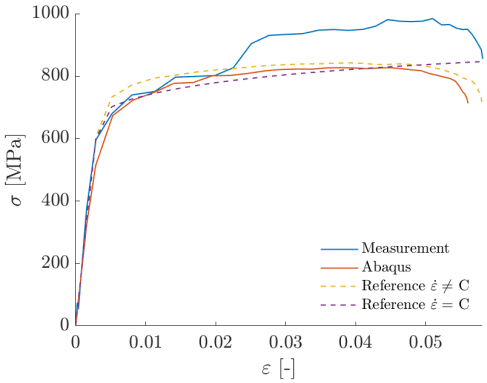

(b) $v_0 = 3$ m/s
$m_d = 40$ kg
$\alpha = 90°$
$b_{grip} = 35$ mm

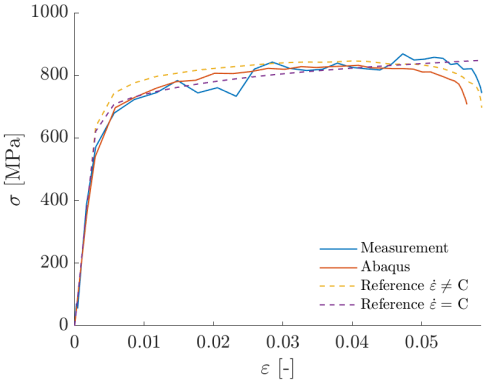

(c) $v_0 = 3$ m/s
$m_d = 40$ kg
$\alpha = 90°$
$b_{grip} = 40$ mm

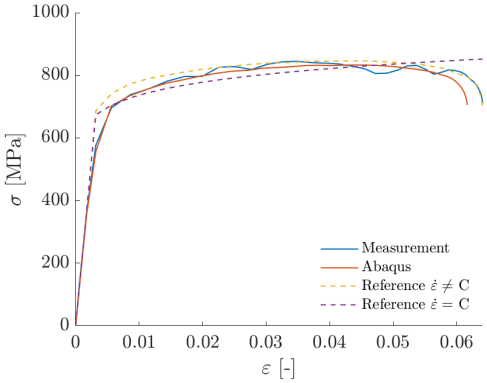

(d) $v_0 = 3$ m/s
$m_d = 40$ kg
$\alpha = 60°$
$b_{grip} = 35$ mm

Figure 5.28: Effect of various parameters on the stress-strain curve at a similar average strain rate

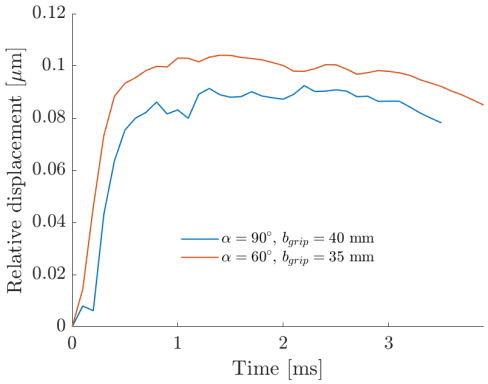

Figure 5.29: Relative in-plane displacement of the reference points in the grip section

Chapter 6

Guideline

This chapter provides a guideline to carry out experiments based on the test method discussed in this thesis and the results presented.

Steps to be taken

1. Perform quasi-static experiments to determine the stress-strain curve at very low strain rates.
2. Use the material data obtained from the quasi-static experiments in a set of FE simulations to determine the desired specimen dimensions, drophead mass, impact velocity and setup parameters for the impact test:
    - Use the impact velocity to tune the strain rate. In general, the velocity should be as low as possible, while being sufficiently high to reach the desired strain rate.
    - Use the drophead mass to tune the duration of the experiment. In general, the drophead mass should be as high as possible, while maintaining the desired strain rate.
    - Adjust the width of the grip section to make sure no plasticity is present in the grip section, while keeping it as narrow as possible for optimal measurement accuracy.
    - Tune the different parameters, from both specimen and setup, such that bending waves are minimised.
    - The length of the specimen should, in general, be kept as low as possible. However, the section between the gauge section and impact section should not be made too short, since a buffer zone is needed between gauge and impact section.
    - The angle α should be between 45° and 75°, preferably around 60° for optimal measurement accuracy.
3. Design the experimental setup using the information of the previous step and considering the following:
    - Ensure a matching drophead and specimen radius.
    - The drophead should be dropped properly in the centre of the specimen.
    - The drophead should not be overly smooth to ensure sufficient friction between drophead and specimen.

- It might be convenient to have a set of different dropheads of which the mass can be further tuned by means of, for example, additional blocks of mass that can be attached to or removed from the drophead.

4. Using DIC as a measurement method, pay attention to the following:
   - The speckle pattern
     Should be random and matte, have high contrast and should not fracture.
   - Camera, lens and environment
     Exposure, lighting of the experiment, field of view, depth of field, line of sight and fish-eye effect.
   - Image spatial resolution versus speckle size
     A single speckle should be captured by at least 3 pixels, but should not be too big.
   - Frame rate
     Should be sufficiently high.
   - Out-of-plane displacements
     Should be avoided when using 2D DIC for the quasi-static experiments.
   - Field of view
     The angle between the 3D DIC cameras should be sufficient, while the line of sight should be kept as optimal as possible.

Chapter 7

Conclusions

In the introduction the main question guiding the research presented in this thesis was posed:

> *How can the effect of strain rate on the tensile stress-strain curve at intermediate strain rates of 10-100 s^{-1} be measured by means of DIC?*

This chapter presents the conclusions of the previous chapters in order to formulate an answer on this question.

7.1 Test method

The test method proposed in this thesis consists of two parts. The first part is a test using a universal testing machine to determine material behaviour at low strain rates of 0.001-10 s^{-1}. A regular dogbone specimen with a longer grip section is used for the UTM tests, which provides the material data to design specimens for the second part. The second part is an impact test where a drophead impacts a specimen, causing it to strain. The specimens are U-shaped strips with a dogbone at either side to test material behaviour at higher strain rates of 10-100 s^{-1}. For both tests, strains are recorded in the grip and gauge sections by means of a DIC system.

The main benefits of the proposed test method are:

- A single system records all measurements, so no time synchronisation of different sensors is needed.
- The DIC system records a complete strain field, providing insight in the strain distribution over the specimen.
- The drophead does not need any sensors and can thus be a piece of material in the right shape with the correct weight.
- A droptower is not strictly needed, another method of dropping the drophead precisely onto the specimen is also sufficient (for example, a drophead guided by a PVC pipe dropped from a height).
- The same experimental setup can easily be used for tests at different strain rates.

7.2 Analytical model

Two analytical models have been developed, one for the universal testing machine tests and one for the impact tests. For each of these, two different material models have been used to model a simplification of mild steel, which in both cases only account for plasticity, while neglecting the contribution of the linear elastic part. The first is the perfectly plastic model, in which the plastic regime is simplified to a constant flow stress for all strains. The second is the linear plastic material model, in which the effect of strain hardening is accounted for by the assumption of a linear stress strain curve in the plastic regime between the yield stress and the ultimate stress. Furthermore, for both models, only deformation of the gauge section is taken into account, while the grip sections and impact section (only in case of the impact test) are assumed to be rigid.

The analytical models for the UTM tests and the impact tests have been compared to a finite element model of the same specimen. For the impact tests, a comparison between three specimen geometries showed that a specimen with a narrow gauge section had the best agreement with the analytical model. The analytical models overestimate the strain in the gauge section, because elastic strain, which is present in the finite element models, is not taken into account by the analytical models. When plastic strain in the gauge section becomes the most dominant component of the strain, both analytical and FE strain curves show good agreement. This is also reflected by the strain rate, which is initially overestimated by the analytical model, after which both models show good agreement. Finally, the stress-strain curves show that both material models provide a decent match with the FE results, thereby verifying the FE models.

It should be noted, however, that, even though the analytical models show reasonable agreement to the FEA results in some cases and can be used to verify the FEA simulations, they do have a limited range of validity related to the underlying assumptions that were made. For example, the assumption of a rigid impact section disregards the energy absorption by the impact section as a result of plastic deformation, while in case of a significant impact there will be plasticity in the impact section absorbing a significant amount of energy. Furthermore, bending waves are not accounted for as a result of the assumption that strain is only in-plane, which is also preferable for the actual experiment, but not necessarily the case. Lastly, the simplification of the material inherently results in an approximation of the stress-strain behaviour of the specimen, which is different from the actual material behaviour.

7.3 Numerical simulations

Numerical simulations of the impact test have been done by means of an explicit, dynamic, non-linear impact simulation using finite element analysis. A mild steel specimen, which is modelled using thin shells, is impacted by a drophead, which is modelled as a rigid solid, at a set impact velocity. The mild steel material model for the specimen is strain rate dependent.

Strain in the grip and gauge section of the specimen are determined by direct FEA output and by post-processing the displacements of two reference points in each section as if they were DIC measurements. The strain in the grip section is converted to stress in the grip section via Hooke's law. The ratio between the cross-sectional areas of the grip and gauge section is then

used to convert the stress from grip to gauge section. Combined with the strains recorded in the gauge section, a stress-strain curve for a certain strain rate can be constructed. The measurement accuracy is defined by the difference between the data obtained directly from the FEA output and the DIC measurements by means of the reference point displacements.

A parametric study has been done using the FE model to determine the effect of various parameters on the strain rate in the gauge section and the measurement accuracy to provide guidelines for the dimensions of the test specimen and the parameters of the experimental setup. The following two lists detail the effect of each tested parameter on either the strain rate in the gauge section or the measurement accuracy based on which the test specimens or experimental setup can be tuned for the highest measurement accuracy at a given target strain rate.

Effects of various parameters on strain rate in the gauge section:

Grip section width As long as a sufficiently wide grip section is selected such that it does not deform plastically, the width of the grip section has negligible influence on the strain rate in the gauge section.

Mass and velocity A higher impact velocity results in a higher initial strain rate, while a heavier drophead takes longer to slow down and therefore results in a smoother strain rate curve and a longer measurement duration.

Bending waves The presence of bending waves decreases the strain rate, since part of the energy is now absorbed by the bending waves instead of axial strain in the specimen.

Length A longer specimen has a lower average strain rate, because the energy from the drophead is distributed over a longer specimen.

Angle α Variation in angle α has hardly any direct effect on the strain rate, but does have an effect on the presence of bending waves and through this on the strain rate.

Mismatch and misalignment A mismatch or misalignment between the specimen and drophead introduces larger bending waves resulting in a lower average strain rate.

Friction More friction results in a higher strain rate because more energy is transferred from the drophead to the specimen.

Effects of various parameters on measurement accuracy:

Grip section width Selecting the correct width of the grip section for the most accurate measurements is trade-off between, on the one hand, selecting a grip section that is wide enough to avoid plasticity, while, on the other hand, keeping it as narrow as possible to avoid measurement inaccuracies resulting from too little strain to be measured.

Mass and velocity In general, a higher mass results in smoother and more accurate measurements. Furthermore, a higher impact velocity results in less bending waves and therefore more accurate measurements. But, when the overall energy input is too high, the grip section will deform plastically rendering the measurement invalid.

Bending waves The presence of bending waves decreases the measurement accuracy, since the out-of-plane bending introduces a non-homogeneous strain through the thickness of the specimen.

Length In general a shorter grip section and shorter section between the gauge section and impact section yields the most accurate measurements. However, the section between the gauge section and impact section should not be made too short, since a buffer zone is needed between gauge and impact section for accurate measurements in the gauge section. Furthermore, a short grip section is also beneficial for the DIC measurements, since a smaller field of view of the camera is required, thereby increasing the accuracy of the DIC measurements.

Angle α The highest measurement accuracy is obtained for alpha in the range of 45° to 75° with the best results around an angle of 60°.

Mismatch and misalignment In general, a longer distance between the measurement section and impact location of the drophead results in a loss of measurement accuracy. However, the effect of a mismatch or misalignment between the specimen and drophead is strongly affected by the angle α of the specimen. Lower values of α reduce the effect of a mismatch and misalignment, but the best results are still obtained for a perfectly matched specimen and drophead that is dropped nicely in the centre of the specimen.

Friction Some friction is beneficial for the measurement accuracy, but once sufficient friction is present, there is no further impact on the measurement accuracy.

Chapter 8

Recommendations

The test method presented in this thesis is only a single step towards a generally accepted best test method for testing intermediate strain rates. The next step would be to perform a set of experiments, using different measurement methods to compare the results and validate the proposed measurement method. Furthermore, the same material should be tested using multiple different test methods at the same strain rate to validate the proposed test method. One could, for example, test at 10 s^{-1} using the proposed test method and a (fast) hydraulic test machine. Further research to improve and expand the proposed test method can be done in several different directions:

Different materials Investigate the test methodology for different materials for both the specimen and drophead. One could even consider a different material for the impact section compared to the grip and gauge sections, when the specimen is not made from a single sheet of material. For the drophead, a different material could, for example, influence stress waves, bending waves or the transmission of impact energy.

Strain measurements on both sides of the specimen Investigate the possibility to measure strain on two sides of the specimen to: on the one hand, measure bending waves and, on the other hand, have the possibility to average the strain between both sides of the specimen to eliminate the influence of bending waves on the measured strains, as was shown by Yang et al. (2014).

Damping between specimen and drophead Investigate the effect of a layer of damping material between the specimen and the drophead to mitigate stress waves and bending waves in the specimen.

Shape and size of the drophead Investigate the effect of the shape and size of the drophead, one could think of a solid U-shape as a drophead or the effect of a larger radius for both drophead and specimen.

Linear elasticity in analytical model Expand the analytical model to include linear elastic material behaviour.

Appendix A

Derivation of analytical model impact specimen

In this appendix, the analytical model given in chapter 3 is derived in more detail. The setup of the impact test is described in section 2.3. Figure A.1 illustrates the setup and simplifications for the analytical computations. The top of the specimen is clamped and the middle section (yellow) is impacted by the drophead (green). The dogbone part (blue) is simplified to three rectangles, of which the grip section, L_{grip}, and section towards the middle, L_{tm}, are assumed to be rigid, while the gauge section deforms plastically, similar to the assumptions for the analytical model of the flat specimen. Next, the middle section is also assumed to be rigid such that the displacement of the two dogbones is directly given by the displacement of the drophead, $u_d(t)$, and the angle α. Finally, since the strain is small compared to the total length, the angle α is assumed to stay constant during the deformation.

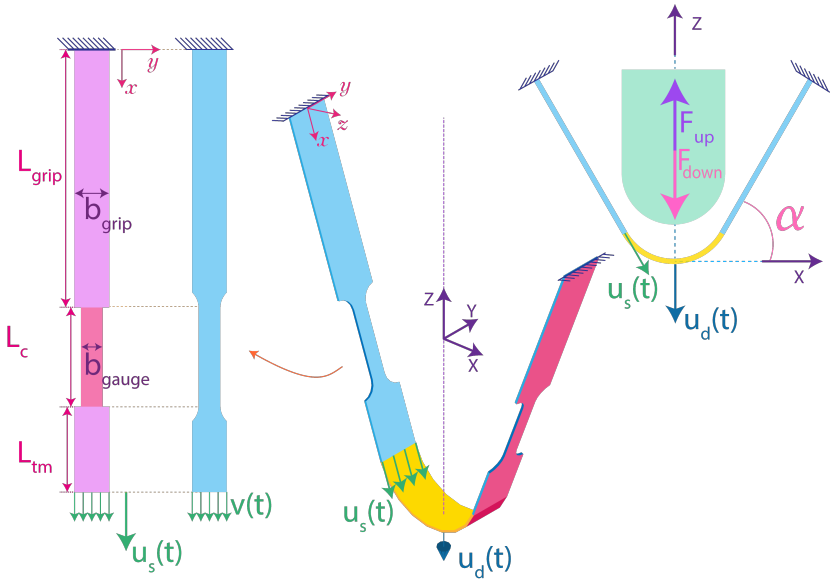

Figure A.1: Definitions analytical model

A.1 Perfectly plastic

The stress strain curve of the rigid perfectly plastic case is given in figure A.2.

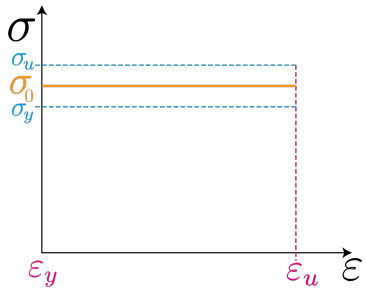

Figure A.2: Stress-strain curve for rigid perfectly plastic material

Start with Newtons second law of motion in the drophead:

$$\begin{aligned} \Sigma F_Z &= F_{up} \\ &= m_d \cdot \frac{\mathrm{d}^2 u_d(t)}{\mathrm{d}t^2} \end{aligned} \tag{A.1}$$

F_{up} is the force exerted by the specimen on the drophead:

$$F_{up} = -2 \cdot \sigma_0 \cdot A_0 \cdot \sin(\alpha) \tag{A.2}$$

Resulting in:

$$\Sigma F_Z = -2 \cdot \sigma_0 \cdot A_0 \cdot \sin(\alpha) = m_d \cdot \frac{\mathrm{d}^2 u_d(t)}{\mathrm{d}t^2} \tag{A.3}$$

Divide by m_d :

$$\frac{\mathrm{d}^2 u_d(t)}{\mathrm{d}t^2} = -\frac{\sigma_0 \cdot 2 \cdot A_0 \cdot \sin(\alpha)}{m_d} \tag{A.4}$$

Integrate the acceleration to get the velocity:

$$\begin{aligned} \int \frac{\mathrm{d}^2 u_d(t)}{\mathrm{d}t^2} \mathrm{d}t = \frac{\mathrm{d}u_d(t)}{\mathrm{d}t} &= v_d(t) \\ &= \int \left(-\frac{2 \cdot \sigma_0 \cdot A_0 \cdot \sin(\alpha)}{m_d} \right) \mathrm{d}t \\ &= -\frac{2 \cdot \sigma_0 \cdot A_0 \cdot \sin(\alpha) \cdot t}{m_d} + c \end{aligned} \tag{A.5}$$

The velocity at $t = 0$ is the impact velocity v_0:

$$c = v_0 \tag{A.6}$$

$$v_d(t) = -\frac{2 \cdot \sigma_0 \cdot A_0 \cdot \sin(\alpha) \cdot t}{m_d} + v_0 \tag{A.7}$$

Integrate the velocity to get displacement:

$$\begin{aligned}\int \frac{\mathrm{d}u_d(t)}{\mathrm{d}t}\mathrm{d}t &= u_d(t) \\ &= \int \left(-\frac{2\cdot\sigma_0\cdot A_0\cdot\sin(\alpha)\cdot t}{m_d} + v_0\right)\mathrm{d}t \\ &= -\frac{\sigma_0\cdot A_0\cdot\sin(\alpha)\cdot t^2}{m_d} + v_0\cdot t + c\end{aligned} \tag{A.8}$$

The displacement at $t = 0$ is 0:

$$c = 0 \tag{A.9}$$

$$u_d(t) = -\frac{\sigma_0\cdot A_0\cdot\sin(\alpha)\cdot t^2}{m_d} + v_0\cdot t \tag{A.10}$$

Use the displacement to determine the engineering strain:

$$\varepsilon_e(t) = \frac{\Delta L(t)}{L_{c,0}} \tag{A.11}$$

$$\Delta L(t) = u_s(t) = \frac{u_d(t)}{\sin(\alpha)} \tag{A.12}$$

$$\varepsilon_e(t) = \frac{u_d(t)}{L_{c,0}\cdot\sin(\alpha)} = -\frac{\sigma_0\cdot A_0\cdot t^2}{m_d\cdot L_{c,0}} + \frac{v_0}{L_{c,0}\cdot\sin(\alpha)}\cdot t \tag{A.13}$$

And the engineering strain rate:

$$\dot{\varepsilon}_e = \frac{v_d(t)}{L_{c,0}\cdot\sin(\alpha)} \tag{A.14}$$

$$= -\frac{2\cdot\sigma_0\cdot A_0\cdot t}{m_d\cdot L_{c,0}} + \frac{v_0}{L_{c,0}\cdot\sin(\alpha)} \tag{A.15}$$

A.2 Linear plastic

The stress strain curve of the rigid linear plastic case is given in figure A.3.

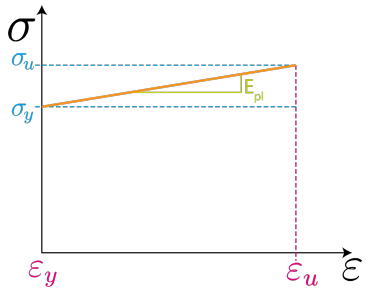

Figure A.3: Stress-strain curve for rigid linear plastic material

.

Start with Newtons second law of motion in the drophead:

$$\Sigma F_Z = m_d \cdot \frac{\mathrm{d}^2 u_d(t)}{\mathrm{d}t^2} \tag{A.16}$$

F_{up} is the force exerted by the specimen on the drophead:

$$F_{up} = -\left(\sigma_y + E_{pl} \cdot \varepsilon_e\right) \cdot 2 \cdot A_0 \cdot \sin(\alpha) \tag{A.17}$$

Resulting in:

$$\begin{aligned} \Sigma F_Z &= -\left(\sigma_y + E_{pl} \cdot \varepsilon_e\right) \cdot 2 \cdot A_0 \cdot \sin(\alpha) \\ &= -2 \cdot \sigma_y \cdot A_0 \cdot \sin(\alpha) - 2 \cdot E_{pl} \cdot \varepsilon_e \cdot A_0 \cdot \sin(\alpha) \end{aligned} \tag{A.18}$$

Divide by m_d :

$$\frac{\mathrm{d}^2 u_d(t)}{\mathrm{d}t^2} = -\frac{2 \cdot \sigma_y \cdot A_0 \cdot \sin(\alpha)}{m_d} - \frac{2 \cdot E_{pl} \cdot \varepsilon_e \cdot A_0 \cdot \sin(\alpha)}{m_d} \tag{A.19}$$

Use the displacement to determine the engineering strain:

$$\varepsilon_e = \frac{u_d(t)}{L_{c,0} \cdot \sin(\alpha)} \tag{A.20}$$

$$\frac{\mathrm{d}^2 u_d(t)}{\mathrm{d}t^2} = -\frac{2 \cdot \sigma_y \cdot A_0 \cdot \sin(\alpha)}{m_d} - \frac{2 \cdot E_{pl} \cdot A_0}{L_{c,0} \cdot m_d} \cdot u_d(t) \tag{A.21}$$

This is a second order linear ODE:

$$\frac{\mathrm{d}^2 u_d(t)}{\mathrm{d}t^2} = -C_1 - C_2 \cdot u_d(t) \tag{A.22}$$

in which:

$$C_1 = \frac{2 \cdot \sigma_y \cdot A_0 \cdot \sin(\alpha)}{m_d}$$

$$C_2 = \frac{2 \cdot E_{pl} \cdot A_0}{L_{c,0} \cdot m_d}$$

The solution is:

$$u_d(t) = -\frac{C_1}{C_2} + C_3 \ \sin\left(\sqrt{C_2}\cdot t\right) + C_4 \ \cos\left(\sqrt{C_2}\cdot t\right) \tag{A.23}$$

The displacement at $t = 0$ is 0:

$$u_d(0) = -\frac{C_1}{C_2} + C_4 \Rightarrow \frac{C_1}{C_2} = C_4 = \frac{\sigma_y \cdot L_{c,0}}{E_{pl}} \tag{A.24}$$

The velocity at $t = 0$ is the impact velocity v_0:

$$\frac{\mathrm{d}u_d(t)}{\mathrm{d}t} = v_d(t) = C_3\sqrt{C_2} \ \cos\left(\sqrt{C_2}\cdot t\right) - C_4\sqrt{C_2} \ \sin\left(\sqrt{C_2}\cdot t\right) \tag{A.25}$$

$$v_d(0) = C_3\sqrt{C_2} = v_0 \quad \Rightarrow \quad \frac{v_0}{\sqrt{C_2}} = C_3 \tag{A.26}$$

The displacement of the drophead is:

$$u_d(t) = -\frac{C_1}{C_2} + C_3 \ \sin\left(\sqrt{C_2}\cdot t\right) + C_4 \ \cos\left(\sqrt{C_2}\cdot t\right) \tag{A.27}$$

in which:

$$C_1 = \frac{2\cdot\sigma_y\cdot A_0\cdot\sin(\alpha)}{m_d}$$

$$C_2 = \frac{2\cdot E_{pl}\cdot A_0}{L_{c,0}\cdot m_d}$$

$$C_3 = \frac{v_0}{\sqrt{C_2}} = \frac{v_0\cdot\sqrt{L_{c,0}\cdot m_d}}{\sqrt{2\cdot E_{pl}\cdot A_0}}$$

$$C_4 = \frac{C_1}{C_2} = \frac{\sigma_y\cdot L_{c,0}\cdot\sin(\alpha)}{E_{pl}}$$

Resulting in:

$$u_d(t) = -\frac{\sigma_y\cdot L_{c,0}\cdot\sin(\alpha)}{E_{pl}} + \frac{v_0\cdot\sqrt{L_{c,0}\cdot m_d}}{\sqrt{2\cdot E_{pl}\cdot A_0}} \ \sin\left(\sqrt{\frac{2\cdot E_{pl}\cdot A_0}{L_{c,0}\cdot m_d}}\cdot t\right) + \frac{\sigma_y\cdot L_{c,0}\cdot\sin(\alpha)}{E_{pl}} \ \cos\left(\sqrt{\frac{2\cdot E_{pl}\cdot A_0}{L_{c,0}\cdot m_d}}\cdot t\right) \tag{A.28}$$

Use the displacement to determine the strain:

$$\varepsilon_e(t) = \frac{u_d(t)}{L_{c,0}\cdot\sin(\alpha)} = \frac{-\frac{C_1}{C_2} + C_3 \ \sin\left(\sqrt{C_2}\cdot t\right) + C_4 \ \cos\left(\sqrt{C_2}\cdot t\right)}{L_{c,0}\cdot\sin(\alpha)} \tag{A.29}$$

$$= -\frac{\sigma_y}{E_{pl}} + \frac{v_0\cdot\sqrt{m_d}}{\sin(\alpha)\cdot\sqrt{L_{c,0}\cdot E_{pl}\cdot 2\cdot A_0}} \ \sin\left(\sqrt{\frac{2\cdot E_{pl}\cdot A_0}{L_{c,0}\cdot m_d}}\cdot t\right) + \frac{\sigma_y}{E_{pl}} \ \cos\left(\sqrt{\frac{2\cdot E_{pl}\cdot A_0}{L_{c,0}\cdot m_d}}\cdot t\right)$$

And the engineering strain rate:

$$\dot{\varepsilon}_e = \frac{v_d(t)}{L_{c,0}\cdot\sin(\alpha)} \tag{A.30}$$

$$= \frac{C_3\sqrt{C_2} \ \cos\left(\sqrt{C_2}\cdot t\right) - C_4\sqrt{C_2} \ \sin\left(\sqrt{C_2}\cdot t\right)}{L_{c,0}\cdot\sin(\alpha)}$$

$$= \frac{v_0}{L_{c,0}\cdot\sin(\alpha)} \ \cos\left(\sqrt{\frac{2\cdot E_{pl}\cdot A_0}{L_{c,0}\cdot m_d}}\cdot t\right) - \frac{\sigma_y}{\sqrt{E_{pl}}}\sqrt{\frac{2\cdot A_0}{L_{c,0}\cdot m_d}} \ \sin\left(\sqrt{\frac{2\cdot E_{pl}\cdot A_0}{L_{c,0}\cdot m_d}}\cdot t\right)$$

Appendix B

Python code to generate model

This appendix provides python code which can be used to generate the FEA models in Abaqus 2018.

Main.py

This file is used as the main file from which all other files are called and in which most of the variables are defined.

```
from abaqus import *
from abaqusConstants import *
backwardCompatibility.setValues(includeDeprecated=True, reportDeprecated=False)
from caeModules import *
import sketch
import part
import regionToolset
import section
import material
import assembly
import step
import load
import mesh
import job
import visualization

modelname='MyModelName'
jobname= modelname

# Variabels drophead
r=50.0 #[mm] Radius of drophead
m_drophead= 0.03 # [*1000 kg] mass of drophead (0.03 = 30 kg)
v_0 = -(float(17)*100) # [mm/s] initial velocity of drophead (15 is 1.5 m/s)
rho=7800 # [kg/m^3]
h=((m_drophead*1000)/rho-4./6.*(r/1000)**3.*pi)/(pi*(r/1000)**2)*1000 #[mm] Height of drophead

# Variabels specimen
B=35.0 # [mm] Width of specimen
t = 2.0 # [mm] thickness
alpha = float(60) # [deg] Python works in radians, whereas Abaqus works in degrees.
alphaRad = radians(alpha) # [rad] alpha in rad
alphaMiddle= radians(90-alpha) # [rad] angle of semicircle
r_specimen = float(valueSpecimen) + t/2 # [mm] radius of specimen
b = 12.5 # [mm]
```

```
L_L = 150.0 # [mm]
R = 12.5 # [mm]
L_c = 57.0 # [mm]
L_tm = 50.0 # [mm]
L_R= sqrt(R**2 - (R-((B-b)/2))**2 ) # [mm]
L = L_L+L_c+2*L_R+L_tm # [mm]
MeshSize = B/16 # Mesh size aan boven kant specimen

# General variables
Duration=0.005 # [s]
SRF=str(float(3)/10) # Strain rate factor
FricCoeff=0.5 # Friction Coefficient
dx = float(value) # [mm] offset of drophead tov middle of specimen
dy = 0.5+ (-sqrt(r_specimen**2 - abs(dx)**3 )+r_specimen)# [mm] clearance between drophead and specimen

myModel = mdb.Model(name=modelname)

# # # Choose rigid or deformable drophead # # #
# Comment the lines that run the other files

# # # For rigid drophead:
execfile('C:\...\...\PartsSpecimen.py')
execfile('C:\...\...\PartsRigidDrophead.py')
execfile('C:\...\...\Material.py')
execfile('C:\...\...\Section.py')
execfile('C:\...\...\Instance.py')
execfile('C:\...\...\Sets.py')
execfile('C:\...\...\Meshen.py')
execfile('C:\...\...\Step.py')
execfile('C:\...\...\Output.py')
execfile('C:\...\...\Contact.py')
execfile('C:\...\...\BC.py')
# # # # # # # # # # # # # # # # # # # # # # # # #

# # # For deformable drophead:
execfile('C:\...\...\PartsSpecimen.py')
execfile('C:\...\...\PartsDeformableDrophead.py')
execfile('C:\...\...\Material.py')
execfile('C:\...\...\Section.py')
execfile('C:\...\...\SectionDeformableDrophead.py')
execfile('C:\...\...\InstanceDeformableDrophead.py')
execfile('C:\...\...\Sets.py')
execfile('C:\...\...\Meshen.py')
execfile('C:\...\...\MeshenDeformableDrophead.py')
execfile('C:\...\...\Step.py')
execfile('C:\...\...\OutputDeformableDrophead.py')
execfile('C:\...\...\ContactDeformableDrophead.py')
execfile('C:\...\...\BCDeformableDrophead.py')
# # # # # # # # # # # # # # # # # # # # # # # # #

# # #
# # # # # # # # # Job # # # # # # # # # # # # #
# # #
myJob=mdb.Job(name=jobname, model=myModel, description='Description of the job')
myJob.writeInput(consistencyChecking=OFF)
```

PartsSpecimen.py

This file is used to generate the specimen part.

```
# # #
# # # # # # # # # Specimen Geometry # # # # # # # # # # # #
# # #
SketchSpecimen = myModel.ConstrainedSketch(name='Sketch side view of specimen', sheetSize=100)
```

```
PartSpecimen = myModel.Part(name='Specimen', dimensionality=THREE_D, type=DEFORMABLE_BODY)

# Sketch Specimen
P1 = (-abs(cos(alphaMiddle))*r_specimen, -abs(sin(alphaMiddle))*r_specimen)
P2 = (abs(cos(alphaMiddle))*r_specimen, -abs(sin(alphaMiddle))*r_specimen)
P3 = ( abs(cos(alphaMiddle))*r_specimen+abs(cos(alphaRad))*L , -abs(sin(alphaMiddle))*r_specimen+abs(sin
    (alphaRad))*L )
P4 = ( -abs(cos(alphaMiddle))*r_specimen-abs(cos(alphaRad))*L , -abs(sin(alphaMiddle))*r_specimen+abs(
    sin(alphaRad))*L )
SketchSpecimen.ArcByCenterEnds(center=(0.0, 0.0), point1=P1, point2=P2, direction=COUNTERCLOCKWISE)
SketchSpecimen.Line(point1=P2, point2=P3)
SketchSpecimen.Line(point1=P1, point2=P4)
PartSpecimen.BaseShellExtrude(sketch=SketchSpecimen, depth=B)

# Cutsketch for specimen
# cutsketch is made in plane, this plane is later projected on the plane of the specimen.
CutSketchSpecimen = myModel.ConstrainedSketch(name='Cut sketch for specimen', sheetSize=100)
C1 = ( L_L , 0.0 )
C2 = ( (L_L+L_R) , (B-b)/2 )
C3 = ( (L_L+L_R+L_c), (B-b)/2 )
C4 = ( (L_L+2*L_R+L_c) , 0.0 )
CM1 = ( (L_L+L_R) , ((B-b)/2-R))
CM2 = ( (L_L+L_R+L_c) , ((B-b)/2-R) )
C11 = ( L_L , B )
C12 = ( (L_L+L_R) , B-(B-b)/2 )
C13 = ( (L_L+L_R+L_c), B-(B-b)/2 )
C14 = ( (L_L+2*L_R+L_c) , B )
CM11 = ( (L_L+L_R) , ((B-b)/2+b+R))
CM12 = ( (L_L+L_R+L_c) , ((B-b)/2+b+R) )
CutSketchSpecimen.ArcByCenterEnds(center=CM1 , point1=C1, point2=C2, direction=CLOCKWISE)
CutSketchSpecimen.ArcByCenterEnds(center=CM2 , point1=C3, point2=C4, direction=CLOCKWISE)
CutSketchSpecimen.Line(point1=C2, point2=C3)
CutSketchSpecimen.Line(point1=C1, point2=C4)
CutSketchSpecimen.ArcByCenterEnds(center=CM11 , point1=C11, point2=C12, direction=COUNTERCLOCKWISE)
CutSketchSpecimen.ArcByCenterEnds(center=CM12 , point1=C13, point2=C14, direction=COUNTERCLOCKWISE)
CutSketchSpecimen.Line(point1=C12, point2=C13)
CutSketchSpecimen.Line(point1=C11, point2=C14)
y_revolve=P2[0]/cos(alphaRad) # Distance where two lines cross each other measured from the bottom of
    the dogbone
CutSketchSpecimen.ConstructionLine(point1=(y_revolve+L, 0 ) , angle=90)

# Cut out using the cutsketch
f, e = PartSpecimen.faces, PartSpecimen.edges
SP=f.getByBoundingBox(xMax= P1[0])
SUE=e.findAt((P1[0], P1[1], B/2), )
transf = PartSpecimen.MakeSketchTransform(sketchPlane=SP[0], sketchUpEdge=SUE, sketchPlaneSide=SIDE1,
    sketchOrientation=RIGHT, origin=(-abs(cos(alphaMiddle))*r_specimen-abs(cos(alphaRad))*L , -abs(sin(
    alphaMiddle))*r_specimen+abs(sin(alphaRad))*L, 0))
s = myModel.ConstrainedSketch(name='TijdelijkeCutSketch', sheetSize=224.84, gridSpacing=5.62, transform=
    transf)
g, v, d, c = s.geometry, s.vertices, s.dimensions, s.constraints
PartSpecimen.projectReferencesOntoSketch(sketch=s, filter=COPLANAR_EDGES)
s.retrieveSketch(sketch=CutSketchSpecimen)

# If alpha is 90 deg, don't use cutrevolve but extrude
if alpha == 90.0:
PartSpecimen.CutExtrude(sketchPlane=SP[0], sketchUpEdge=SUE, sketchPlaneSide=SIDE1, sketchOrientation=
    RIGHT, sketch=s)
else:
PartSpecimen.CutRevolve(sketchPlane=SP[0], sketchUpEdge=SUE, sketchPlaneSide=SIDE1, sketchOrientation=
    RIGHT, sketch=s, angle=180.0, flipRevolveDirection=OFF)

del myModel.sketches['TijdelijkeCutSketch']

# Make partitions
PartitionSketchSpecimen = myModel.ConstrainedSketch(name='Partition sketch for specimen', sheetSize=100)
```

```
PP1 = ( 0.0 , B/2 )
PP2 = ( L_L , B/2 )
PP3 = ( (L_L+2*L_R+L_c+(B-b)/3) , B/2 )
PP4 = ( L , B/2 )
PartitionSketchSpecimen.Line(point1=PP1, point2=PP4)
PartitionSketchSpecimen.Line(point1=PP3, point2=C4)
PartitionSketchSpecimen.Line(point1=PP3, point2=C14)

# Make square in the middle of the gauge section, Smal
SQM = ( (L_L+L_R+L_c/2) , B/2 )
SQA1 = ( (L_L+L_R+L_c/2-25.0) , (B-b)/2 )
SQE1 = ( (L_L+L_R+L_c/2-25.0) , B-(B-b)/2)
SQA3 = ( (L_L+L_R+L_c/2) , (B-b)/2 )
SQE3 = ( (L_L+L_R+L_c/2) , B-(B-b)/2)
SQA5 = ( (L_L+L_R+L_c/2+25.0) , (B-b)/2 )
SQE5 = ( (L_L+L_R+L_c/2+25.0) , B-(B-b)/2)
PartitionSketchSpecimen.Line(point1=SQA1, point2=SQE1)
PartitionSketchSpecimen.Line(point1=SQA3, point2=SQE3)
PartitionSketchSpecimen.Line(point1=SQA5, point2=SQE5)
PartitionSketchSpecimen.Line(point1=C2, point2=C12)
PartitionSketchSpecimen.Line(point1=C3, point2=C13)

# Create reference points in grip section: Breed
CBA1 = ( L_L/4 , 0 )
CBA3 = ( L_L/2 , 0 )
CBA5 = ( L_L*3/4 , 0 )
CBC1 = ( L_L/4 , B/2 )
CBC3 = ( L_L/2 , B/2 )
CBC5 = ( L_L*3/4 , B/2 )
CBE1 = ( L_L/4 , B )
CBE3 = ( L_L/2 , B )
CBE5 = ( L_L*3/4 , B )
PartitionSketchSpecimen.Line(point1=CBA1, point2=CBC1)
PartitionSketchSpecimen.Line(point1=CBC1, point2=CBE1)
PartitionSketchSpecimen.Line(point1=CBA3, point2=CBC3)
PartitionSketchSpecimen.Line(point1=CBC3, point2=CBE3)
PartitionSketchSpecimen.Line(point1=CBA5, point2=CBC5)
PartitionSketchSpecimen.Line(point1=CBC5, point2=CBE5)

# First partition sketch
f, e = PartSpecimen.faces, PartSpecimen.edges
SUE= e.getByBoundingBox(zMax=B+0.001, zMin=B-0.001, xMin=P4[0], xMax=P1[0])
SP=f.getByBoundingBox(xMax= P1[0])
transf = PartSpecimen.MakeSketchTransform(sketchPlane=SP[0], sketchUpEdge=SUE[0], sketchOrientation=TOP,
      origin=(P4[0], P4[1], 0))

s = myModel.ConstrainedSketch(name='TijdelijkePartitionSketch', sheetSize=224.84, gridSpacing=5.62,
     transform=transf)
g, v, d, c = s.geometry, s.vertices, s.dimensions, s.constraints
s.retrieveSketch(sketch=PartitionSketchSpecimen)
PartSpecimen.PartitionFaceBySketch(sketchUpEdge=SUE[0], faces=SP[0], sketch=s, sketchOrientation=TOP)
del myModel.sketches['TijdelijkePartitionSketch']

# Second partition sketch, is voor de andere kant
SUE= e.getByBoundingBox(zMax=B+0.001, zMin=B-0.001, xMin=P2[0], xMax=P3[0])
SP=f.getByBoundingBox(xMin= P2[0])
transf = PartSpecimen.MakeSketchTransform(sketchPlane=SP[0], sketchUpEdge=SUE[0], sketchPlaneSide=SIDE1,
      sketchOrientation=BOTTOM, origin=(P3[0], P3[1], B))
s = myModel.ConstrainedSketch(name='TijdelijkePartitionSketch', sheetSize=224.84, gridSpacing=5.62,
     transform=transf)
g, v, d, c = s.geometry, s.vertices, s.dimensions, s.constraints
s.retrieveSketch(sketch=PartitionSketchSpecimen)
PartSpecimen.PartitionFaceBySketch(sketchUpEdge=SUE[0], faces=SP[0], sketch=s, sketchOrientation=BOTTOM)
del myModel.sketches['TijdelijkePartitionSketch']

# Make partition impact section
```

```
P11 = (-abs(cos(alphaMiddle))*r_specimen, -abs(sin(alphaMiddle))*r_specimen, B/2)
P21 = (abs(cos(alphaMiddle))*r_specimen, -abs(sin(alphaMiddle))*r_specimen, B/2 )
SP = f.getByBoundingBox(yMax= P2[1])
PartSpecimen.PartitionFaceByShortestPath(point1=P11, point2=P21, faces=SP[0])

P00 = (0, -r_specimen, 0)
P01 = (0 , -r_specimen, B )
SP = f.getByBoundingBox(yMax= P2[1])
PartSpecimen.PartitionFaceByShortestPath(point1=P00, point2=P01, faces=SP)

# Edges partition
e1 = PartSpecimen.edges
#Breed: Grip section
e11 = e1.getByBoundingBox(
  xMin= P4[0]+abs(cos(alphaRad))*CBA5[0] - 1.E-6,
  xMax= P4[0]+abs(cos(alphaRad))*CBA5[0] + 1.E-6,
  yMin= P4[1]-abs(sin(alphaRad))*CBA5[0] - 1.E-6,
  yMax= P4[1]-abs(sin(alphaRad))*CBA5[0] + 1.E-6)
PartSpecimen.PartitionEdgeByPoint(edge=e11[1], point=PartSpecimen.InterestingPoint(edge=e11[1], rule=
    MIDDLE))
PartSpecimen.PartitionEdgeByPoint(edge=e11[0], point=PartSpecimen.InterestingPoint(edge=e11[0], rule=
    MIDDLE))
e11 = e1.getByBoundingBox(
  xMin= P4[0]+abs(cos(alphaRad))*CBA3[0] - 1.E-6,
  xMax= P4[0]+abs(cos(alphaRad))*CBA3[0] + 1.E-6,
  yMin= P4[1]-abs(sin(alphaRad))*CBA3[0] - 1.E-6,
  yMax= P4[1]-abs(sin(alphaRad))*CBA3[0] + 1.E-6)
PartSpecimen.PartitionEdgeByPoint(edge=e11[1], point=PartSpecimen.InterestingPoint(edge=e11[1], rule=
    MIDDLE))
PartSpecimen.PartitionEdgeByPoint(edge=e11[0], point=PartSpecimen.InterestingPoint(edge=e11[0], rule=
    MIDDLE))
e11 = e1.getByBoundingBox(
  xMin= P4[0]+abs(cos(alphaRad))*CBA1[0] - 1.E-6,
  xMax= P4[0]+abs(cos(alphaRad))*CBA1[0] + 1.E-6,
  yMin= P4[1]-abs(sin(alphaRad))*CBA1[0] - 1.E-6,
  yMax= P4[1]-abs(sin(alphaRad))*CBA1[0] + 1.E-6)
PartSpecimen.PartitionEdgeByPoint(edge=e11[1], point=PartSpecimen.InterestingPoint(edge=e11[1], rule=
    MIDDLE))
PartSpecimen.PartitionEdgeByPoint(edge=e11[0], point=PartSpecimen.InterestingPoint(edge=e11[0], rule=
    MIDDLE))
#Smal: Gauge section
e11 = e1.getByBoundingBox(
  xMin= P4[0]+abs(cos(alphaRad))*SQA1[0] - 1.E-6,
  xMax= P4[0]+abs(cos(alphaRad))*SQA1[0] + 1.E-6,
  yMin= P4[1]-abs(sin(alphaRad))*SQA1[0] - 1.E-6,
  yMax= P4[1]-abs(sin(alphaRad))*SQA1[0] + 1.E-6)
PartSpecimen.PartitionEdgeByPoint(edge=e11[1], point=PartSpecimen.InterestingPoint(edge=e11[1], rule=
    MIDDLE))
PartSpecimen.PartitionEdgeByPoint(edge=e11[0], point=PartSpecimen.InterestingPoint(edge=e11[0], rule=
    MIDDLE))
e11 = e1.getByBoundingBox(
  xMin= P4[0]+abs(cos(alphaRad))*SQA3[0] - 1.E-6,
  xMax= P4[0]+abs(cos(alphaRad))*SQA3[0] + 1.E-6,
  yMin= P4[1]-abs(sin(alphaRad))*SQA3[0] - 1.E-6,
  yMax= P4[1]-abs(sin(alphaRad))*SQA3[0] + 1.E-6)
PartSpecimen.PartitionEdgeByPoint(edge=e11[1], point=PartSpecimen.InterestingPoint(edge=e11[1], rule=
    MIDDLE))
PartSpecimen.PartitionEdgeByPoint(edge=e11[0], point=PartSpecimen.InterestingPoint(edge=e11[0], rule=
    MIDDLE))
e11 = e1.getByBoundingBox(
  xMin= P4[0]+abs(cos(alphaRad))*SQA5[0] - 1.E-6,
  xMax= P4[0]+abs(cos(alphaRad))*SQA5[0] + 1.E-6,
  yMin= P4[1]-abs(sin(alphaRad))*SQA5[0] - 1.E-6,
  yMax= P4[1]-abs(sin(alphaRad))*SQA5[0] + 1.E-6)
PartSpecimen.PartitionEdgeByPoint(edge=e11[1], point=PartSpecimen.InterestingPoint(edge=e11[1], rule=
    MIDDLE))
```

```
PartSpecimen.PartitionEdgeByPoint(edge=e11[0], point=PartSpecimen.InterestingPoint(edge=e11[0], rule=
    MIDDLE))
```

PartsRigidDrophead.py

```
# # #
# # # # # # # # # Drophead Geometry # # # # # # # # # # # #
# # #
SketchDrophead = myModel.ConstrainedSketch(name='Sketch of the drophead', sheetSize=100)
PartDrophead = myModel.Part(name='ZDrophead', dimensionality=THREE_D, type=ANALYTIC_RIGID_SURFACE)

# Sketch Drophead
SketchDrophead.ArcByCenterEnds(center=(0.0, 0.0), point1=(0.0,-r), point2=(r, 0.0), direction=
    COUNTERCLOCKWISE)
SketchDrophead.Line(point1=(r, 0.0), point2=(r, h))
SketchDrophead.Line(point1=(r, h), point2=(0.0, h))
SketchDrophead.ConstructionLine(point1=(0.0, 0.0), angle=90.0)
PartDrophead.AnalyticRigidSurfRevolve(sketch=SketchDrophead)

# Assign reference point to Drophead
PartDrophead.ReferencePoint(point=(0.0, -r, 0.0))

# create set for bottom of drophead
q = PartDrophead.referencePoints
refPoints=(q[2], )
OnderkantDropheadSet=PartDrophead.Set(referencePoints=refPoints, name='OnderkantDrophead')

# Create inertia for drophead
region=PartDrophead.sets['OnderkantDrophead']
PartDrophead.engineeringFeatures.PointMassInertia(name='MassDrophead', region=region, mass=m_drophead)
```

PartsDeformableDrophead.py

```
# # #
# # # # # # # # # Drophead Geometry # # # # # # # # # # # #
# # #
SketchDrophead = myModel.ConstrainedSketch(name='Sketch of the drophead', sheetSize=100)
SketchDropheadExtrusion = myModel.ConstrainedSketch(name='Sketch of the drophead extrustion', sheetSize
    =100)
PartDrophead = myModel.Part(name='ZDrophead', dimensionality=THREE_D, type=DEFORMABLE_BODY)

# Sketch Drophead hemisphere
SketchDrophead.ArcByCenterEnds(center=(0.0, 0.0), point1=(0.0,-r), point2=(0.0, r), direction=
    COUNTERCLOCKWISE)
SketchDrophead.Line(point1=(0.0, r), point2=(0.0, -r))
SketchDrophead.ConstructionLine(point1=(0.0, 0.0), angle=90.0)
PartDrophead.BaseSolidRevolve(sketch=SketchDrophead,angle=180.0)

# Add extrusion to hemisphere
SketchDropheadExtrusion.CircleByCenterPerimeter(center=(0.0, 0.0), point1=(r, 0.0))
f, e = PartDrophead.faces, PartDrophead.edges
transf = PartDrophead.MakeSketchTransform(sketchPlane=f[2], sketchUpEdge=e[2], sketchPlaneSide=SIDE1,
    sketchOrientation=RIGHT, origin=(0.0, 0.0, 0.0))
TempExtrusionSketch = myModel.ConstrainedSketch(name='Temporary extrusion sketch', sheetSize=223.6,
    gridSpacing=5.59, transform=transf)
PartDrophead.projectReferencesOntoSketch(sketch=TempExtrusionSketch, filter=COPLANAR_EDGES)
TempExtrusionSketch.retrieveSketch(sketch=SketchDropheadExtrusion)
PartDrophead.SolidExtrude(sketchPlane=f[2], sketchUpEdge=e[2], sketchPlaneSide=SIDE1, sketchOrientation=
    RIGHT, sketch=TempExtrusionSketch, depth=h, flipExtrudeDirection=OFF)
del myModel.sketches['Temporary extrusion sketch']

c1, v1, d1 = PartDrophead.cells, PartDrophead.vertices, PartDrophead.datums

# Add principle datum axis Z
```

```
zAxisDatum=PartDrophead.DatumAxisByPrincipalAxis(principalAxis=ZAXIS)

# Create partitions
# Split hemisphere from cilinder
NormalDatum = PartDrophead.datums[zAxisDatum.id]
PartDrophead.PartitionCellByPlanePointNormal(point=v1[1], normal=NormalDatum, cells=c1[0])

# Create square partition on both circular faces
r1=30.0
f, e = PartDrophead.faces, PartDrophead.edges
SP=f.getByBoundingBox(zMax=-h+0.1)
SUE=e.getByBoundingBox(zMax=-h+0.1)
transf = PartDrophead.MakeSketchTransform(sketchPlane=SP[0], sketchUpEdge=SUE[0], sketchPlaneSide=SIDE1,
      origin=(0.0, 0.0, -h))
PartitionSketch = myModel.ConstrainedSketch(name='Partition sketch for drophead', sheetSize=955.56,
     gridSpacing=23.88, transform=transf)
PartitionSketch.Line(point1 = (r, 0.0) , point2 = (r1, 0.0) )
PartitionSketch.Line(point1 = (r1, 0.0) , point2 = (0.0, -r1) )
PartitionSketch.Line(point1 = (0.0, -r1) , point2 = (0.0, -r) )
PartitionSketch.Line(point1 = (0.0, r) , point2 = (0.0, r1) )
PartitionSketch.Line(point1 = (0.0, r1) , point2 = (-r1, 0.0) )
PartitionSketch.Line(point1 = (-r1, 0.0) , point2 = (-r, 0.0) )
PartitionSketch.Line(point1 = (-r1, 0.0) , point2 = (0.0, -r1) )
PartitionSketch.Line(point1 = (0.0, r1) , point2 = (r1, 0.0) )
PartDrophead.PartitionFaceBySketch(sketchUpEdge=SUE[0], faces=SP[0], sketch=PartitionSketch)

SP=f.getByBoundingBox(zMax=0.0+0.1, zMin=0.0-0.1)
SUE=e.getByBoundingBox(zMax=0.0+0.1, zMin=0.0-0.1)
transf = PartDrophead.MakeSketchTransform(sketchPlane=SP[0], sketchUpEdge=SUE[0], sketchPlaneSide=SIDE1,
      origin=(0.0, 0.0, 0.0))
TempPartitionSketch=myModel.ConstrainedSketch(name='Temporary partition sketch for drophead', sheetSize
     =955.56, gridSpacing=23.88, transform=transf)
TempPartitionSketch.retrieveSketch(sketch=PartitionSketch)
PartDrophead.PartitionFaceBySketch(sketchUpEdge=SUE[0], faces=SP[0], sketch=TempPartitionSketch)
del myModel.sketches['Temporary partition sketch for drophead']

# Use the face partitions to partition drophead
pickedCells = c1.getByBoundingBox(zMax=0.0+0.1)
pickedEdges=e.findAt(
  (( (r-r1)/2+r1 , 0.0 , -h) , ) ,
  ((  0.0 , (r-r1)/2+r1 , -h) , ) ,
  (( r1/2, r1/2 , -h) , ) ,
  (( sqrt(0.5)*r, sqrt(0.5)*r , -h) , ) ,)
PartDrophead.PartitionCellByExtrudeEdge(line=NormalDatum, cells=pickedCells, edges=pickedEdges, sense=
     FORWARD)

pickedCells = c1.findAt((( -sqrt(0.5)*r, -sqrt(0.5)*r , -h) , ) ,)
pickedEdges=e.findAt(
  (( -(r-r1)/2-r1 , 0.0 , -h) , ) ,
  ((  0.0 , -(r-r1)/2-r1 , -h) , ) ,
  (( -r1/2, -r1/2 , -h) , ) ,
  (( -sqrt(0.5)*r, -sqrt(0.5)*r , -h) , ) ,)
PartDrophead.PartitionCellByExtrudeEdge(line=NormalDatum, cells=pickedCells, edges=pickedEdges, sense=
     FORWARD)

pickedCells = c1.findAt(((0.0, 0.0 , -h) , ) ,)
pickedEdges=e.findAt(
  (( r1/2, r1/2 , -h) , ) ,
  (( -r1/2, r1/2 , -h) , ) ,
  (( -r1/2, -r1/2 , -h) , ) ,
  (( r1/2, -r1/2 , -h) , ) ,)
PartDrophead.PartitionCellByExtrudeEdge(line=NormalDatum, cells=pickedCells, edges=pickedEdges, sense=
     FORWARD)

# Use the same face partitions for partition the hemisphere
pickedCells = c1.getByBoundingBox(zMin=0.0-0.1)
```

```
pickedEdges=e.findAt(
  (( (r-r1)/2+r1 , 0.0 ,0.0) , ) ,
  ((  0.0 , (r-r1)/2+r1 , 0.0) , ) ,
  (( r1/2, r1/2 , 0.0) , ) ,
  (( sqrt(0.5)*r, sqrt(0.5)*r , 0.0) , ) ,)
PartDrophead.PartitionCellByExtrudeEdge(line=NormalDatum, cells=pickedCells, edges=pickedEdges, sense=
    FORWARD)

pickedCells = c1.findAt((( -sqrt(0.5)*r, -sqrt(0.5)*r , 0.0) , ) ,)
pickedEdges=e.findAt(
  (( -(r-r1)/2-r1 , 0.0 , 0.0) , ) ,
  ((  0.0 , -(r-r1)/2-r1 , 0.0) , ) ,
  (( -r1/2, -r1/2 ,0.0) , ) ,
  (( -sqrt(0.5)*r, -sqrt(0.5)*r , 0.0) , ) ,)
PartDrophead.PartitionCellByExtrudeEdge(line=NormalDatum, cells=pickedCells, edges=pickedEdges, sense=
    FORWARD)

pickedCells = c1.findAt(((0.0, 0.0 , 0.0) , ) ,)
pickedEdges=e.findAt(
  (( r1/2, r1/2 , 0.0) , ) ,
  (( -r1/2, r1/2 , 0.0) , ) ,
  (( -r1/2, -r1/2 , 0.0) , ) ,
  (( r1/2, -r1/2 , 0.0) , ) ,)
PartDrophead.PartitionCellByExtrudeEdge(line=NormalDatum, cells=pickedCells, edges=pickedEdges, sense=
    FORWARD)
```

Material.py

```
# # #
# # # # # # # # # Material # # # # # # # # # # # # #
# # #
MaterialSteel = myModel.Material('Steel')
MaterialSteel.Elastic(table=((210.E3 , 0.3), ))
MaterialSteel.Density(table=((7.8E-09, ), ))
MaterialSteel.Plastic(rate=OFF, table=(
  (350.0, 0.0),
  (381.8449394, 0.005),
  (403.4111867, 0.01),
  (416.5869563, 0.015),
  (426.1954757, 0.02),
  (433.80078, 0.025),
  (440.1154005, 0.03),
  (445.5259947, 0.035),
  (450.2666001, 0.04),
  (454.4899625, 0.045),
  (458.3014449, 0.05),
  (461.7768789, 0.055),
  (464.9727094, 0.06),
  (467.9321162, 0.065),
  (470.6888889, 0.07),
  (473.2699794, 0.075),
  (475.6972393, 0.08),
  (477.9886375, 0.085),
  (480.1591333, 0.09),
  (482.2213162, 0.095),
  (484.1858847, 0.1),
  (486.0620084, 0.105),
  (487.8576079, 0.11),
  (489.5795733, 0.115),
  (491.2339359, 0.12),
  (492.8260069, 0.125),
  (494.3604873, 0.13),
  (495.8415593, 0.135),
  (497.27296, 0.14),
  (498.6580427, 0.145),
  (499.999828, 0.15)))
```

```
MaterialSteel.plastic.RateDependent(table=((40.4, 5.0), ))

# Material Orientation
e1 = PartSpecimen.edges
e11 = e1.getByBoundingBox(
  xMin= P4[0]+abs(cos(alphaRad))*SQM[0] - 1.E-6,
  xMax= P4[0]+abs(cos(alphaRad))*SQM[0] + 1.E-6,
  yMin= P4[1]-abs(sin(alphaRad))*SQM[0] - 1.E-6,
  yMax= P4[1]-abs(sin(alphaRad))*SQM[0] + 1.E-6,
  zMax= B/2)
e12 = e1.getByBoundingBox(
  xMin= P4[0]+abs(cos(alphaRad))* SQM[0] - 1.E-6,
  xMax= P4[0]+abs(cos(alphaRad))*(SQM[0]+25.0) + 1.E-6,
  yMin= P4[1]-abs(sin(alphaRad))*(SQM[0]+25.0) - 1.E-6,
  yMax= P4[1]-abs(sin(alphaRad))* SQM[0] + 1.E-6,
  zMin= B/2 - 1.E-6,
  zMax= B/2 + 1.E-6 )
myCsys=PartSpecimen.DatumCsysByTwoLines(CARTESIAN, line1=e12[0], line2=e11[0], name='TweedeCsys')
```

Section.py

```
# # #
# # # # # # # # # Section # # # # # # # # # # # # #
# # #
# Section maken
Section = myModel.HomogeneousShellSection(name='SpecimenSection', material='Steel', thickness=t)

# Section toekennen
f = PartSpecimen.faces
region = regionToolset.Region(faces=f[0:len(f)])
PartSpecimen.SectionAssignment(region=region, sectionName='SpecimenSection')
```

SectionDeformableDrophead.py

```
# # #
# # # # # # # # # Section # # # # # # # # # # # # #
# # #
# Create section for drophead
SectionDH = myModel.HomogeneousSolidSection(name='DropheadSection', material='Steel', thickness=None)

# Section toekennen
c1 = PartDrophead.cells
region = regionToolset.Region(cells=c1[0:len(c1)])
PartDrophead.SectionAssignment(region=region, sectionName='DropheadSection')
```

Instance.py

```
# # #
# # # # # # # # # Instance # # # # # # # # # # # # #
# # #
# Instance maken van beide parts (assembly maken)
myAssembly = myModel.rootAssembly
DropheadInstance = myAssembly.Instance(name='Drophead', part=PartDrophead, dependent=ON)
SpecimenInstance = myAssembly.Instance(name='Specimen', part=PartSpecimen, dependent=ON)

# Instances positioneren
myAssembly.translate(instanceList=('Drophead', ), vector=(dx, -(r_specimen-r)+t/2+dy , B/2))
```

InstanceDeformableDrophead.py

```
# # #
# # # # # # # # # Instance # # # # # # # # # # # # #
# # #
# Instance maken van beide parts (assembly maken)
myAssembly = myModel.rootAssembly
```

```
DropheadInstance = myAssembly.Instance(name='Drophead', part=PartDrophead, dependent=ON)
SpecimenInstance = myAssembly.Instance(name='Specimen', part=PartSpecimen, dependent=ON)

f = DropheadInstance.faces
TopDrophead=f.getByBoundingBox(zMax=-h+0.1)
TopDropheadSet = myAssembly.Set(faces=TopDrophead, name='DropheadTop')

# Instances positioneren
myAssembly.rotate(instanceList=('Drophead', ), axisPoint=(0.0, 0.0, r), axisDirection=(1.0, 0.0, 0.0),
    angle=90.0)
myAssembly.translate(instanceList=('Drophead', ), vector=(dx, -(r_specimen-r)-r+t/2+dy , B/2-r))
```

Sets.py

```
# # #
# # # # # # # # # Sets # # # # # # # # # # # # #
# # #
# Create geometry set 'BovenkantSpecimen'
e1, f1 = SpecimenInstance.edges, SpecimenInstance.faces
BovenkantSpecimenSet=myAssembly.Set(edges=e1.findAt(
  (( -abs(cos(alphaMiddle))*r_specimen-abs(cos(alphaRad))*L , -abs(sin(alphaMiddle))*r_specimen+abs(sin(
      alphaRad))*L, B/4),),
  (( -abs(cos(alphaMiddle))*r_specimen-abs(cos(alphaRad))*L , -abs(sin(alphaMiddle))*r_specimen+abs(sin(
      alphaRad))*L, 3*B/4),),
  (( abs(cos(alphaMiddle))*r_specimen+abs(cos(alphaRad))*L , -abs(sin(alphaMiddle))*r_specimen+abs(sin(
      alphaRad))*L, 3*B/4),),
  (( abs(cos(alphaMiddle))*r_specimen+abs(cos(alphaRad))*L , -abs(sin(alphaMiddle))*r_specimen+abs(sin(
      alphaRad))*L, B/4), ), ), name='BovenkantSpecimen')

# Create geometry set 'AllFacesSpecimen'
f = PartSpecimen.faces
AllFacesSpecimenSet=PartSpecimen.Set(faces=f, name='AllFacesSpecimen')

# Create assembly set 'FacesBreedSpecimen'
fBreed=f1.getByBoundingBox(yMin=P3[1]-abs(sin(alphaRad))*L_L*3/4, yMax= P3[1]-abs(sin(alphaRad))*CBC1
    [0])
FacesBreedSet= myAssembly.Set(faces=fBreed, name='FacesBreedSpecimen')

# Create assembly set 'FacesSmalSpecimen'
fSmal=f1.getByBoundingBox(yMin= P3[1]-abs(sin(alphaRad))*SQA5[0], yMax= P3[1]-abs(sin(alphaRad))*SQA1
    [0])
FacesSmalSet= myAssembly.Set(faces=fSmal, name='FacesSmalSpecimen')

# Create assembly set 'NodeBreedSpecimen'
v = SpecimenInstance.vertices
v1= v.getByBoundingBox(
  xMin= P4[0]+abs(cos(alphaRad))*CBC3[0] - 1.E-6,
  xMax= P4[0]+abs(cos(alphaRad))*CBC3[0] + 1.E-6,
  yMin= P4[1]-abs(sin(alphaRad))*CBC3[0] - 1.E-6,
  yMax= P4[1]-abs(sin(alphaRad))*CBC3[0] + 1.E-6,
  zMin= B/2 - 1.E-6,
  zMax= B/2 + 1.E-6 )
BreedNodeSet= myAssembly.Set(vertices=v1, name='BreedNode')

# Create assembly set 'SmalNode'
v = SpecimenInstance.vertices
v1= v.getByBoundingBox(
  xMin= P4[0]+abs(cos(alphaRad))*SQM[0] - 1.E-6,
  xMax= P4[0]+abs(cos(alphaRad))*SQM[0] + 1.E-6,
  yMin= P4[1]-abs(sin(alphaRad))*SQM[0] - 1.E-6,
  yMax= P4[1]-abs(sin(alphaRad))*SQM[0] + 1.E-6,
  zMin= B/2 - 1.E-6,
  zMax= B/2 + 1.E-6 )
SmalNodeSet= myAssembly.Set(vertices=v1, name='SmalNode')

# Create assembly set 'BreedA' and 'SmalA'
```

```
v = SpecimenInstance.vertices
v1= v.getByBoundingBox(
  xMin= P4[0]+abs(cos(alphaRad))*CBA1[0] - 1.E-6,
  xMax= P4[0]+abs(cos(alphaRad))*CBA1[0] + 1.E-6,
  yMin= P4[1]-abs(sin(alphaRad))*CBA1[0] - 1.E-6,
  yMax= P4[1]-abs(sin(alphaRad))*CBA1[0] + 1.E-6,
  zMin= B - 1.E-6,
  zMax= B + 1.E-6 )
v2= v.getByBoundingBox(
  xMin= P4[0]+abs(cos(alphaRad))*CBA5[0] - 1.E-6,
  xMax= P4[0]+abs(cos(alphaRad))*CBA5[0] + 1.E-6,
  yMin= P4[1]-abs(sin(alphaRad))*CBA5[0] - 1.E-6,
  yMax= P4[1]-abs(sin(alphaRad))*CBA5[0] + 1.E-6,
  zMin= B - 1.E-6,
  zMax= B + 1.E-6 )
BreedNodeSetA= myAssembly.Set(vertices=(v1,v2), name='BreedA')
myList=[v1,v2]
v1= v.getByBoundingBox(
  xMin= P4[0]+abs(cos(alphaRad))*SQA1[0] - 1.E-6,
  xMax= P4[0]+abs(cos(alphaRad))*SQA1[0] + 1.E-6,
  yMin= P4[1]-abs(sin(alphaRad))*SQA1[0] - 1.E-6,
  yMax= P4[1]-abs(sin(alphaRad))*SQA1[0] + 1.E-6,
  zMin= B-(B-b)/2 - 1.E-6,
  zMax= B-(B-b)/2 + 1.E-6 )
v2= v.getByBoundingBox(
  xMin= P4[0]+abs(cos(alphaRad))*SQA5[0] - 1.E-6,
  xMax= P4[0]+abs(cos(alphaRad))*SQA5[0] + 1.E-6,
  yMin= P4[1]-abs(sin(alphaRad))*SQA5[0] - 1.E-6,
  yMax= P4[1]-abs(sin(alphaRad))*SQA5[0] + 1.E-6,
  zMin= B-(B-b)/2 - 1.E-6,
  zMax= B-(B-b)/2 + 1.E-6 )
SmalNodeSetA= myAssembly.Set(vertices=(v1,v2), name='SmalA')
myList.append(v1)
myList.append(v2)

# Create assembly set 'BreedB' and 'SmalB'
v = SpecimenInstance.vertices
v1= v.getByBoundingBox(
  xMin= P4[0]+abs(cos(alphaRad))*CBA1[0] - 1.E-6,
  xMax= P4[0]+abs(cos(alphaRad))*CBA1[0] + 1.E-6,
  yMin= P4[1]-abs(sin(alphaRad))*CBA1[0] - 1.E-6,
  yMax= P4[1]-abs(sin(alphaRad))*CBA1[0] + 1.E-6,
  zMin= B*3/4 - 1.E-6,
  zMax= B*3/4 + 1.E-6 )
v2= v.getByBoundingBox(
  xMin= P4[0]+abs(cos(alphaRad))*CBA5[0] - 1.E-6,
  xMax= P4[0]+abs(cos(alphaRad))*CBA5[0] + 1.E-6,
  yMin= P4[1]-abs(sin(alphaRad))*CBA5[0] - 1.E-6,
  yMax= P4[1]-abs(sin(alphaRad))*CBA5[0] + 1.E-6,
  zMin= B*3/4 - 1.E-6,
  zMax= B*3/4 + 1.E-6 )
BreedNodeSetB= myAssembly.Set(vertices=(v1,v2), name='BreedB')
myList.append(v1)
myList.append(v2)
v1= v.getByBoundingBox(
  xMin= P4[0]+abs(cos(alphaRad))*SQA1[0] - 1.E-6,
  xMax= P4[0]+abs(cos(alphaRad))*SQA1[0] + 1.E-6,
  yMin= P4[1]-abs(sin(alphaRad))*SQA1[0] - 1.E-6,
  yMax= P4[1]-abs(sin(alphaRad))*SQA1[0] + 1.E-6,
  zMin= (B-b)/2+3./4.*b - 1.E-6,
  zMax= (B-b)/2+3./4.*b + 1.E-6 )
v2= v.getByBoundingBox(
  xMin= P4[0]+abs(cos(alphaRad))*SQA5[0] - 1.E-6,
  xMax= P4[0]+abs(cos(alphaRad))*SQA5[0] + 1.E-6,
  yMin= P4[1]-abs(sin(alphaRad))*SQA5[0] - 1.E-6,
  yMax= P4[1]-abs(sin(alphaRad))*SQA5[0] + 1.E-6,
```

```
  zMin= (B-b)/2+3./4.*b - 1.E-6,
  zMax= (B-b)/2+3./4.*b + 1.E-6 )
SmalNodeSetB= myAssembly.Set(vertices=(v1,v2), name='SmalB')
myList.append(v1)
myList.append(v2)

# Create assembly set 'BreedC' and 'SmalC'
v = SpecimenInstance.vertices
v1= v.getByBoundingBox(
  xMin= P4[0]+abs(cos(alphaRad))*CBA1[0] - 1.E-6,
  xMax= P4[0]+abs(cos(alphaRad))*CBA1[0] + 1.E-6,
  yMin= P4[1]-abs(sin(alphaRad))*CBA1[0] - 1.E-6,
  yMax= P4[1]-abs(sin(alphaRad))*CBA1[0] + 1.E-6,
  zMin= B/2 - 1.E-6,
  zMax= B/2 + 1.E-6 )
v2= v.getByBoundingBox(
  xMin= P4[0]+abs(cos(alphaRad))*CBA5[0] - 1.E-6,
  xMax= P4[0]+abs(cos(alphaRad))*CBA5[0] + 1.E-6,
  yMin= P4[1]-abs(sin(alphaRad))*CBA5[0] - 1.E-6,
  yMax= P4[1]-abs(sin(alphaRad))*CBA5[0] + 1.E-6,
  zMin= B/2 - 1.E-6,
  zMax= B/2 + 1.E-6 )
BreedNodeSetC= myAssembly.Set(vertices=(v1,v2), name='BreedC')
myList.append(v1)
myList.append(v2)
v1= v.getByBoundingBox(
  xMin= P4[0]+abs(cos(alphaRad))*SQA1[0] - 1.E-6,
  xMax= P4[0]+abs(cos(alphaRad))*SQA1[0] + 1.E-6,
  yMin= P4[1]-abs(sin(alphaRad))*SQA1[0] - 1.E-6,
  yMax= P4[1]-abs(sin(alphaRad))*SQA1[0] + 1.E-6,
  zMin= B/2 - 1.E-6,
  zMax= B/2 + 1.E-6 )
v2= v.getByBoundingBox(
  xMin= P4[0]+abs(cos(alphaRad))*SQA5[0] - 1.E-6,
  xMax= P4[0]+abs(cos(alphaRad))*SQA5[0] + 1.E-6,
  yMin= P4[1]-abs(sin(alphaRad))*SQA5[0] - 1.E-6,
  yMax= P4[1]-abs(sin(alphaRad))*SQA5[0] + 1.E-6,
  zMin= B/2 - 1.E-6,
  zMax= B/2 + 1.E-6 )
SmalNodeSetC= myAssembly.Set(vertices=(v1,v2), name='SmalC')
myList.append(v1)
myList.append(v2)

# Create assembly set 'BreedD' and 'SmalD'
v = SpecimenInstance.vertices
v1= v.getByBoundingBox(
  xMin= P4[0]+abs(cos(alphaRad))*CBA1[0] - 1.E-6,
  xMax= P4[0]+abs(cos(alphaRad))*CBA1[0] + 1.E-6,
  yMin= P4[1]-abs(sin(alphaRad))*CBA1[0] - 1.E-6,
  yMax= P4[1]-abs(sin(alphaRad))*CBA1[0] + 1.E-6,
  zMin= B/4 - 1.E-6,
  zMax= B/4 + 1.E-6 )
v2= v.getByBoundingBox(
  xMin= P4[0]+abs(cos(alphaRad))*CBA5[0] - 1.E-6,
  xMax= P4[0]+abs(cos(alphaRad))*CBA5[0] + 1.E-6,
  yMin= P4[1]-abs(sin(alphaRad))*CBA5[0] - 1.E-6,
  yMax= P4[1]-abs(sin(alphaRad))*CBA5[0] + 1.E-6,
  zMin= B/4 - 1.E-6,
  zMax= B/4 + 1.E-6 )
BreedNodeSetD= myAssembly.Set(vertices=(v1,v2), name='BreedD')
v1= v.getByBoundingBox(
  xMin= P4[0]+abs(cos(alphaRad))*SQA1[0] - 1.E-6,
  xMax= P4[0]+abs(cos(alphaRad))*SQA1[0] + 1.E-6,
  yMin= P4[1]-abs(sin(alphaRad))*SQA1[0] - 1.E-6,
  yMax= P4[1]-abs(sin(alphaRad))*SQA1[0] + 1.E-6,
  zMin= (B-b)/2+b/4 - 1.E-6,
```

```
  zMax= (B-b)/2+b/4 + 1.E-6 )
v2= v.getByBoundingBox(
  xMin= P4[0]+abs(cos(alphaRad))*SQA5[0] - 1.E-6,
  xMax= P4[0]+abs(cos(alphaRad))*SQA5[0] + 1.E-6,
  yMin= P4[1]-abs(sin(alphaRad))*SQA5[0] - 1.E-6,
  yMax= P4[1]-abs(sin(alphaRad))*SQA5[0] + 1.E-6,
  zMin= (B-b)/2+b/4 - 1.E-6,
  zMax= (B-b)/2+b/4 + 1.E-6 )
SmalNodeSetD= myAssembly.Set(vertices=(v1,v2), name='SmalD')

# Create assembly set 'BreedE' and 'SmalE'
v = SpecimenInstance.vertices
v1= v.getByBoundingBox(
  xMin= P4[0]+abs(cos(alphaRad))*CBA1[0] - 1.E-6,
  xMax= P4[0]+abs(cos(alphaRad))*CBA1[0] + 1.E-6,
  yMin= P4[1]-abs(sin(alphaRad))*CBA1[0] - 1.E-6,
  yMax= P4[1]-abs(sin(alphaRad))*CBA1[0] + 1.E-6,
  zMin= - 1.E-6,
  zMax= 1.E-6 )
v2= v.getByBoundingBox(
  xMin= P4[0]+abs(cos(alphaRad))*CBA5[0] - 1.E-6,
  xMax= P4[0]+abs(cos(alphaRad))*CBA5[0] + 1.E-6,
  yMin= P4[1]-abs(sin(alphaRad))*CBA5[0] - 1.E-6,
  yMax= P4[1]-abs(sin(alphaRad))*CBA5[0] + 1.E-6,
  zMin= -1.E-6,
  zMax= 1.E-6 )
BreedNodeSetE= myAssembly.Set(vertices=(v1,v2), name='BreedE')
v1= v.getByBoundingBox(
  xMin= P4[0]+abs(cos(alphaRad))*SQA1[0] - 1.E-6,
  xMax= P4[0]+abs(cos(alphaRad))*SQA1[0] + 1.E-6,
  yMin= P4[1]-abs(sin(alphaRad))*SQA1[0] - 1.E-6,
  yMax= P4[1]-abs(sin(alphaRad))*SQA1[0] + 1.E-6,
  zMin= (B-b)/2 - 1.E-6,
  zMax= (B-b)/2 + 1.E-6 )
v2= v.getByBoundingBox(
  xMin= P4[0]+abs(cos(alphaRad))*SQA5[0] - 1.E-6,
  xMax= P4[0]+abs(cos(alphaRad))*SQA5[0] + 1.E-6,
  yMin= P4[1]-abs(sin(alphaRad))*SQA5[0] - 1.E-6,
  yMax= P4[1]-abs(sin(alphaRad))*SQA5[0] + 1.E-6,
  zMin= (B-b)/2 - 1.E-6,
  zMax= (B-b)/2 + 1.E-6 )
SmalNodeSetE= myAssembly.Set(vertices=(v1,v2), name='SmalE')

BoeiendStukSet = myAssembly.Set(vertices=myList, name='BoeiendStuk')

# Create geometry set 'ContactOppSpecimen'
f11=f1.getByBoundingBox(yMax= P2[1])
ContactOppSpecimenSet = myAssembly.Set(faces=f11, name='ContactOppSpecimen')

# Create geometry set 'HalfSpecimen'
f = PartSpecimen.faces
f11=f.getByBoundingBox(xMax= 0.0)
HalfSpecimenSet = PartSpecimen.Set(faces=f11, name='HalfSpecimen')

# Material orientation
f = PartSpecimen.faces
faces = f.getByBoundingBox(yMin= P1[1], yMax= P3[1], xMax=0)
region = regionToolset.Region(faces=faces)
orientation = PartSpecimen.datums[myCsys.id]
PartSpecimen.MaterialOrientation(region=region, localCsys=orientation, axis=AXIS_3)
```

Meshen.py

```
# # #
# # # # # # # # # Meshen of specimen# # # # # # # # # # # #
# # #
```

```
# assign element type
regionSpecimen=PartSpecimen.faces
regionSpecimenOvergang=PartSpecimen.faces.getByBoundingBox(yMax= P3[1]-abs(sin(alphaRad))*L_L*3/4+0.01,
    yMin= P3[1]-abs(sin(alphaRad))*C2[0]-0.01)
elemType = mesh.ElemType(elemCode=S4R)
PartSpecimen.setElementType(regions=AllFacesSpecimenSet, elemTypes=(elemType, ))

# assign global seed for part
PartSpecimen.seedPart(size=MeshSize)

# assign edge seed for smal part
e = PartSpecimen.edges
pickedEdges = e.findAt(
  ((P4[0]+abs(cos(alphaRad))*(C2[0]+SQA1[0])/2, P4[1]-abs(sin(alphaRad))*(C2[0]+SQA1[0])/2, C2[1]),),
  ((P4[0]+abs(cos(alphaRad))*(C2[0]+SQA1[0])/2, P4[1]-abs(sin(alphaRad))*(C2[0]+SQA1[0])/2, SQM[1]),),
  ((P4[0]+abs(cos(alphaRad))*(C2[0]+SQA1[0])/2, P4[1]-abs(sin(alphaRad))*(C2[0]+SQA1[0])/2, C12[1]),),
  ((P4[0]+abs(cos(alphaRad))*(SQA3[0]+SQA1[0])/2, P4[1]-abs(sin(alphaRad))*(SQA3[0]+SQA1[0])/2, C2[1]),)
      ,
  ((P4[0]+abs(cos(alphaRad))*(SQA3[0]+SQA1[0])/2, P4[1]-abs(sin(alphaRad))*(SQA3[0]+SQA1[0])/2, SQM[1])
      ,),
  ((P4[0]+abs(cos(alphaRad))*(SQA3[0]+SQA1[0])/2, P4[1]-abs(sin(alphaRad))*(SQA3[0]+SQA1[0])/2, C12[1])
      ,),
  ((P4[0]+abs(cos(alphaRad))*(SQA3[0]+SQA5[0])/2, P4[1]-abs(sin(alphaRad))*(SQA3[0]+SQA5[0])/2, C2[1]),)
      ,
  ((P4[0]+abs(cos(alphaRad))*(SQA3[0]+SQA5[0])/2, P4[1]-abs(sin(alphaRad))*(SQA3[0]+SQA5[0])/2, SQM[1])
      ,),
  ((P4[0]+abs(cos(alphaRad))*(SQA3[0]+SQA5[0])/2, P4[1]-abs(sin(alphaRad))*(SQA3[0]+SQA5[0])/2, C12[1])
      ,),
  ((P4[0]+abs(cos(alphaRad))*(C3[0]+SQA5[0])/2, P4[1]-abs(sin(alphaRad))*(C3[0]+SQA5[0])/2, C2[1]),),
  ((P4[0]+abs(cos(alphaRad))*(C3[0]+SQA5[0])/2, P4[1]-abs(sin(alphaRad))*(C3[0]+SQA5[0])/2, SQM[1]),),
  ((P4[0]+abs(cos(alphaRad))*(C3[0]+SQA5[0])/2, P4[1]-abs(sin(alphaRad))*(C3[0]+SQA5[0])/2, C12[1]),),
  ((P3[0]-abs(cos(alphaRad))*(C2[0]+SQA1[0])/2, P4[1]-abs(sin(alphaRad))*(C2[0]+SQA1[0])/2, C2[1]),),
  ((P3[0]-abs(cos(alphaRad))*(C2[0]+SQA1[0])/2, P4[1]-abs(sin(alphaRad))*(C2[0]+SQA1[0])/2, SQM[1]),),
  ((P3[0]-abs(cos(alphaRad))*(C2[0]+SQA1[0])/2, P4[1]-abs(sin(alphaRad))*(C2[0]+SQA1[0])/2, C12[1]),),
  ((P3[0]-abs(cos(alphaRad))*(SQA3[0]+SQA1[0])/2, P4[1]-abs(sin(alphaRad))*(SQA3[0]+SQA1[0])/2, C2[1]),)
      ,
  ((P3[0]-abs(cos(alphaRad))*(SQA3[0]+SQA1[0])/2, P4[1]-abs(sin(alphaRad))*(SQA3[0]+SQA1[0])/2, SQM[1])
      ,),
  ((P3[0]-abs(cos(alphaRad))*(SQA3[0]+SQA1[0])/2, P4[1]-abs(sin(alphaRad))*(SQA3[0]+SQA1[0])/2, C12[1])
      ,),
  ((P3[0]-abs(cos(alphaRad))*(SQA3[0]+SQA5[0])/2, P4[1]-abs(sin(alphaRad))*(SQA3[0]+SQA5[0])/2, C2[1]),)
      ,
  ((P3[0]-abs(cos(alphaRad))*(SQA3[0]+SQA5[0])/2, P4[1]-abs(sin(alphaRad))*(SQA3[0]+SQA5[0])/2, SQM[1])
      ,),
  ((P3[0]-abs(cos(alphaRad))*(SQA3[0]+SQA5[0])/2, P4[1]-abs(sin(alphaRad))*(SQA3[0]+SQA5[0])/2, C12[1])
      ,),
  ((P3[0]-abs(cos(alphaRad))*(C3[0]+SQA5[0])/2, P4[1]-abs(sin(alphaRad))*(C3[0]+SQA5[0])/2, C2[1]),),
  ((P3[0]-abs(cos(alphaRad))*(C3[0]+SQA5[0])/2, P4[1]-abs(sin(alphaRad))*(C3[0]+SQA5[0])/2, SQM[1]),),
  ((P3[0]-abs(cos(alphaRad))*(C3[0]+SQA5[0])/2, P4[1]-abs(sin(alphaRad))*(C3[0]+SQA5[0])/2, C12[1]),),
  )
PartSpecimen.seedEdgeBySize(edges=pickedEdges, size=(MeshSize*b/B), constraint=FIXED)

# assign edge seed for smal part midden
e = PartSpecimen.edges
pickedEdges = e.findAt(
  ((P4[0]+abs(cos(alphaRad))*SQA1[0], P4[1]-abs(sin(alphaRad))*SQA1[0], (B-b)/2+b/8 ),),
  ((P4[0]+abs(cos(alphaRad))*SQA1[0], P4[1]-abs(sin(alphaRad))*SQA1[0], (B-b)/2+b*3/8 ),),
  ((P4[0]+abs(cos(alphaRad))*SQA1[0], P4[1]-abs(sin(alphaRad))*SQA1[0], (B-b)/2+b*5/8 ),),
  ((P4[0]+abs(cos(alphaRad))*SQA1[0], P4[1]-abs(sin(alphaRad))*SQA1[0], (B-b)/2+b*7/8 ),),
  ((P4[0]+abs(cos(alphaRad))*SQA3[0], P4[1]-abs(sin(alphaRad))*SQA3[0], (B-b)/2+b/8 ),),
  ((P4[0]+abs(cos(alphaRad))*SQA3[0], P4[1]-abs(sin(alphaRad))*SQA3[0], (B-b)/2+b*3/8 ),),
  ((P4[0]+abs(cos(alphaRad))*SQA3[0], P4[1]-abs(sin(alphaRad))*SQA3[0], (B-b)/2+b*5/8 ),),
  ((P4[0]+abs(cos(alphaRad))*SQA3[0], P4[1]-abs(sin(alphaRad))*SQA3[0], (B-b)/2+b*7/8 ),),
  ((P4[0]+abs(cos(alphaRad))*SQA5[0], P4[1]-abs(sin(alphaRad))*SQA5[0], (B-b)/2+b/8 ),),
  ((P4[0]+abs(cos(alphaRad))*SQA5[0], P4[1]-abs(sin(alphaRad))*SQA5[0], (B-b)/2+b*3/8 ),),
  ((P4[0]+abs(cos(alphaRad))*SQA5[0], P4[1]-abs(sin(alphaRad))*SQA5[0], (B-b)/2+b*5/8 ),),
```

```
  ((P4[0]+abs(cos(alphaRad))*SQA5[0], P4[1]-abs(sin(alphaRad))*SQA5[0], (B-b)/2+b*7/8 ),),
  ((P3[0]-abs(cos(alphaRad))*SQA1[0], P4[1]-abs(sin(alphaRad))*SQA1[0], (B-b)/2+b/8 ),),
  ((P3[0]-abs(cos(alphaRad))*SQA1[0], P4[1]-abs(sin(alphaRad))*SQA1[0], (B-b)/2+b*3/8 ),),
  ((P3[0]-abs(cos(alphaRad))*SQA1[0], P4[1]-abs(sin(alphaRad))*SQA1[0], (B-b)/2+b*5/8 ),),
  ((P3[0]-abs(cos(alphaRad))*SQA1[0], P4[1]-abs(sin(alphaRad))*SQA1[0], (B-b)/2+b*7/8 ),),
  ((P3[0]-abs(cos(alphaRad))*SQA3[0], P4[1]-abs(sin(alphaRad))*SQA3[0], (B-b)/2+b/8 ),),
  ((P3[0]-abs(cos(alphaRad))*SQA3[0], P4[1]-abs(sin(alphaRad))*SQA3[0], (B-b)/2+b*3/8 ),),
  ((P3[0]-abs(cos(alphaRad))*SQA3[0], P4[1]-abs(sin(alphaRad))*SQA3[0], (B-b)/2+b*5/8 ),),
  ((P3[0]-abs(cos(alphaRad))*SQA3[0], P4[1]-abs(sin(alphaRad))*SQA3[0], (B-b)/2+b*7/8 ),),
  ((P3[0]-abs(cos(alphaRad))*SQA5[0], P4[1]-abs(sin(alphaRad))*SQA5[0], (B-b)/2+b/8 ),),
  ((P3[0]-abs(cos(alphaRad))*SQA5[0], P4[1]-abs(sin(alphaRad))*SQA5[0], (B-b)/2+b*3/8 ),),
  ((P3[0]-abs(cos(alphaRad))*SQA5[0], P4[1]-abs(sin(alphaRad))*SQA5[0], (B-b)/2+b*5/8 ),),
  ((P3[0]-abs(cos(alphaRad))*SQA5[0], P4[1]-abs(sin(alphaRad))*SQA5[0], (B-b)/2+b*7/8 ),),
  )
PartSpecimen.seedEdgeBySize(edges=pickedEdges, size=(MeshSize*b/B), constraint=FIXED)

# use structured meshing
PartSpecimen.setMeshControls(regions=regionSpecimen, technique=SWEEP)
PartSpecimen.setMeshControls(regions=regionSpecimenOvergang, technique=FREE, algorithm=MEDIAL_AXIS)

# Generate mesh
PartSpecimen.generateMesh()

# Element sets maken
q = PartSpecimen.nodes
q1= q.getByBoundingBox(
  xMin= P4[0]+abs(cos(alphaRad))*SQM[0] - 1.E-4,
  xMax= P4[0]+abs(cos(alphaRad))*SQM[0] + 1.E-4,
  yMin= P4[1]-abs(sin(alphaRad))*SQM[0] - 1.E-4,
  yMax= P4[1]-abs(sin(alphaRad))*SQM[0] + 1.E-4,
  zMin= B/2 - 1.E-6,
  zMax= B/2 + 1.E-6 )
q11=q1[0].getElements()
PartSpecimen.SetFromElementLabels(elementLabels=(q11[0].label, q11[1].label, q11[2].label, q11[3].label)
     , name='ElMidSmal' )
q2 = q.getByBoundingBox(
  xMin= P4[0]+abs(cos(alphaRad))*CBC3[0] - 1.E-4,
  xMax= P4[0]+abs(cos(alphaRad))*CBC3[0] + 1.E-4,
  yMin= P4[1]-abs(sin(alphaRad))*CBC3[0] - 1.E-4,
  yMax= P4[1]-abs(sin(alphaRad))*CBC3[0] + 1.E-4,
  zMin= B/2 - 1.E-6,
  zMax= B/2 + 1.E-6 )
q22=q2[0].getElements()
PartSpecimen.SetFromElementLabels(elementLabels=(q22[0].label, q22[1].label, q22[2].label, q22[3].label)
     , name='ElMidBreed' )

q = PartSpecimen.nodes
q3 = q.getByBoundingBox(
  xMin= P4[0] - MeshSize/2,
  xMax= P4[0] + MeshSize/2,
  yMin= P4[1] - MeshSize/2,
  yMax= P4[1] + MeshSize/2,
  zMin= 0 - MeshSize/2,
  zMax= B + MeshSize/2)
PartSpecimen.Set(nodes=q3, name='BovenkantSpecimenNodes')
```

MeshenDeformableDrophead.py

```
# # #
# # # # # # # # # Meshen of specimen# # # # # # # # # # #
# # #
NrElDH1=7 # number of elements along the edges of the middle square
NrElDH2=3 # Number of elements along the diagonal egdes from square to side
SizeBias1=7.0 # Mesh sizes for bias in drophead
SizeBias2=25.0
```

```
# assign element type
c1 = PartDrophead.cells
regionDH = regionToolset.Region(cells=c1[0:len(c1)])
elemTypeDH = mesh.ElemType(elemCode=C3D8)
PartDrophead.setElementType(regions=regionDH, elemTypes=(elemTypeDH, ))

# assign edge seed for square and edge of drophead
e = PartDrophead.edges
pickedEdges = e.findAt(
  (( r1/2, r1/2 , 0.0) , ) ,
  (( -r1/2, r1/2 , 0.0) , ) ,
  (( -r1/2, -r1/2 , 0.0) , ) ,
  (( r1/2, -r1/2 , 0.0) , ) ,
  (( r1/2, r1/2 , -h) , ) ,
  (( -r1/2, r1/2 , -h) , ) ,
  (( -r1/2, -r1/2 , -h) , ) ,
  (( r1/2, -r1/2 , -h) , ) ,
  (( -sqrt(0.5)*r, sqrt(0.5)*r , 0) , ) ,
  (( -sqrt(0.5)*r, -sqrt(0.5)*r , 0) , ) ,
  (( sqrt(0.5)*r, -sqrt(0.5)*r , 0) , ) ,
  (( sqrt(0.5)*r, sqrt(0.5)*r , 0) , ) ,
  (( -sqrt(0.5)*r, sqrt(0.5)*r , -h) , ) ,
  (( -sqrt(0.5)*r, -sqrt(0.5)*r , -h) , ) ,
  (( sqrt(0.5)*r, -sqrt(0.5)*r , -h) , ) ,
  (( sqrt(0.5)*r, sqrt(0.5)*r , -h) , ) , )
PartDrophead.seedEdgeByNumber(edges=pickedEdges, number=NrElDH1, constraint=FIXED)

# assign edge seed for diagonal egdes from square to side
pickedEdges = e.findAt(
  (( (r-r1)/2+r1 , 0.0 , -h) , ) ,
  ((  0.0 , (r-r1)/2+r1 , -h) , ) ,
  (( -(r-r1)/2-r1 , 0.0 , -h) , ) ,
  ((  0.0 , -(r-r1)/2-r1 , -h) , ) ,
  (( (r-r1)/2+r1 , 0.0 , 0) , ) ,
  ((  0.0 , (r-r1)/2+r1 , 0) , ) ,
  (( -(r-r1)/2-r1 , 0.0 , 0) , ) ,
  ((  0.0 , -(r-r1)/2-r1 , 0) , ) , )
PartDrophead.seedEdgeByNumber(edges=pickedEdges, number=NrElDH2, constraint=FIXED)

# Determine the direction of the edges, the directions of end1Edges and end2Edges are opposite
pickedEdges = e.findAt(
  (( r1, 0.0 , -h/2) , ) ,
  (( 0.0, r1 , -h/2) , ) ,
  (( -r1, 0.0 , -h/2) , ) ,
  (( 0.0 , -r1 , -h/2) , ) ,
  (( r, 0.0 , -h/2) , ) ,
  (( -r, 0.0 , -h/2) , ) ,
  (( 0.0, -r , -h/2) , ) ,
  (( 0.0, r , -h/2) , ) , )
pickedEdges1=[]
pickedEdges2=[]
for i in range(len(pickedEdges)):
  CheckDirection=pickedEdges[i].getVertices()
  if CheckDirection[0]<CheckDirection[1]:
    pickedEdges1.append(pickedEdges[i])
  else:
    pickedEdges2.append(pickedEdges[i])

PartDrophead.seedEdgeByBias(biasMethod=SINGLE, end1Edges=pickedEdges1,
end2Edges=pickedEdges2, minSize=SizeBias1, maxSize=SizeBias2, constraint=FIXED)

pickedEdges = e.findAt(
  (( r1, 0.0 , r1/2) , ) ,
  (( 0.0, r1 , r1/2) , ) ,
  (( -r1, 0.0 , r1/2) , ) ,
  (( 0.0 , -r1 , r1/2) , ) , )
```

```
PartDrophead.seedEdgeBySize(edges=pickedEdges, size=SizeBias1, constraint=FINER)

# Assign structured meshing on the entire drophead
PartDrophead.setMeshControls(regions=c1, technique=STRUCTURED)

# Then change that by assigning sweep mesh to side cells
c11 = c1.findAt(
  (( r1 , 0.1 , -h/2) , ) ,
  (( r1 , -0.1 , -h/2) , ) ,
  (( -r1 , 0.1 , -h/2) , ) ,
  (( -r1 , -0.1 , -h/2) , ) , )
PartDrophead.setMeshControls(regions=c11, technique=SWEEP, algorithm=ADVANCING_FRONT)
c11 = c1.findAt(
  (( r1 , 0.1 , r1/2) , ) ,
  (( r1 , -0.1 , r1/2) , ) ,
  (( -r1 , 0.1 , r1/2) , ) ,
  (( -r1 , -0.1 , r1/2) , ) , )
PartDrophead.setMeshControls(regions=c11, technique=SWEEP, algorithm=MEDIAL_AXIS)

# Generate mesh
PartDrophead.generateMesh()

RadiusEl=(r1*2/NrElDH1)
# Make Node set for element on the bottom of the drophead
q = PartDrophead.nodes
q1= q.getByBoundingCylinder(
  center1= (0.0 , 0.0 , r + 1.E-4 ),
  center2= (0.0 , 0.0 , r -SizeBias1/3),
  radius= (RadiusEl + 1.E-4))
q2=[q1[0].label, q1[1].label, q1[2].label, q1[3].label]
PartDrophead.SetFromNodeLabels(nodeLabels=(q2), name='NodesOnderkantDrophead')
```

Step.py

```
# # #
# # # # # # # # # Step # # # # # # # # # # # # #
# # #
# Drop
myModel.ExplicitDynamicsStep(name='Drop', previous='Initial', timePeriod=Duration)
```

Output.py

```
# # #
# # # # # # # # # Field Output Requests # # # # # # # # # # # #
# # #
del myModel.fieldOutputRequests['F-Output-1']
region=myModel.rootAssembly.sets['BoeiendStuk']
myModel.FieldOutputRequest(name='FieldOutput', createStepName='Drop', region=region, variables=('UT',) ,
      timeInterval=1e-04, timeMarks=ON)

# # #
# # # # # # # # # History Output Requests # # # # # # # # # # # #
# # #
del myModel.historyOutputRequests['H-Output-1']
region = myAssembly.instances['Drophead'].sets['OnderkantDrophead']
myModel.HistoryOutputRequest(name='Drophead', createStepName='Drop', variables=('U2', 'V2'),
     timeInterval=1e-04, region=region)
region = BreedNodeSet
myModel.HistoryOutputRequest(name='Breed', createStepName='Drop', variables=('U1', 'U2', 'U3'),
     timeInterval=1e-04, region=region)
region = SmalNodeSet
myModel.HistoryOutputRequest(name='Smal', createStepName='Drop', variables=('U1', 'U2', 'U3'),
     timeInterval=1e-04, region=region)

region=myAssembly.instances['Specimen'].sets['ElMidSmal']
```

```
myModel.HistoryOutputRequest(name='ElSmal', createStepName='Drop', variables=('S11', 'S22', 'LE11', '
    LE22', 'PEEQ'), timeInterval=1e-04, region=region)
myModel.HistoryOutputRequest(name='ElSmalER', createStepName='Drop', variables=('ER11', 'ER22'),
    timeInterval=1e-05, region=region, filter=ANTIALIASING)

region=myAssembly.instances['Specimen'].sets['ElMidBreed']
myModel.HistoryOutputRequest(name='ElBreed', createStepName='Drop', variables=('S11', 'S22', 'LE11', '
    LE22', 'PEEQ'), timeInterval=1e-04, region=region)
myModel.HistoryOutputRequest(name='ElBreedER', createStepName='Drop', variables=('ER11', 'ER22'),
    timeInterval=1e-05, region=region, filter=ANTIALIASING)

region=myModel.rootAssembly.instances['Specimen'].sets['BovenkantSpecimenNodes']
myModel.HistoryOutputRequest(name='Proef', createStepName='Drop', variables=('RT', ), timeInterval=1e
    -04, region=region)
```

OutputDeformableDrophead.py

```
# # #
# # # # # # # # # Field Output Requests # # # # # # # # # # # #
# # #
del myModel.fieldOutputRequests['F-Output-1']
region =myModel.rootAssembly.sets['BoeiendStuk']
myModel.FieldOutputRequest(name='FieldOutput', createStepName='Drop', region=region, variables=('UT',) ,
     timeInterval=1e-04, timeMarks=ON)

# # #
# # # # # # # # # History Output Requests # # # # # # # # # # # #
# # #
del myModel.historyOutputRequests['H-Output-1']
region = myAssembly.instances['Drophead'].sets['NodesOnderkantDrophead']
myModel.HistoryOutputRequest(name='Drophead', createStepName='Drop', variables=('U2', 'V2'),
    timeInterval=1e-04, region=region)
region = BreedNodeSet
myModel.HistoryOutputRequest(name='Breed', createStepName='Drop', variables=('U1', 'U2', 'U3'),
    timeInterval=1e-04, region=region)
region = SmalNodeSet
myModel.HistoryOutputRequest(name='Smal', createStepName='Drop', variables=('U1', 'U2', 'U3'),
    timeInterval=1e-04, region=region)

region=myAssembly.instances['Specimen'].sets['ElMidSmal']
myModel.HistoryOutputRequest(name='ElSmal', createStepName='Drop', variables=('S11', 'S22', 'LE11', '
    LE22', 'PEEQ'), timeInterval=1e-04, region=region)
myModel.HistoryOutputRequest(name='ElSmalER', createStepName='Drop', variables=('ER11', 'ER22'),
    timeInterval=1e-05, region=region, filter=ANTIALIASING)

region=myAssembly.instances['Specimen'].sets['ElMidBreed']
myModel.HistoryOutputRequest(name='ElBreed', createStepName='Drop', variables=('S11', 'S22', 'LE11', '
    LE22', 'PEEQ'), timeInterval=1e-04, region=region)
myModel.HistoryOutputRequest(name='ElBreedER', createStepName='Drop', variables=('ER11', 'ER22'),
    timeInterval=1e-05, region=region, filter=ANTIALIASING)

region=myModel.rootAssembly.instances['Specimen'].sets['BovenkantSpecimenNodes']
myModel.HistoryOutputRequest(name='Proef', createStepName='Drop', variables=('RT', ), timeInterval=1e
    -04, region=region)
```

Contact.py

```
# # #
# # # # # # # # # Contact # # # # # # # # # # # #
# # #
# contact interaction properties
ContactPropertie=myModel.ContactProperty('BoemProp')
ContactPropertie.TangentialBehavior( )
ContactPropertie.NormalBehavior( )
# Uncomment when contact is not frictionless
```

```
# ContactPropertie.tangentialBehavior.setValues(formulation=PENALTY, table=((FricCoeff, ), ),
    maximumElasticSlip=FRACTION, fraction=0.005)

# Contact interaction
f1= DropheadInstance.faces
f11=f1.getByBoundingBox(yMax=r)
DropheadContact = regionToolset.Region(side1Faces=f11)

myModel.SurfaceToSurfaceContactExp(name='Boem', createStepName='Drop', master=DropheadContact , slave=
    ContactOppSpecimenSet , sliding=FINITE, interactionProperty='BoemProp')
```

ContactDeformableDrophead.py

```
# # #
# # # # # # # # # Contact # # # # # # # # # # # #
# # #
# contact interaction properties
ContactPropertie=myModel.ContactProperty('BoemProp')
ContactPropertie.TangentialBehavior( )
ContactPropertie.NormalBehavior( )
# Uncomment when contact is not frictionless
# ContactPropertie.tangentialBehavior.setValues(formulation=PENALTY, table=((FricCoeff, ), ),
    maximumElasticSlip=FRACTION, fraction=0.005)

# Contact interaction
f1= DropheadInstance.faces
f20=f1.getClosest(coordinates=((r, dy-r/2, r),),)
f21=f1.getClosest(coordinates=((r, dy-r/2, -r),),)
f22=f1.getClosest(coordinates=((-r, dy-r/2, -r),),)
f23=f1.getClosest(coordinates=((-r, dy-r/2, r),),)
f24=f1.getClosest(coordinates=((0, dy-r, 0),),)
InteractionSurfDHSet=myAssembly.Set(faces=f1.findAt(((f20[0][1]),), ((f21[0][1]),), ((f22[0][1]), ), ((
    f23[0][1]),), ((f24[0][1]),) ), name='IntSurfDH')
DropheadContact = regionToolset.Region(side1Faces=InteractionSurfDHSet.faces)

myModel.SurfaceToSurfaceContactExp(name='Boem', createStepName='Drop', master=DropheadContact, slave=
    ContactOppSpecimenSet, sliding=FINITE, interactionProperty='BoemProp')
```

BC.py

```
# # #
# # # # # # # # # Boundary Conditions # # # # # # # # # # # #
# # #
# constrict movement drophead
region = myAssembly.instances['Drophead'].sets['OnderkantDrophead']
myModel.DisplacementBC( name='ConstrictDrophead', createStepName='Initial', region=region, u1=SET, u3=
    SET, ur1=SET, ur2=SET, ur3=SET)

# Clamp specimen
myModel.EncastreBC(name='Inklemming Specimen', createStepName='Initial', region=BovenkantSpecimenSet)

# # #
# # # # # # # # # Predefined Field # # # # # # # # # # # #
# # #
# (drophead velocity)
region = myAssembly.instances['Drophead'].sets['OnderkantDrophead']
myModel.Velocity(name='DropheadVelocity', region=region, velocity1=0.0, velocity2=v_0, velocity3=0.0,
    omega=0.0)
myAssembly.regenerate()

# # #
# # # # # # # # # Keyword file aanpassen # # # # # # # # # # # #
# # #
# Find the line where steel is defined
myModel.keywordBlock.synchVersions()
blockPrefix='*Material'
```

```
pos=0
for block in myModel.keywordBlock.sieBlocks:
  if block[0:len(blockPrefix)].lower()==blockPrefix.lower():
    break
  else:
    pos=pos+1

myModel.keywordBlock.replace(pos, """*Material, name=Steel, srate factor="""+SRF)
```

BCDeformableDrophead.py

```
# # #
# # # # # # # # # Boundary Conditions # # # # # # # # # # # # #
# # #
# constrict movement drophead
myModel.DisplacementBC( name='ConstrictDrophead', createStepName='Initial', region=TopDropheadSet, u1=
     SET, u3=SET)

# Clamp specimen
myModel.EncastreBC(name='Inklemming Specimen', createStepName='Initial', region=BovenkantSpecimenSet)

# # #
# # # # # # # # # Predefined Field # # # # # # # # # # # # #
# # #
# drophead velocity
DropheadComplete = regionToolset.Region(cells=DropheadInstance.cells)
myModel.Velocity(name='DropheadVelocity', region=DropheadComplete, velocity1=0.0, velocity2=v_0,
     velocity3=0.0, omega=0.0)
myAssembly.regenerate()

# # #
# # # # # # # # # Adjust keyword file for SRF # # # # # # # # # # # #
# # #
# Find the line where steel is defined
myModel.keywordBlock.synchVersions()
blockPrefix='*Material'
pos=0
for block in myModel.keywordBlock.sieBlocks:
  if block[0:len(blockPrefix)].lower()==blockPrefix.lower():
    break
  else:
    pos=pos+1

myModel.keywordBlock.replace(pos, """*Material, name=Steel, srate factor="""+SRF)
```

Appendix C

Abaqus input file

This appendix provides an example input file for Abaqus 2018.

```
*Heading
 Description of the job
** Job name: MyJobName Model name: MyModelName
** Generated by: Abaqus/CAE 2018
*Preprint, echo=NO, model=NO, history=NO, contact=NO
**
** PARTS
**
*Part, name=Specimen
*Node

     [Plenty of nodes]

*Element, type=S4R

     [Plenty of elements]

*Element, type=S3

     [A few elements]

*Element, type=S3
4065, 5410, 5422, 5421
7794, 8542, 8554, 8553
*Nset, nset=_PickedSet19, internal, generate
     1,  10625,     1
*Elset, elset=_PickedSet19, internal, generate
    1,  9986,    1
*Nset, nset=AllFacesSpecimen, generate
     1,  10625,     1
*Elset, elset=AllFacesSpecimen, generate
    1,  9986,    1
*Nset, nset=HalfSpecimen

     [Plenty of nodes]

*Elset, elset=HalfSpecimen

     [Plenty of elements]

*Elset, elset=ElMidSmal
 6337, 6586, 6849, 6881
*Elset, elset=ElMidBreed
```

```
 8005, 8035, 8514, 8784
*Nset, nset=BovenkantSpecimenNodes
   80,   81,   85, 1986, 1987, 1988, 1989, 1990, 1991, 1992, 2185, 2186, 2187, 2188, 2189, 2190
 2191,
** Region: (SpecimenSection:Picked)
*Elset, elset=_I1, internal

     [Plenty of elements]

** Section: SpecimenSection
*Shell Section, elset=_I1, material=Steel
2., 5
*Orientation, name=Ori-1
         0.,         -1.,          0.,          0.,          0.,         -1.
3, 0.
** Region: (SpecimenSection:Picked), (Material Orientation:Picked)
*Elset, elset=_I2, internal

     [Plenty of elements]

** Section: SpecimenSection
*Shell Section, elset=_I2, material=Steel, orientation=Ori-1
2., 5
*End Part
**
*Part, name=ZDrophead
*End Part
**
**
** ASSEMBLY
**
*Assembly, name=Assembly
**
*Instance, name=Drophead, part=ZDrophead
         0.,         0.5,         10.
*Node
      1,          0.,        -50.,          0.
*Nset, nset=Drophead-RefPt_, internal
1,
*Nset, nset=OnderkantDrophead
 1,
*Surface, type=REVOLUTION, name=RigidSurface_, internal
START,          0., 456.374183872498
 LINE,         50., 456.374183872498
 LINE,         50.,          0.
 CIRCL,          0.,        -50.,          0.,          0.
*Rigid Body, ref node=Drophead-RefPt_, analytical surface=RigidSurface_
*Element, type=MASS, elset=OnderkantDrophead_MassDrophead_
1, 1
*Mass, elset=OnderkantDrophead_MassDrophead_
0.03,
*End Instance
**
*Instance, name=Specimen, part=Specimen
*End Instance
**
*Nset, nset=BoeiendStuk, instance=Specimen
 48, 50, 51, 59, 60, 61, 66, 70, 71, 79, 82, 83
*Nset, nset=BovenkantSpecimen, instance=Specimen
   38,   39,   80,   81,   84,   85, 1184, 1185, 1186, 1187, 1188, 1189, 1190, 1986, 1987, 1988
 1989, 1990, 1991, 1992, 2086, 2087, 2088, 2089, 2090, 2091, 2092, 2185, 2186, 2187, 2188, 2189
 2190, 2191
*Elset, elset=BovenkantSpecimen, instance=Specimen
 5018, 5019, 5020, 5021, 5022, 5023, 5024, 5025, 8747, 8748, 8749, 8750, 8751, 8752, 8753, 8754
 9227, 9228, 9229, 9230, 9231, 9232, 9233, 9234, 9979, 9980, 9981, 9982, 9983, 9984, 9985, 9986
*Nset, nset=BreedA, instance=Specimen
```

```
 71, 83
*Nset, nset=BreedB, instance=Specimen
 70, 82
*Nset, nset=BreedC, instance=Specimen
 66, 79
*Nset, nset=BreedD, instance=Specimen
 65, 78
*Nset, nset=BreedE, instance=Specimen
 67, 77
*Nset, nset=BreedNode, instance=Specimen
 74,
*Nset, nset=ContactOppSpecimen, instance=Specimen

     [Plenty of nodes]

*Elset, elset=ContactOppSpecimen, instance=Specimen

     [Plenty of elements]

*Nset, nset=FacesBreedSpecimen, instance=Specimen

     [Plenty of nodes]

*Elset, elset=FacesBreedSpecimen, instance=Specimen

     [Plenty of elements]

*Nset, nset=FacesSmalSpecimen, instance=Specimen

     [Plenty of nodes]

*Elset, elset=FacesSmalSpecimen, instance=Specimen

     [Plenty of elements]

*Nset, nset=SmalA, instance=Specimen
 51, 61
*Nset, nset=SmalB, instance=Specimen
 50, 60
*Nset, nset=SmalC, instance=Specimen
 48, 59
*Nset, nset=SmalD, instance=Specimen
 47, 58
*Nset, nset=SmalE, instance=Specimen
 49, 57
*Nset, nset=SmalNode, instance=Specimen
 53,
*Surface, type=NODE, name=ContactOppSpecimen_CNS_, internal
ContactOppSpecimen, 1.
*End Assembly
**
** MATERIALS
**
*Material, name=Steel,srate factor=0.3
*Density
 7.8e-09,
*Elastic
210000., 0.3
*Plastic
    350.,   0.
 381.845, 0.005
 403.411, 0.01
 416.587, 0.015
 426.195, 0.02
 433.801, 0.025
 440.115, 0.03
```

```
 445.526, 0.035
 450.267, 0.04
  454.49, 0.045
 458.301, 0.05
 461.777, 0.055
 464.973, 0.06
 467.932, 0.065
 470.689, 0.07
  473.27, 0.075
 475.697, 0.08
 477.989, 0.085
 480.159, 0.09
 482.221, 0.095
 484.186,  0.1
 486.062, 0.105
 487.858, 0.11
  489.58, 0.115
 491.234, 0.12
 492.826, 0.125
  494.36, 0.13
 495.842, 0.135
 497.273, 0.14
 498.658, 0.145
    500., 0.15
*Rate Dependent
 40.4,5.
**
** INTERACTION PROPERTIES
**
*Surface Interaction, name=BoemProp
*Friction
0.,
*Surface Behavior, pressure-overclosure=HARD
**
** BOUNDARY CONDITIONS
**
** Name: ConstrictDrophead Type: Displacement/Rotation
*Boundary
Drophead.OnderkantDrophead, 1, 1
Drophead.OnderkantDrophead, 3, 3
Drophead.OnderkantDrophead, 4, 4
Drophead.OnderkantDrophead, 5, 5
Drophead.OnderkantDrophead, 6, 6
** Name: Inklemming Specimen Type: Symmetry/Antisymmetry/Encastre
*Boundary
BovenkantSpecimen, ENCASTRE
**
** PREDEFINED FIELDS
**
** Name: DropheadVelocity Type: Velocity
*Initial Conditions, type=VELOCITY
Drophead.OnderkantDrophead, 1, 0.
Drophead.OnderkantDrophead, 2, -1700.
Drophead.OnderkantDrophead, 3, 0.
** ----------------------------------------------------------------
**
** STEP: Drop
**
*Step, name=Drop, nlgeom=YES
*Dynamic, Explicit
, 0.01
*Bulk Viscosity
0.06, 1.2
**
** INTERACTIONS
**
```

```
** Interaction: Boem
*Contact Pair, interaction=BoemProp, mechanical constraint=KINEMATIC, cpset=Boem
Drophead.RigidSurface_, ContactOppSpecimen_CNS_
**
** OUTPUT REQUESTS
**
*Restart, write, number interval=1, time marks=NO
**
** FIELD OUTPUT: FieldOutput
**
*Output, field, time interval=0.0001, time marks=YES
*Node Output, nset=BoeiendStuk
UT,
**
** HISTORY OUTPUT: ElBreedER
**
*Output, history, filter=ANTIALIASING, time interval=1e-05
*Element Output, elset=Specimen.ElMidBreed
ER11, ER22
**
** HISTORY OUTPUT: ElSmalER
**
*Element Output, elset=Specimen.ElMidSmal
ER11, ER22
**
** HISTORY OUTPUT: Proef
**
*Output, history, time interval=0.0001
*Node Output, nset=Specimen.BovenkantSpecimenNodes
RT,
**
** HISTORY OUTPUT: Breed
**
*Node Output, nset=BreedNode
U1, U2, U3
**
** HISTORY OUTPUT: ElBreed
**
*Element Output, elset=Specimen.ElMidBreed
LE11, LE22, PEEQ, S11, S22
**
** HISTORY OUTPUT: ElSmal
**
*Element Output, elset=Specimen.ElMidSmal
LE11, LE22, PEEQ, S11, S22
**
** HISTORY OUTPUT: Drophead
**
*Node Output, nset=Drophead.OnderkantDrophead
U2, V2
**
** HISTORY OUTPUT: Smal
**
*Node Output, nset=SmalNode
U1, U2, U3
*End Step
```

Bibliography

Alabi, A., Moore, P., Wrobel, L., Campbell, J., and He, W. (2018). "Tensile behaviour of s690ql and s960ql under high strain rate". *Journal of Constructional Steel Research*, vol. 150. doi:10.1016/j.jcsr.2018.08.009.

ASTM E112-13 (2013). "ASTM E112-13, Standard test methods for determining average grain size". Standard, ASTM International, West Conshohocken, PA.

ASTM E8 (2016). "ASTM E8 / E8M-16ae1, Standard test methods for tensions testing of metallic materials". Standard, ASTM International, West Conshohocken, PA.

Bruce, D., Matlock, D., Speer, J., and De, A. (2004). "Assessment of the strain-rate dependent tensile properties of automotive sheet steels". *SAE Technical Papers*. doi: 10.4271/2004-01-0507.

Chan, J. J. (2009). *Design of fixtures and specimens for high strain-rate tensile testing on a drop tower*. BsC Thesis, Massachusetts Institute of Technology.

Cowper, G. and Symonds, P. (1957). "Strain hardening and strain-rate effects in the impact loading loading of cantilever beams". Report no. 28, Brown University Division of applied mathematics.

Dassault Systèmes Simulia Corp (2017). *Abaqus User assistance 2018*. Dassault Systèmes Simulia Corp, United States.

Gray, I., George T. (2000). "Classic Split-Hopkinson Pressure Bar Testing". In *Mechanical Testing and Evaluation*. ASM International. ISBN 978-1-62708-176-4. doi:10.31399/asm.hb.v08.a0003296.

Huh, H., Kim, S.-B., Song, J.-H., and Lim, J.-H. (2008). "Dynamic tensile characteristics of trip-type and dp-type steel sheets for an auto-body". *International Journal of Mechanical Sciences*, vol. 50, pp. 918–931. doi:10.1016/j.ijmecsci.2007.09.004.

ISO 6892-1 (2016). "ISO 6892-1:2016, Metallic materials - tensile testing - part 1: Method of test at room temperature". Standard, International Organization for Standardization, Geneva, CH.

Jones, N. (2012). *Structural impact*. Cambridge University Press. ISBN 978-1-107-01096-3.

Limess Messtechnik & Software GmbH (2020). "Q400 DIC - measurement system for deformation and strain based on digital image correlation". URL https://www.limess.com/en/products/q400-digital-image-correlation#technical-specifications. Accessed on September 9, 2020.

Meriam, J., Kraige, L., and Palm, I., W.J. (2003). *Engineering mechanics dynamics*. Wiley & sons. ISBN 0-471-26606-x.

Pape, G. (2002). *Flow stress and ductile failure at varying strain rates*. Ph.D. thesis, Delft University of Technology.

Perogamvros, N., Mitropoulos, T., and Lampeas, G. (2016). "Drop tower adaptation for medium strain rate tensile testing". *Experimental Mechanics*, vol. 56, pp. 419–436. doi: 10.1007/s11340-015-0112-3.

Reedlunn, B., Daly, S., Hector, L., Zavattieri, P., and Shaw, J. (2013). "Tips and tricks for characterizing shape memory wire part 5: Full-field strain measurement by digital image correlation". *Experimental Techniques*, vol. 37, pp. 62–78. doi:10.1111/j.1747-1567.2011.00717.x.

Rusinek, A., Cheriguene, R., Bäumer, A., and Larour, P. (2008). "Dynamic behaviour of high-strength sheet steel in dynamic tension: Experimental and numerical analyses". *The Journal of Strain Analysis for Engineering Design*, vol. 43, pp. 37–53. doi:10.1243/03093247JSA320.

Shim, J. and Mohr, D. (2009). "Using split hopkinson pressure bars to perform large strain compression tests on polyurea at low, intermediate and high strain rates". *International Journal of Impact Engineering*, vol. 36. doi:10.1016/j.ijimpeng.2008.12.010.

Spronk, S. (2018). *Investigation of the rate-dependency of carbon/epoxy and glass/polyamide-6 composites in tension, mode-I delamination and low-velocity impact*. Ph.D. thesis, Ghent University.

Sutton, M. A., Orteu, J.-J., and Schreier, H. W. (2009). *Image correlation for shape, motion and deformation measurements*. Springer US. ISBN 978-0-387-78746-6.

Yang, X., Hector, L. G., and Wang, J. (2014). "A combined theoretical/experimental approach for reducing ringing artifacts in low dynamic testing with servo-hydraulic load frames". *Experimental Mechanics*, vol. 54, pp. 775–789. doi:10.1007/s11340-014-9850-x.